Remote Sensing for Regional Assessment and Analysis of Minnesota Lake and River Water Quality

A DISSERTATION
SUBMITTED TO THE FACULTY OF THE GRADUATE SCHOOL
OF THE UNIVERSITY OF MINNESOTA
BY

Leif Gordon Olmanson

IN PARTIAL FULFILLMENT OF THE REQUIREMENTS
FOR THE DEGREE OF
DOCTOR OF PHILOSOPHY

Marvin E. Bauer

May 2012

Acknowledgements

The completion of my dissertation and subsequent PhD has been a long journey, which started long before my graduate education. Although the journey to complete my PhD has been long, it has been thought-provoking and rewarding. My interest in geography and other natural resource sciences began at Gustavus Adolphus College with many memorable field trips and lectures taught by various professors, including: Jim Welsh, Mark Johnson and Joe Carlson from Geology; Bob Bellig from Biology; and Robert Douglas and Robert Moline from Geography. Many thanks to these great professors for sparking my interest in natural resource assessment! While I have always been interested in finding better ways of doing things, the tools to bring together my interests were introduced to me at the University of Minnesota.

My first eye opening experiences came in 1994 with Professor Robert McMaster's Introduction to Geographic Information Systems (GIS) course and subsequent Urban GIS and Analysis course co-taught with Professor William Craig. They made me aware of the endless potential of this emerging technology. Later in the fall of 1994 I met Professor Patrick Brezonik, who was co-teaching a Water Resources policy course and encouraged me to enroll in the newly formed Water Resources Science graduate program. That winter while taking the Water Resources Science Interdisciplinary Seminar, also taught by Patrick Brezonik, I met Steve Kloiber. In that course Steve and I completed a project together where we evaluated all the lake water quality data that had been collected in the Twin Cities Metropolitan Area (TCMA) and found there was a paucity of data and a great need for better methods for regional water

quality assessment. My final realization came in the spring of 1996 when I took the Advanced Remote Sensing course taught by Marvin Bauer. In that course I had the opportunity to explore Landsat imagery and quickly discovered that the images contained information about water quality and may be the answer for regional assessment of lake water quality in Minnesota. After convincing Professor Bauer that lakes are not black and that there is actual information in the imagery, I conducted my class project investigating the use of Landsat imagery for water quality assessment. That work continued in my Water Resources Science Plan B thesis "Satellite Remote Sensing of the Trophic State Condition of lakes in the Twin Cities Metropolitan Area" which was completed and my master's degree awarded in 1997.

Shortly after completion of my master's degree in Water Resources Science, I was hired by Patrick Brezonik and Marvin Bauer to conduct research using remote sensing and GIS for assessment of water quality for a number of different projects throughout the years. These projects are what made this dissertation possible. Therefore, I give special thanks and acknowledgement to Patrick Brezonik and Marvin Bauer for giving me the opportunity to work on these interesting projects. In addition, I thank the Minnesota Pollution Control Agency, North American Lake Management Society – U.S. EPA, Legislative Commission on Minnesota Resources, NASA – Upper Great Lakes Regional Earth Sciences Application Center, Minnesota Department of Natural Resources, Metropolitan Council - Twin Cities Water Quality Initiative Grant Program, and the University of Minnesota for funding and research support.

This dissertation would not have been possible without the help, support, patience and excellent guidance of my principal advisors Marvin Bauer and Patrick Brezonik, who I have been working with for 15 years. Marvin Bauer has been invaluable on an academic, professional, and a personal level, for which I am extremely grateful. Not only was he readily available for me throughout the years, but he also provided me with an excellent atmosphere for doing research. Patrick Brezonik, has really helped me during the construction and completion of each chapter. I am grateful for their wisdom, knowledge and commitment to the highest standards. They have always read and responded to the drafts of each chapter of my work quicker than I could have hoped for. I will also be forever grateful to them for strongly encouraging me to finish my PhD.

I also wish to thank the other members of my dissertation committee, Joseph Knight and Kenneth Brooks, for generously offering their time, support, guidance and good will throughout the review of this document.

I acknowledge the insightful work of Joseph Shapiro, whose efforts started the CLMP program in 1973, and the efforts of hundreds of citizen volunteers who collected the Secchi transparency data that made calibration of satellite imagery for lake clarity assessments in Minnesota possible. I also thank Sean Vaughn of the Minnesota Department of Natural Resources for development of the catchment delineations used in Chapter 3. I greatly appreciate the MERIS data that were provided by the European Space Agency; Landsat and MODIS data that were provided by United States Geological Survey (USGS) and National Aeronautics and Space Administration (NASA); and AWiFS imagery that was provided by the USDA Foreign Agricultural Service through

the AmericaView program. For assistance with field data coordination, collection and sample analysis for Chapter 5, special thanks go to Bruce Wilson (MPCA), Steve Kloiber (Metropolitan Council), Kent Johnson (Metropolitan Council), and sampling crews from the Minnesota Pollution Control Agency, Metropolitan Council, Minnesota Department of Natural Resources, and Minnesota Department of Agriculture. They were dispatched on short notice to collect water samples. Weather forecasts from KARE 11 meteorologist Jonathan Yuhas were invaluable in planning for data acquisitions under clear conditions.

Last but not least, none of this would have been possible without the love and patience of my wife Kristin and children, Anders, Britta and Bjorn. I would like to express my heart-felt gratitude to my family for the constant source of love, support and strength all these years.

Dedication

I dedicate this dissertation to my parents, M. Donald Olmanson, M.D. and Barbara Olmanson, who inspired my love and respect of the great outdoors. They taught me about hard work, perseverance, and resourcefulness; all traits that were very useful in the completion of this dissertation.

Abstract

Beginning soon after the launch of the first Landsat satellite, researchers began investigating the use of Landsat imagery to monitor the water quality of our lakes and coastlines. The earliest use of Landsat imagery was for simple qualitative observations which included locating and mapping pollution and pollution plumes. Shortly thereafter, field measurements of water quality were correlated with Landsat data and later these correlations were used for quantitative assessment of water quality (e.g., turbidity, chlorophyll and water clarity).

This dissertation expands on this earlier work and describes results of research to develop and use remote sensing tools for regional water quality assessment to improve the understanding and management of Minnesota's lakes and rivers. It includes four major components. First, a 20-year, 1985–2005, comprehensive water clarity database for more than 10,500 lakes at approximately five-year intervals for the time period 1985–2005, which includes almost 100,000 individual estimates of lake water clarity, was compiled and evaluated. Second, the results of a statistical analysis of the Landsat database for geospatial and temporal trends of water clarity over the 20-year period, as well as trends related to land cover/use and lake morphometry, are reported. Third, the advantages of improved spectral and temporal resolution and disadvantages of the lower spatial resolution of the global MODIS and MERIS systems are evaluated for regional-scale measurements of lake water clarity and chlorophyll of large lakes in Minnesota and compared with Landsat. Finally, aerial hyperspectral spectrometers were used to collect

imagery with high spatial and spectral resolution for use in identifying, measuring and mapping optically related water quality characteristics of major rivers in Minnesota for three time periods that represent different water quality and flow regimes.

Table of Contents

List of Tables

List of Figures

Chapter 1

Remote Sensing for Regional Assessment and Analysis of Minnesota Lake and River Water Quality

1.1 Introduction

In many parts of the world lakes are important subsistence, recreational and aesthetic resources that add to the economic strength and quality of life. Protecting and monitoring lake water quality are chief concerns for many national, regional and local organizations. For successful lake management, it is important to have long-term water quality information at a broad regional and local level. Regrettably, only a relatively small number of lakes are regularly monitored by ground-based methods, and historical water quality data are deficient for most lakes. Although it is not possible to go back in time and collect water quality information using traditional field methods, Landsat images have been acquired and archived on a regular basis since the early 1970s, enabling historical water quality assessments of all lakes. Additionally, global systems such as MODIS and MERIS have been acquiring and archiving imagery on a regular basis since the early 2000s enabling more recent historical water quality assessments of large lakes.

Landsat imagery has been used to characterize certain water quality characteristics of lakes for 40 years. Some of the earliest uses of Landsat imagery were for simple qualitative observations. These included locating and mapping pollution and pollution plumes (e.g., Lind, 1973; Pluhowski, 1973). Shortly thereafter, Landsat imagery

was correlated to field based measurements (e.g., Yarger, 1973; McCauley, 1974; Brooks, 1975) and finally used for quantitative assessment of water quality (e.g., turbidity, chlorophyll and water clarity, frequently expressed in terms of Secchi depth) (e.g., Brown et al., 1977a; Lillesand et al., 1983; Ritchie et al., 1990; Lathrop et al., 1991, 1992; Dekker and Peters, 1993), but until recent times these reports usually described investigative efforts involving only one or a few lakes and/or short observation periods. One early exception was the work of Martin et al. (1983), who used semi-automated procedures to assess the trophic status of around 3,000 lakes in Wisconsin using Landsat Multispectral Scanner (MSS) imagery. Dekker et al. (2002) described procedures using analytical optical modeling that could be used for retrospective analysis of Landsat and SPOT imagery for regional water quality assessment where there is no concurrent field data. Kloiber et al. (2002a) and Olmanson et al. (2001) described an efficient and practical procedure using empirical methods based on Landsat imagery for routine, regional-scale assessments of lakes for water clarity, and Kloiber et al. (2002b) used this approach to assess spatial patterns and temporal trends in approximately 500 lakes in the seven-county Twin Cities Metropolitan Area (TCMA) of Minneapolis-St. Paul, Minnesota. Olmanson et al. (2002) expanded this work to a statewide level, reporting the first census of water clarity for Minnesota lakes.

This dissertation describes results of research to continue and expand the use of remote sensing tools to improve the understanding and management of lakes and rivers in Minnesota. It includes four major components. First, the procedures used in Kloiber et al. (2002b) and Olmanson et al. (2002) were expanded to complete a 20-year, 1985–2005,

comprehensive water clarity database for more than 10,500 lakes at approximately five-year intervals for the time period 1985–2005, which includes almost 100,000 individual estimates of lake water clarity and is the largest database on lake clarity produced from Landsat imagery to date. Second, the results of a statistical analysis of the Landsat database for geospatial and temporal trends of water clarity over the 20-year period, as well as trends related to land cover/use and lake morphometry, are reported. Third, the advantages of improved spectral and temporal resolution and disadvantages of the lower spatial resolution of the global MODIS and MERIS systems are evaluated for regional-scale measurements of lake water clarity and chlorophyll of large lakes in Minnesota and compared with Landsat. Finally, aerial hyperspectral spectrometers were used to collect imagery with high spatial and spectral resolution for use in measuring optically related water quality characteristics of major rivers of Minnesota.

1.2 Study Area

Minnesota is the northernmost continental U.S. State and is known as the "Land of 10,000 Lakes." It has approximately 12,000 lakes that are four hectares (ha) or larger in area, as well as 6,564 natural rivers and countless streams that stretch approximately 150,000 km. These water bodies vary greatly at local, regional and statewide scales by size, depth, ecology, and water quality. The wide diversity allows for many recreational and tourism opportunities but makes their management challenging. Of the lakes that have been studied to date, 26 percent have been found to be impaired by anthropogenic eutrophication and of the 17 percent of the state's river and stream miles assessed for the

2010 Impaired Waters List, 40 percent were found to be impaired (P. Anderson, Minnesota Pollution Control Agency, personal communications, 2010 & 2011).

Minnesota has seven ecoregions that differ in terms of their aggregate land use, geology, soils, vegetation, climate, wildlife, and hydrologic characteristics (Omernik, 1987). The Northern Lakes and Forest (NLF) and Northern Minnesota Wetlands (NMW), which have land cover dominated by forest, lakes and wetlands, generally have the highest water clarity in the state. The Northern Glacial Plains (NGP), Red River Valley (RRV) and Western Corn Belt Plains (WCBP) generally have low water clarity and are dominated by agricultural land cover.

1.3 Synopsis of the chapters

This dissertation is divided into four principal chapters, all of which are intended for publication in international research journals. Two have been published (Chapter 2 and 4), one has been submitted (Chapter 5) for publication and the remaining chapter (Chapter 3) is in preparation for submission. Each chapter provides background, rationale, goals, methods, results, discussion, and conclusions.

Chapter 2 (Olmanson et al., 2008) was published in *Remote Sensing of Environment* and documents a series of Minnesota statewide assessments that include more than 10,500 lakes each at approximately five-year intervals for the period 1985–2005. More recently, additional assessments were completed for 1975 using Landsat multispectral scanner (MSS) imagery and for 2008 using Landsat Thematic Mapper (TM) and Enhanced Thematic Mapper plus (ETM+) imagery. These assessments have

demonstrated strong relationships (average R^2 of 0.83 and range 0.71–0.96) between the spectral-radiometric responses of Landsat TM, ETM+ and MSS data and in situ observations of water clarity measured in terms of Secchi disk transparency (SD). Data for all lakes and years are available at http://water.umn.edu/, and a web-based mapping tool called "Lake Browser" enables searches and displays of results for individual lakes. This database is used routinely by scientists, teachers, agencies, and the public for research, education, water management and recreational purposes.

Chapter 3 describes a geospatial and temporal analysis of the twenty-year Landsat water clarity database 1985–2005, using GIS in relation to land use/land cover and lake morphometric characteristics. Lake clarity in Minnesota has a strong geographic pattern; lakes in the south and southwest generally have low clarity, and lakes in the north and northeast tend to have high clarity. Lake depth is a strong factor in water clarity with deep lakes having higher water clarity than shallow lakes. Land use/cover also is a significant factor, with decreasing water clarity associated with increased agricultural and urban areas. Increasing water clarity was associated with increased forest areas. The mean water clarity statewide remained stable from 1985 to 2005, but decreasing water clarity trends were detected in ecoregions dominated by agricultural land use. These patterns are evident at the catchment, watershed, county, ecoregion and statewide levels. Results of this analysis should be useful to lake managers and policy makers in making informed decisions about land development and improve the management of lake resources.

Chapter 4 (Olmanson et al., 2011) was published in *Water Resources Research* and investigates two alternative systems for remote sensing of regional water quality. For the assessments completed in Chapter 2 Landsat imagery was used; however, Landsat 5 imaging was suspended in November 2011(the MSS sensor was reactivated and may allow for imaging to continue). Landsat 7, while still operating, is far beyond its expected service life and could fail at any time. The next Landsat is not scheduled to be launched until early 2013. Two alternative systems, MODIS and MERIS, that could be used for regional assessments and provide imagery at low or no cost were examined. These systems have lower spatial resolution than Landsat, which limits the number of lakes they can assess, but they have improved spectral characteristics and have been used for routine global chlorophyll and other measurements of the oceans. To evaluate the usefulness of these systems for lakes, we used empirical methods similar to those used for regional water clarity assessments with Landsat data in Minnesota. The assessment accuracy for chlorophyll and water clarity (Secchi depth) and the size and number of lakes that could be assessed were determined for calibrated radiance and atmospherically corrected MODIS and MERIS products and were compared to Landsat. MODIS and MERIS systems, which have large swath widths and high temporal coverage are well suited for regional assessments of large lakes, but their low spatial resolution limits the number of lakes that can be assessed. Landsat imagery allows all lakes > 4 ha (more than 12,000 in Minnesota) to be assessed, but its low spectral resolution limits assessments to water clarity. The MERIS system, with spectral and spatial resolution suitable for large (>150 ha) lakes, was the only system with a spectral band set that measured key absorption and

scattering characteristics of phytoplankton that could be used reliably for regional chlorophyll assessments. The atmospherically corrected MERIS products we tested did not perform as well as the calibrated radiance product, and the MODIS atmospherically corrected algorithm using the shortwave infrared (SWIR) bands performed better than the methods used for MERIS and as well as the calibrated radiance product.

Chapter 5 investigates the use of aerial hyperspectral spectrometers to measure and map optically related water quality characteristics of major rivers in the Minneapolis-St. Paul (Twin Cities) metropolitan area, Minnesota. Imagery was collected during three acquisitions (August 2004, 2005 and 2007); each period represented different flow and water quality regimes. For calibration purposes, water samples were collected concurrently with the remote sensing data acquisition, and to obtain a range of conditions for calibrations, we focused our measurements around the confluences of river systems that have different water quality characteristics. Spectral characteristics that distinguish waters dominated by different inherent optical properties (IOPs) were identified and used to develop empirical models to map different water quality characteristics in optically complex waters.

Application of the methods to quantify spatial variations in water quality for important stretches of the Mississippi River and its tributaries indicate that imaging spectrometry can be used to successfully distinguish and map key water quality variables under complex IOP conditions, particularly to separate and map inorganic suspended sediments independently of chlorophyll levels. Maps showing the complex interactions of

sediment and algae in these river segments due to different flow conditions should be useful for water resource managers.

Chapter 2

A 20-year Landsat Water Clarity Census of Minnesota's 10,000 Lakes[1]

A 20-year comprehensive water clarity database assembled from Landsat imagery, primarily Thematic Mapper and Enhanced Thematic Mapper Plus, for Minnesota lakes larger than eight hectares in surface area contains data on more than 10,500 lakes at five-year intervals over the period 1985-2005. The reliability of the data was evaluated by examining the precision of repeated measurements on individual lakes within short time periods using data from adjacent overlapping Landsat paths and by comparing water clarity computed from Landsat data to field-collected Secchi depth data. The agreement between satellite data and field measurements of Secchi depth within Landsat paths was strong (average R^2 of 0.83 and range 0.71-0.96). Relationships between late summer Landsat and field-measured Secchi depth for the combined statewide data similarly were strong (r^2 of 0.77-0.80 for individual time periods and r^2 = 0.78 for the entire database). Lake clarity has strong geographic patterns in Minnesota; lakes in the south and southwest have low clarity, and lakes in the north and northeast tend to have the highest clarity. This pattern is evident at both the individual lake and the ecoregion level. Mean water clarity in the Northern Lakes and Forest and North Central Hardwood Forest ecoregions in central and northern Minnesota remained stable from 1985 to 2005 while decreasing water clarity trends were detected in the Western Corn

[1] Reprinted in slightly revised form from: Olmanson, L.G., Bauer, M.E. & Brezonik, P.L. (2008). A 20-year Landsat water clarity census of Minnesota's 10,000 lakes. *Remote Sensing of Environment,* 112(11), 4086–4097, with permission from Elsevier.

Belt Plains and Northern Glaciated Plains ecoregions in southern Minnesota, where agriculture is the predominant land use. Mean water clarity at the statewide level also remained stable with an average around 2.25 m from 1985 to 2005. This assessment demonstrates that satellite imagery can provide an accurate method for obtaining comprehensive spatial and temporal coverage of key water quality characteristics that can be used to detect trends at different geographic scales.

2.1 Introduction

Minnesota's numerous lakes are important recreational and aesthetic resources that add to the economic vitality and quality of life of the state. Protecting and monitoring lake water quality is a major concern for many state and local agencies and citizen groups. For effective lake management, it is essential to have long-term water quality information on a broad regional and spatial scale. Unfortunately only a small percentage of lakes in Minnesota are regularly monitored by conventional methods, and historical water quality data are sparse or lacking for most lakes. Although it is not possible to go backwards in time and collect historical water quality information using conventional field methods, Landsat images have been collected and archived regularly since the early 1970s, enabling extraction of some historical water quality information on lakes.

Landsat imagery has been used to estimate certain water quality characteristics of lakes (e.g., chlorophyll and water clarity, usually expressed in terms of Secchi depth) for over 30 years (e.g., Brown et al., 1977; Lillesand et al., 1983; Ritchie et al., 1990; Lathrop et al., 1991, 1992; Dekker and Peters 1993), but until recently such reports

largely described exploratory efforts involving only one or a few lakes and/or short observation periods. One early exception is Martin et al. (1983) who used semi-automated procedures to assess the trophic status of around 3000 lakes in Wisconsin using Landsat Multispectral Scanner (MSS) imagery. Kloiber et al. (2002a) and Olmanson et al. (2001) described a practical and efficient procedure to use Landsat Thematic Mapper (TM) and Enhanced Thematic Mapper Plus (ETM+) imagery for routine, regional-scale assessments of lakes for water clarity, and Kloiber et al. (2002b) used this approach to measure spatial patterns and temporal trends of ~500 lakes within the seven-county metropolitan area of Minneapolis-St. Paul Minnesota. Olmanson et al. (2002) expanded this work to a statewide level, reporting the first census of Minnesota lakes for water clarity. Chipman et al. (2004) have conducted census-level analyses on lakes in Wisconsin using similar procedures for over 8000 lakes.

Using these methods we now have completed a 20-year, comprehensive water clarity database for lakes larger than ~8 hectares (20 acres) in area. The database includes results for more than 10,500 lakes based on Landsat imagery at approximately five-year intervals for the time period 1985-2005 and includes almost 100,000 individual estimates of lake water clarity, which may be the largest database on lake clarity produced to date. The objectives of this paper are to describe how the lake water clarity database was assembled, assess its accuracy, and summarize initial analyses to evaluate spatial and temporal trends of lake water clarity in Minnesota over the past 20 years.

2.2 Methods

The long term goal of our Landsat work has been to develop reliable and inexpensive techniques for synoptic measurements of key indicators of lake water quality that can be used by management agencies to complement water quality data obtained by ground-based sampling programs. One of the prime management issues for inland lakes is trophic state, and of the three most common indicators of trophic state – total phosphorus (TP), chlorophyll *a* (chl *a*), and Secchi disk transparency (commonly called Secchi depth, SD) – the latter two are amenable to measurement by satellite imagery. SD is the most commonly measured trophic state indicator, and is strongly correlated with the responses in the blue and red bands of Landsat TM/ETM+ data (Kloiber et. al., 2002a). Most of our work to date has involved calibrating Landsat TM data with ground-based SD measurements and estimating $SD_{Landsat}$ for all lakes in an image from the regression equation developed in the calibration step. The results then can be mapped as distributions of $SD_{Landsat}$ in the lakes, and the estimated $SD_{Landsat}$ can be converted to a trophic state index based on transparency: $TSI(SD_{Landsat}) = 60 - 14.41 \ln(SD_{Landsat})$ (Carlson 1977).

It is important to recognize that other factors besides phytoplankton abundance (as measured by chlorophyll) may affect SD in lakes. Most important of these non-trophic-state factors are humic color and non-phytoplankton turbidity, including soil-derived clays and suspended sediment. For this reason, we report our results based on SD calibrations as satellite-estimated $SD_{Landsat}$ or $TSI(SD_{Landsat})$, which identifies the value as an index based on transparency.

2.2.1 Satellite Imagery and Lake Reference Data

We used imagery from the Landsat 4 MSS, Landsat 5 TM, and Landsat 7 ETM+. The majority of the images were from Landsat 5 TM, which has been operating over the entire period. One Landsat 4 MSS image was used in the 1985 assessment because a clear TM image was not available for path 27 in this time period. Several Landsat 7 ETM+ images were used for 2000 assessment, and some Landsat 7 ETM+ with the scan line corrector off (SLC off) were used for the 2005 assessment. We found that Landsat 7 ETM+ (SLC off) imagery worked as well for water clarity assessment as earlier (intact) ETM+ imagery because only a representative sample of pixels is needed from each lake and the missing data generally did not affect the results.

To create the database we targeted clear paths of consecutive Landsat images from a late summer index period (July 15 - September 15, with a preference for August). This period was found to be the best index period for remote sensing of water clarity in Minnesota (Stadelmann et al., 2001). There are two advantages to using images from this index period: (1) short-term variability in lake water clarity is at a seasonal minimum, and (2) most lakes have their minimum water clarity during this period. In addition, it is preferable to have images from near anniversary dates for change detection.

For water clarity assessments it is critical to use imagery without cloud cover or haze because clouds, cloud shadows, and haze affect spectral radiometric responses and cause erroneous results. Unfortunately, clear paths (five consecutive rows from the same orbital path) of imagery for all of Minnesota are rare. Figure 2.1 illustrates some typical imagery that was used for these assessments. Although these images are clear through

most of the state, path 29 has cloud cover in the middle of the imagery, and path 27 has haze in the northern portion. Therefore, we targeted the best available imagery,

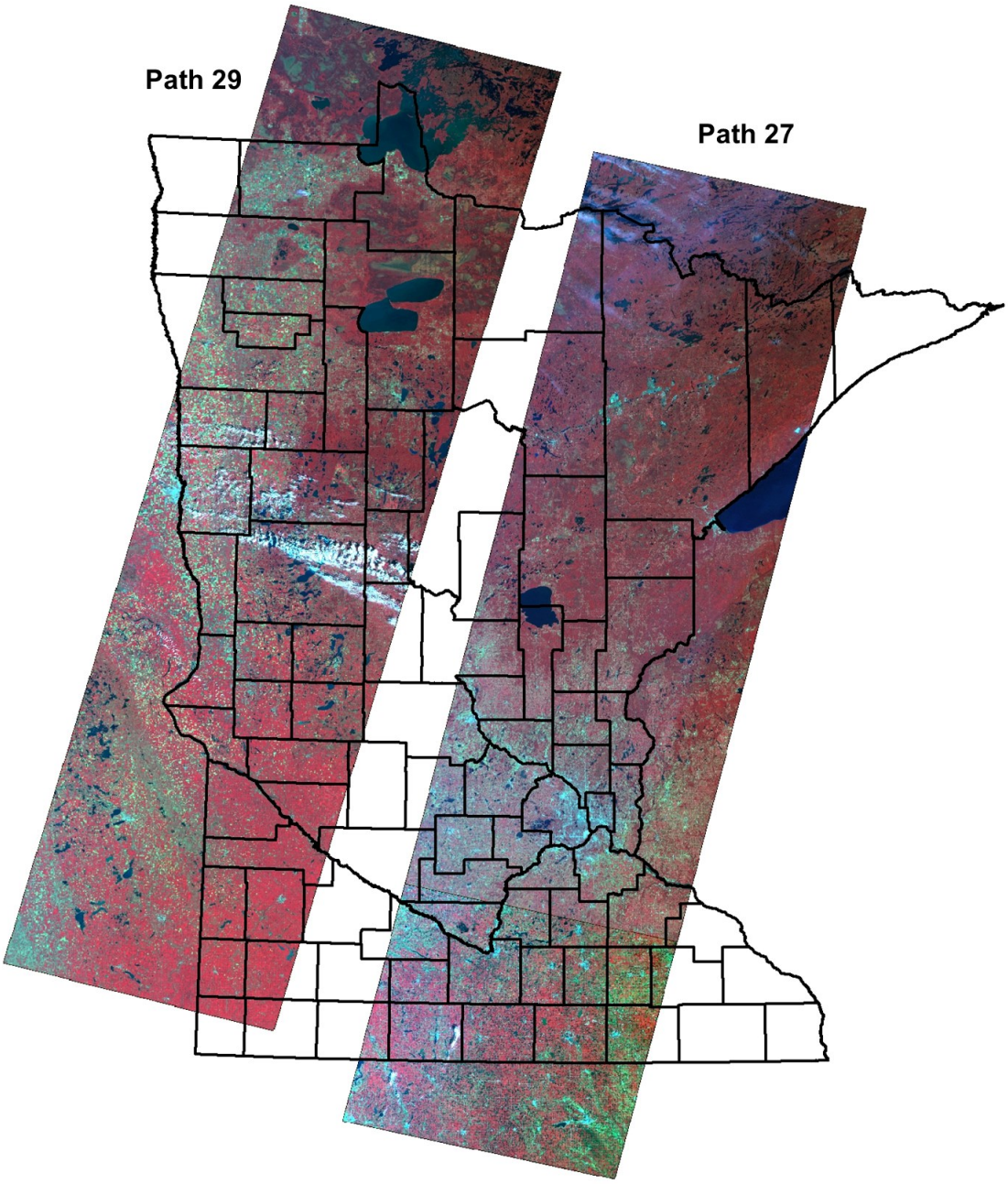

Figure 2.1 Two Landsat paths of consecutive images used to assess water clarity.

avoiding areas with clouds and haze (discussed further in section 2.2). Lakes in areas with cloud cover or haze in one image were assessed using a clear image from a different time. For each time period (nominally 1985, 1990, 1995, 2000 and 2005), 2-4 years (e.g., 2000 used imagery from 1999, 2000 and 2001) were needed to acquire clear imagery for the entire state (Table 2.1). Nonetheless, using paths of consecutive Landsat imagery with 2-5 images collected from the same path at the same time (instead of individual images) had several advantages, including decreased processing time (because several images could be processed simultaneously). The accuracy of the model also was improved because of the larger number of data points available for calibration and greater range of water clarity in calibration datasets with greater spatial coverage (Minnesota lakes tend to have lower clarity in the south and higher clarity in the north).

We acquired and processed more than 100 Landsat images from 37 dates (Table 2.1) and extracted water clarity information for more than 10,500 lakes in each time period. Because of the overlap (about 35%) of successive Landsat paths, the database includes almost 100,000 water clarity data points, with around 60% of the lakes having two or more data points for each time period. The number of times a lake was assessed in each of the time periods depended on the overlap area and number of images used in the assessment. The replicate data from adjacent paths provided useful information to evaluate the reliability of the Landsat results.

Table 2.1 Landsat image data and calibration model statistics for Minnesota water clarity database.

			Number			Estimated		Model Statistics				Number
Image Date	Path	Rows	Images	Sensor	Landsat	% Clear	Days *	N	SD Range (m)	R^2	SEE **	Lakes Assessed
8/13/1984	29	27-29	3	TM	5	75	8	17	0.9 - 5.5	0.91	0.144	3305
9/16/1984	27	26-30	5	MSS	4	95	7	70	0.4 - 7.0	0.80	0.325	4573
8/18/1985	27	29-30	2	TM	5	75	7	37	0.3 - 3.2	0.85	0.223	997
8/3/1986	29	26-28	3	TM	5	50	7	19	0.9 - 5.8	0.71	0.287	2685
8/21/1986	27	26-29	4	TM	5	75	7	105	0.3 - 7.0	0.79	0.324	4405
8/28/1986	28	26-28	3	TM	5	60	3	56	0.6 - 6.1	0.86	0.203	3646
8/30/1986	26	27	1	TM	5	85	9	22	0.9 - 7.3	0.94	0.159	1384
8/1/1987	26	29-30	2	TM	5	85	8	16	0.3 - 6.4	0.90	0.319	244
8/15/1987	28	28-29	2	TM	5	60	10	25	0.3 - 4.3	0.82	0.302	1237
8/7/1990	28	27-30	3	TM	5	85	3	211	0.15 - 9.5	0.77	0.322	4436
8/25/1990	26	29-30	2	TM	5	95	7	29	0.3 - 7.3	0.77	0.362	456
8/30/1990	29	26-29	4	TM	5	100	3	116	0.18 - 7.2	0.77	0.375	3784
8/19/1991	27	27	1	TM	5	75	7	36	0.4 - 8.4	0.88	0.279	1539
8/26/1991	28	29-30	2	TM	5	80	7	27	0.2 - 6.4	0.79	0.338	700
8/28/1991	26	27	1	TM	5	95	7	34	0.6 - 9.9	0.77	0.374	1462
9/4/1991	27	26-30	5	TM	5	85	3	169	0.15 - 9.1	0.79	0.372	4390
7/24/1994	29	28-29	2	TM	5	75	5	52	0.15 - 6.4	0.81	0.267	1534
7/29/1995	27	27-30	4	TM	5	90	3	212	0.15 - 8.2	0.83	0.297	4965
8/14/1995	27	26-28	3	TM	5	70	3	87	0.3 - 7.0	0.84	0.311	2433
8/21/1995	28	26-30	5	TM	5	100	3	278	0.15 - 8.8	0.83	0.265	5456
9/13/1995	29	26-28	3	TM	5	85	3	93	0.4 - 6.7	0.82	0.227	3310
8/25/1996	26	27-30	4	TM	5	90	10	30	0.15 - 8.2	0.86	0.406	1470
7/23/1999	28	26-30	5	ETM+	7	95	3	268	0.25 - 6.8	0.81	0.296	4773
9/11/1999	26	29-30	2	ETM+	7	100	7	21	0.3 - 6.4	0.92	0.317	487
8/10/2000	28	28	1	ETM+	7	70	3	89	0.15 - 7.0	0.89	0.249	972
9/5/2000	26	27	1	TM	5	60	7	16	0.8 - 5.5	0.96	0.141	900
9/12/2000	27	26-30	5	TM	5	95	3	227	0.15 - 14.6	0.82	0.370	4438
8/28/2001	29	26-28	3	TM	5	95	3	124	0.3 - 8.5	0.89	0.220	3768
8/13/2003	26	27	1	TM	5	50	10	21	0.5 - 7.3	0.81	0.381	1247
9/5/2003	27	26-29	4	TM	5	90	3	219	0.15 - 8.1	0.84	0.326	4569
8/5/2004	28	26-28	3	ETM+ slc off	7	50	3	139	0.3 - 8.2	0.84	0.226	2671
8/21/2004	28	26-28	3	ETM+ slc off	7	50	3	171	0.6 - 6.7	0.86	0.240	3694
9/16/2004	26	29-30	2	TM	5	100	7	13	0.3 - 5.5	0.90	0.318	425
7/30/2005	29	26-29	4	ETM+ slc off	7	95	3	141	0.6 - 8.8	0.72	0.297	3760
8/7/2005	29	26-29	4	TM	5	80	3	127	0.3 - 8.2	0.81	0.302	3415
9/1/2005	28	27-30	4	TM	5	75	3	152	0.15 - 5.8	0.85	0.297	2983
9/2/2005	27	28-30	3	ETM+ slc off	7	80	3	127	0.15 - 5.8	0.83	0.343	2450

* SD data used for calibration within No. of days of Landsat overpass

** Standard Error of Estimate

In situ SD data for image calibration is readily available for most of Minnesota because of volunteer efforts of the Citizen Lake Monitoring Program (CLMP), combined with technical resources (training and management) of the Minnesota Pollution Control Agency (MPCA). The CLMP program began in 1973 at the University of Minnesota's Limnological Research Center. Initially, fewer than 200 lakes were monitored each year, but starting in 1985 the number began to increase and reached ~1,100 in 2005. Nonetheless, only about 10% of the lakes statewide (12% in the seven-county Twin Cities metropolitan area) were monitored for water clarity in 2005. In some parts of the state the fraction monitored is much lower. CLMP-monitored lakes tend to be recreational lakes that are larger (median size of 75 ha and average size of 333 ha), than Landsat-monitored lakes (median size of 18 ha and average size of 99 ha). It also should be noted that CLMP lakes are selected by interest of volunteers and not randomly. Therefore, the data cannot be reliably extrapolated to the larger population of Minnesota lakes, and such use may result in biased and misleading conclusions (Peterson et al., 1999).

To calibrate the imagery we used water clarity data (in situ SD) usually collected within $\pm$ 3 days of the image acquisition date, but the window was increased to up to $\pm$10 days in cases where data were sparse. Kloiber et al., 2002a found that ground observations within one day of the satellite yielded the best calibrations, but the larger number of ground observations with the longer time window offsets some of the loss of correlation. Chipman et al., 2004 had similar findings and determined that model parameter values did not change significantly with a wider time window. We found that

for images where in situ data were sparse the larger number of ground observations with longer time window improved the calibration of the imagery. For example, for comparisons of models using in situ data acquired within ±1 and ± 7 days of an August 25, 1996 TM image, the number of ground observations increased from 12 to 26 with the longer time window and R^2 values increased from 0.85 to 0.88, and the standard error of estimate (SEE) decreased from 0.444 to 0.375. We conclude that measurements taken within a few days (±3 to 10 days) of image acquisition provide strong relationships. This is because water clarity (Secchi depth) usually does not exhibit large and rapid fluctuations in a given lake during the relatively stable late summer index period (although there are strong seasonal patterns in clarity) (Stadelmann et al., 2001). For a few images where data were too sparse (less than 15 data points) or not well distributed throughout the range of typical water clarity conditions, supplemental data were acquired from water clarity measurements extracted from the overlap area of adjacent Landsat images (see Olmanson et al., 2002 for more information on this method). The number of SD measurements available for calibration ranged from 13-16 in the Arrowhead and Driftless areas in the northeast and southeast, respectively, to 278 through the middle of the state in Landsat path 28. The average number of measurements used for image calibration was 97. The calibration data generally had a wide range of SD values (Table 2.1).

Field-collected SD data from the CLMP program also were used to validate the accuracy of Landsat water clarity database (discussed in section 2.3). The average water clarity for each field data collection point and each lake polygon (that had field data)

were calculated from late summer (July 15 through September 15) CLMP SD data for each of the time periods.

2.2.2 Image Preprocessing and Classification

The image classification procedures used for this paper are documented by Olmanson et al. (2001), and the rationale for the procedures was described by Kloiber et al. (2002a). Some modifications were made as appropriate when experience and advances in software and computer hardware enabled simpler or improved image processing procedures. We used Leica Geosystems ERDAS Imagine and Esri ArcGIS for image processing. Acquiring a representative sample from the image for each lake was a primary objective, and image samples generally were near the center of a lake, where reflectance from aquatic vegetation, the shoreline, or the lake bottom did not affect the spectral radiometric response.

Initial preprocessing included image rectification using road intersections from a Minnesota Department of Transportation highway GIS data layer as ground control points (GCPs). We used ~40 well distributed GCPs, with a positional accuracy (RMSE) on the order of ±0.25 pixels, or 7.5 m. The next step, if necessary, was to combine consecutive images from the same orbital path and date into one uniform image. We clipped areas covered with clouds from this image and checked for haze by visually inspecting the image using the (RGB) band combination 1,6,6 (TM 1 (Blue), TM 6 (Thermal), TM 6 (Thermal)). Figure 2.2 illustrates a Landsat TM image using the (RGB) band combination 4,2,1 typically used to highlight green vegetation and (RGB) band combination 1,6,6 used to highlight haze as a red color. Areas with high levels of haze

were clipped. Because each image (path) was calibrated individually with field data, we did not perform atmospheric correction or normalization of the image brightness data.

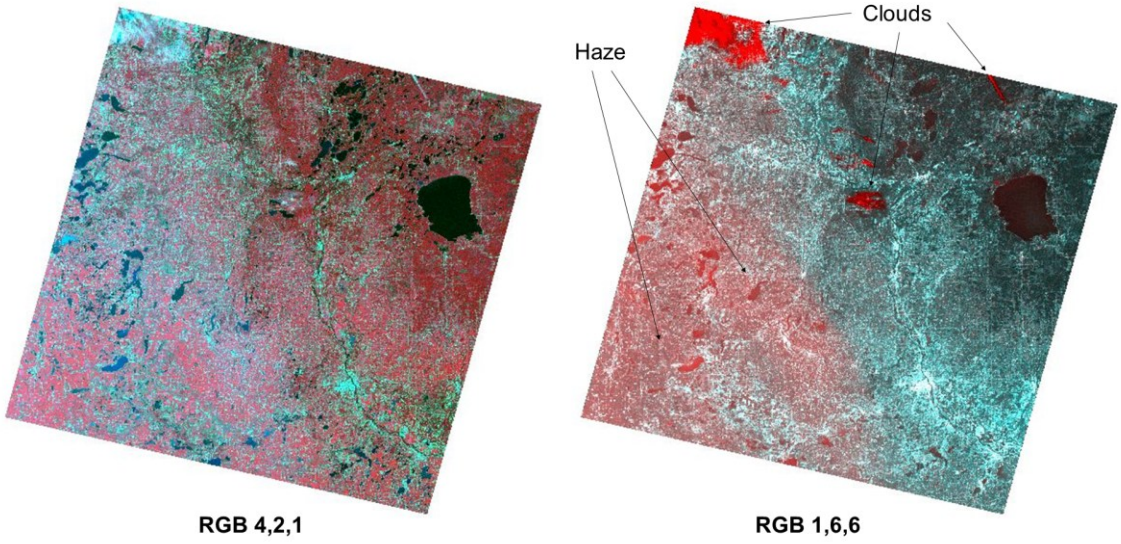

Figure 2.2 Examples of Landsat TM band combinations 4,2,1 (RGB) typically used to highlight green vegetation and 1,6,6 which can be used highlight haze and cloud cover (Path 28/Row 28, August 8, 2000)**.**

Once image preprocessing was complete, a "water-only" image was produced by performing an unsupervised classification method based on ISODATA clustering. Because water features have different spectral characteristics from terrestrial features, water pixels were grouped into one or more distinct classes that could be easily identified. We then masked out terrestrial features to create a water-only image, performed an unsupervised classification on this image, and generated spectral signatures of each class. We used these signatures, along with the location where the pixels occur, to differentiate classes containing open water and shallow water (where sediment and/or macrophytes affect spectral response). These areas tend to have high spatial variability

compared to open-water portions of the lake. Based on this analysis, we removed the affected pixels. Next, the spectral radiometric data from the "open-water" image were obtained to develop relationships with measured SD. For these assessments, we used a lake polygon layer (Olmanson et al., 2001) to help automate the process. The polygon layer used for this purpose has 12,049 polygons delineating lakes or lake basins. Lakes with multiple basins were split into separate polygons. The polygon layer was constructed to include all Minnesota lakes and open water wetlands eight ha and larger. We used the signature editor in ERDAS Imagine to extract spectral data from the image for all lakes in the image.

Using log-transformed SD data as the dependent variable and TM band 1 and the TM1:TM3 ratio as independent variables, we performed least-squares multiple regression using the general form:

$$\ln(SD) = a(TM1/TM3) + b(TM1) + c$$

where a, b and c are coefficients fit to the calibration data by the regression analysis, ln(SD) is the natural logarithm of Secchi depth for a given lake, and TM1 and TM3 are the Landsat brightness values for the selected lake pixels in the blue and red bands, respectively. Kloiber et al., 2002a found that this band combination was a dependable predictor of SD.

The model developed for each path of Landsat images was applied to brightness values (digital numbers) for the sample of pixels from each lake to calculate water clarity ($SD_{Landsat}$). The number of lakes assessed per image (path of consecutive images from same date) ranged from 244 to 4,965 with an average of 2,675 lakes. To create maps the

computed $SD_{Landsat}$ data were linked to the lake polygon layer. The lake-level polygon method has an advantage over pixel-level maps because by generating a single clarity value for each lake the data can be easily included in a water clarity database and used in other analyses. The final image processing step was to edit the maps to remove lakes with faulty results due to such conditions as haze, small clouds, or cloud shadows that were not clipped. This was accomplished using the RGB 1,6,6 band combination to highlight areas with haze which was used to target problem areas.

2.2.3 Water Clarity Database Development

To create the water clarity database the final classifications for each path of Landsat imagery were combined and minimum, maximum and mean water clarity values were calculated for each lake in each time period. The number of lakes assessed for each time period ranged from 10,516 in ~2000 to ~11,241 in ~2005. Because the image processing procedure targeted clear imagery and open water areas, some lakes were not assessed in a given time period. The main reason for some lakes not being assessed was pervasive presence of aquatic vegetation in wetlands and shallow lakes resulting in insufficient unaffected pixels for accurate water clarity assessment. Other reasons included severe phytoplankton blooms (floating mats of phytoplankton were masked off since their spectral characteristics are more similar to green vegetation than water), and clouds or haze.

2.3 Results and Discussion

2.3.1 Evaluation of Landsat Estimates of Lake Clarity

Production of the five semi-decadal lake clarity assessments required 109 Landsat images from 37 dates. Models developed for each path of imagery from the same date showed strong relationships between ground-based water clarity data (SD from the CLMP) and spectral-radiometric responses of the Landsat data. The SD range, R^2, SEE and the number of lakes for each model are listed in Table 2.1. R^2 values for the regression relationships to establish the coefficients of the model equations ranged from 0.71 to 0.96 (average of 0.83) and SEE ranged from 0.141 to 0.406 (average 0.292). Given that ground-based measurements of SD are themselves subject to some imprecision, we consider these relationships to be very good. Similar strong relationships also were found by Kloiber et al. (2002b) and Chipman et al. (2004). In contrast, Nelson et al. (2003) reported low r^2 values (0.43) that they attributed to the distribution of SD values in their calibration dataset. Our study and Chipman et al. (2004) obtained strong relationships for images over a wide range of SD values some of which would be similar to those used in Nelson et al. (2003). Cloud cover was present in much of the imagery used by Nelson et al. (2003) and this likely affected the spectral-radiometric responses.

To evaluate the comparability of the different sensors and images from the different dates used to create the water clarity database we examined lake water clarity data from the overlap areas of adjacent Landsat images. First, we examined how well water clarity results from a September 1, 2005 Landsat 5 TM image compare with results from a September 2, 2005 Landsat 7 (SLC-off) image. Because the images were within

one day of each other we assumed that water clarity conditions would be very similar for both images and the water clarity assessments would be highly correlated; this was the case. Figure 2.3 shows the overlap area of the images and a scatter plot with regression line of the Landsat-inferred TSI($SD_{Landsat}$) values for the overlap area of each image. The two images were calibrated separately, but because of the geographic overlap and closely spaced image acquisition dates, some calibration data from the overlap area were used to calibrate both images. The calibration fits were similar for the two images ($R^2 = 0.85$ for September 1 and $R^2 = 0.83$ for September 2), but the model coefficients (especially 'a') were rather different. Nonetheless, agreement between the two sets of Landsat-inferred TSI($SD_{Landsat}$) values is very strong ($r^2 = 0.94$), and the results parallel the 1:1 line, indicating that water clarity results from the two sensors and dates are highly comparable.

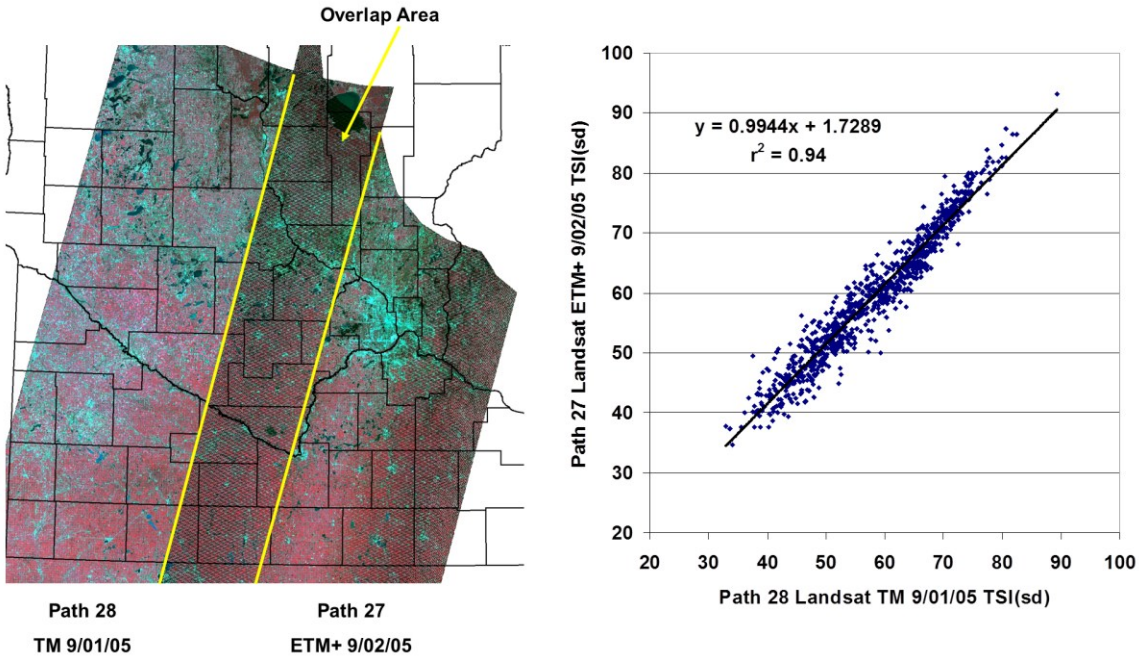

Figure 2.3 Water clarity assessment comparison for Landsat TM vs. ETM+ SLC-off data for 925 lakes in the overlap area of paths 27 and 28.

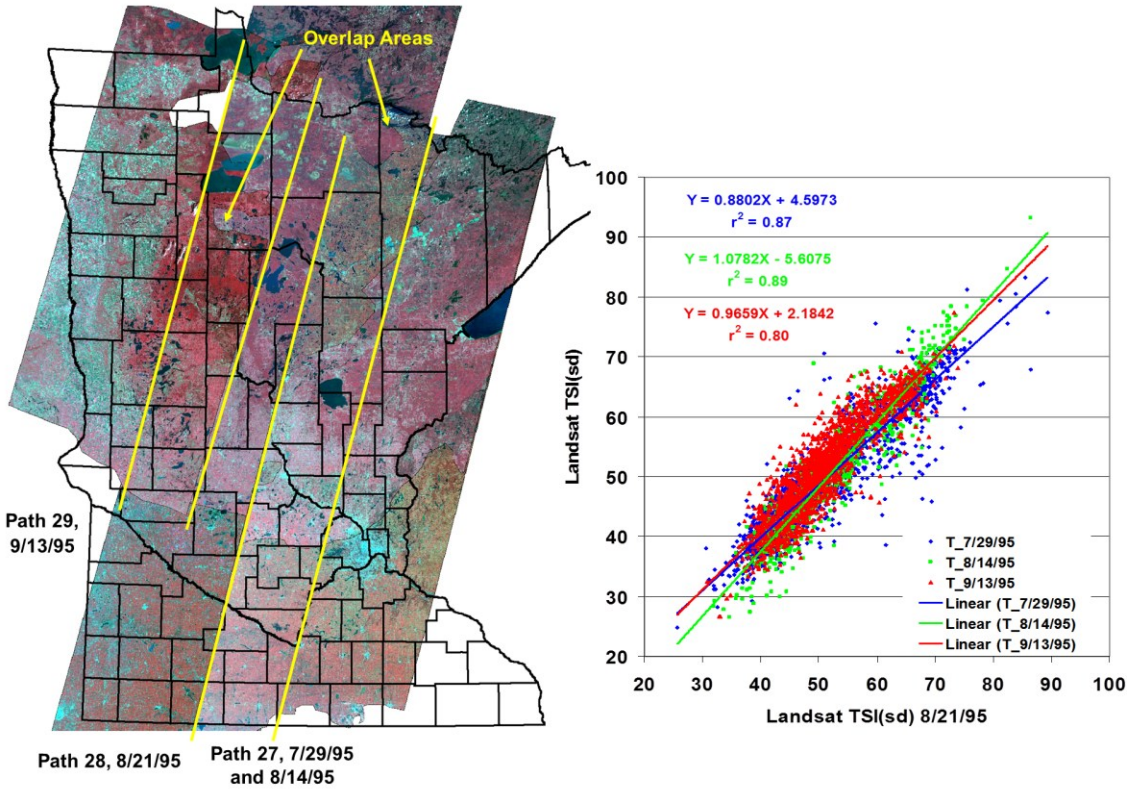

Figure 2.4 Water clarity assessment comparison in the overlap areas of paths 27-29 for 1995 Landsat images.

To evaluate the variability in $SD_{Landsat}$ results over the range of the late summer index period, we examined the overlap areas of three late summer 1995 Landsat TM images (path 27, July 29, Path 27, August 14 and path 29, September 13) with an August 21 path 28 Landsat TM image (Fig. 2.4). Although the relationships are not as strong as those for images acquired within one day, they are still strong with r^2 values of 0.87, 0.89 and 0.80. The range of image dates (July 29-September 13) covers most of the late summer index period (July 15-September 15). The August 14 image is closest in time to the August 21 image, and regression line for the two sets of results is close to parallel with the 1:1 line indicating similar water clarity conditions. The regression line for the

July 29 image is slightly skewed toward higher water clarity in the eutrophic lakes, which may reflect seasonal differences in the early portion of the late summer window. The regression line for the September 13 image is also close to parallel with the 1:1 line indicating a similar distribution of water clarity conditions.

The results in Fig. 2.4 suggest that restricting satellite-based lake clarity assessments to the late summer index window limits, but does not eliminate minor seasonal differences. A further narrowing of the window (e.g., to August images only), might further decrease uncertainties caused by seasonal variations, but considering the frequency of cloud cover in Minnesota (Kloiber et al., 2002a) and that the current eight-day overpass cycle of Landsats 5 and 7 is not sustainable (both Landsat 5 and 7 have exceeded their expected life), this option does not appear to be practical. Considering the availability of other measures for most lakes are sparse and subject to some errors, we regard the accuracy of Landsat water clarity assessment using a two-month late summer index period to be acceptable, especially since this method allows all lakes to be assessed in a uniform way.

The overall objective of this study was to create a comprehensive statewide water clarity database that represents water clarity conditions in five semi-decadal time periods. Therefore, it is important to assess how well the Landsat water clarity database, which consists of the average Landsat water clarity value calculated for each lake polygon (see section 2.2.3), relates to field-measured water clarity data, which is the average late-summer CLMP SD data (see section 2.2.1), for each time period. Regression analyses were conducted with Landsat-derived $TSI(SD_{Landsat})$ as the dependent variable and

average field-measured late-summer TSI(SD) as the independent variable for each time period and for a combined data set containing 6,216 field observations. The r^2 values for the five time periods range from 0.77 to 0.80 (Fig. 2.5), and $r^2 = 0.78$ for the combined dataset (Fig. 2.6), indicating a consistently strong relationship between Landsat-derived and field-measured late-summer SD. However, because small percentages (4.1-8.1%) of the CLMP SD data used to calculate the average late-summer CLMP SD also were used for image calibrations and could bias validation of the relationship, an independent subset was created. The independent subset was the average late-summer CLMP SD data for lakes not used to calibrate any of the images in each time period. Values of r^2 from regression analyses for the independent subset were slightly lower than the full dataset for each time period and range from 0.74 to 0.79 with an average of 0.76, which still represents a consistently strong relationship between Landsat-derived and field-measured late-summer SD. This is especially true considering that some of the reduction in r^2 may be due to data year disparity, since each time period consists of multiple years of data (see section 2.2.1) and removal of the calibration lakes left data from years without imagery to validate the water clarity of a lake. The regression lines closely match the 1:1 line for each time period and for the combined dataset indicating the Landsat-derived and field-measured SD results are comparable. Thus, Landsat images from the late-summer index period provide a reliable estimate of SD for the date of the imagery and the combined database provides a reasonable estimate of late summer water clarity for each time period.

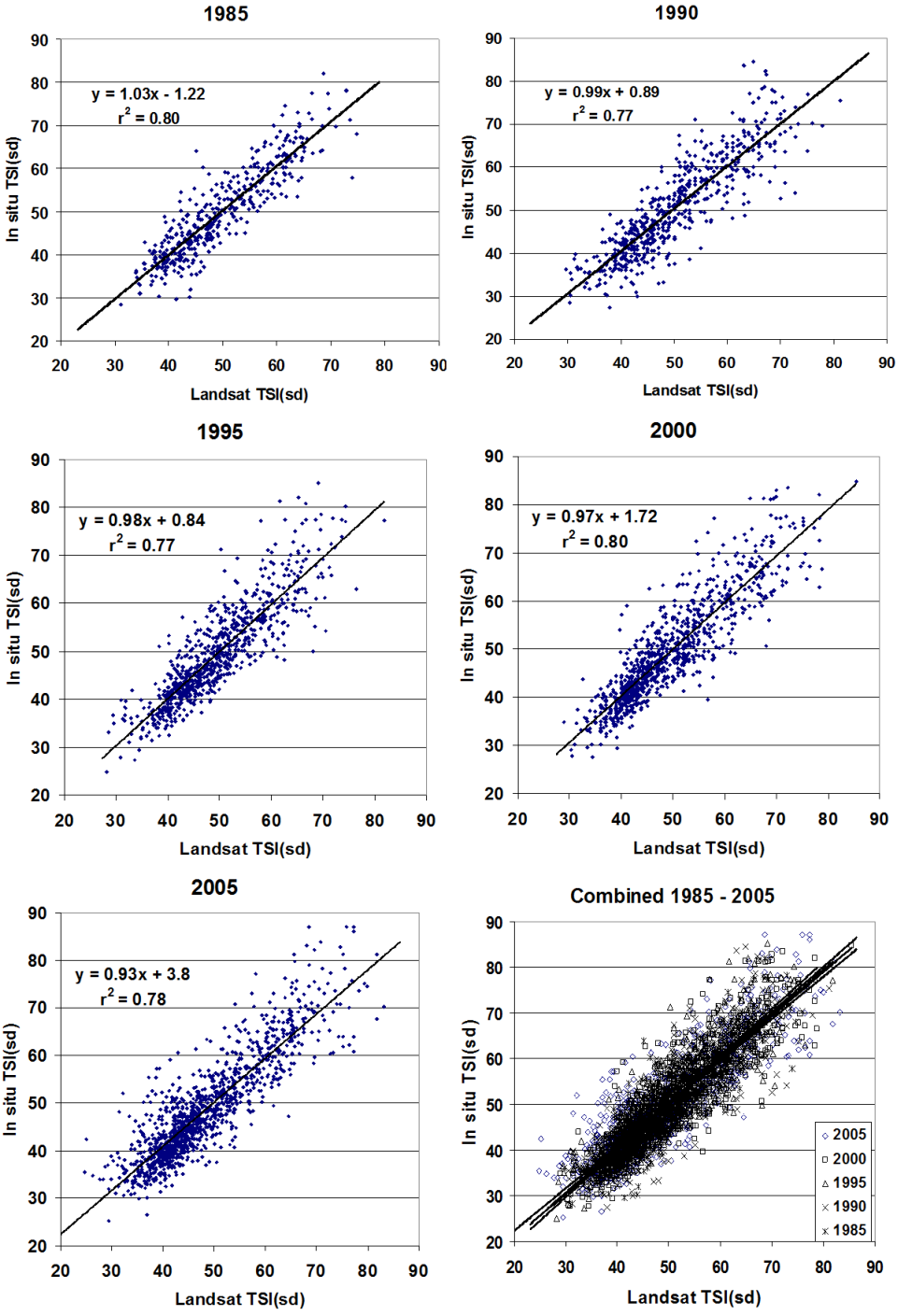

Figure 2.5 Scatter plots of Landsat TSI(sd) vs. In situ late summer lake polygon mean TSI(sd) for each time period.

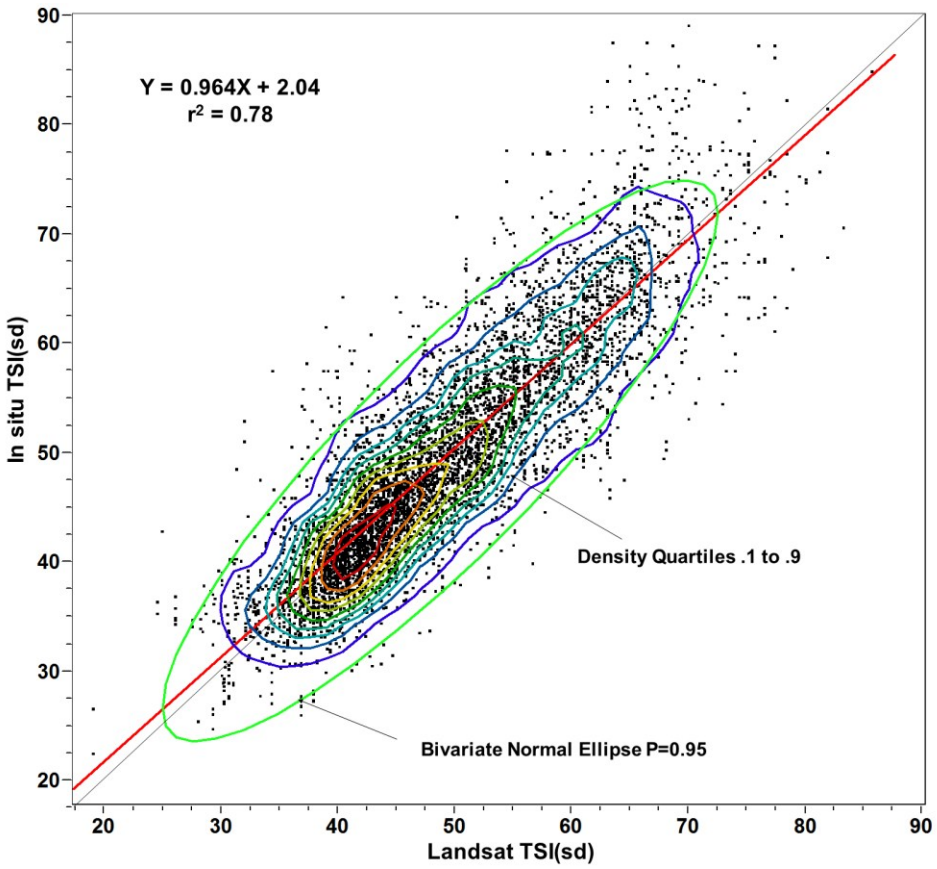

Figure 2.6 Scatter plot of Landsat TSI(sd) vs. In situ late summer mean TSI(sd) for 6216 lake points.

However, there is some lack of agreement for lakes with low water clarity (SD < 0.25 m or TSI > 80), for which Landsat $SD_{Landsat}$ values generally were larger than field-measured values. This may reflect issues related to spatial variability of water clarity. Surface blooms of phytoplankton in eutrophic lakes are subject to concentration or dispersal by wind, which may result in variable concentrations of phytoplankton and SD across a lake (Dekker et al., 2002). The procedure used to extract brightness data from Landsat images targeted the deepest and most central part of the lakes, which also may

have the highest water clarity and may account for the differences from the field measurements for low clarity lakes.

2.3.2 Spatial and Temporal Analyses

Having evaluated the accuracy of the water clarity database and determined that we have a reasonable estimate of water clarity for the entire population of lakes in Minnesota for five semi-decadal time periods from 1985 to 2005, we can investigate spatial patterns and temporal trends of water clarity in Minnesota. To do that we analyzed spatial and temporal distributions of water clarity at the statewide, ecoregion and individual lake scales.

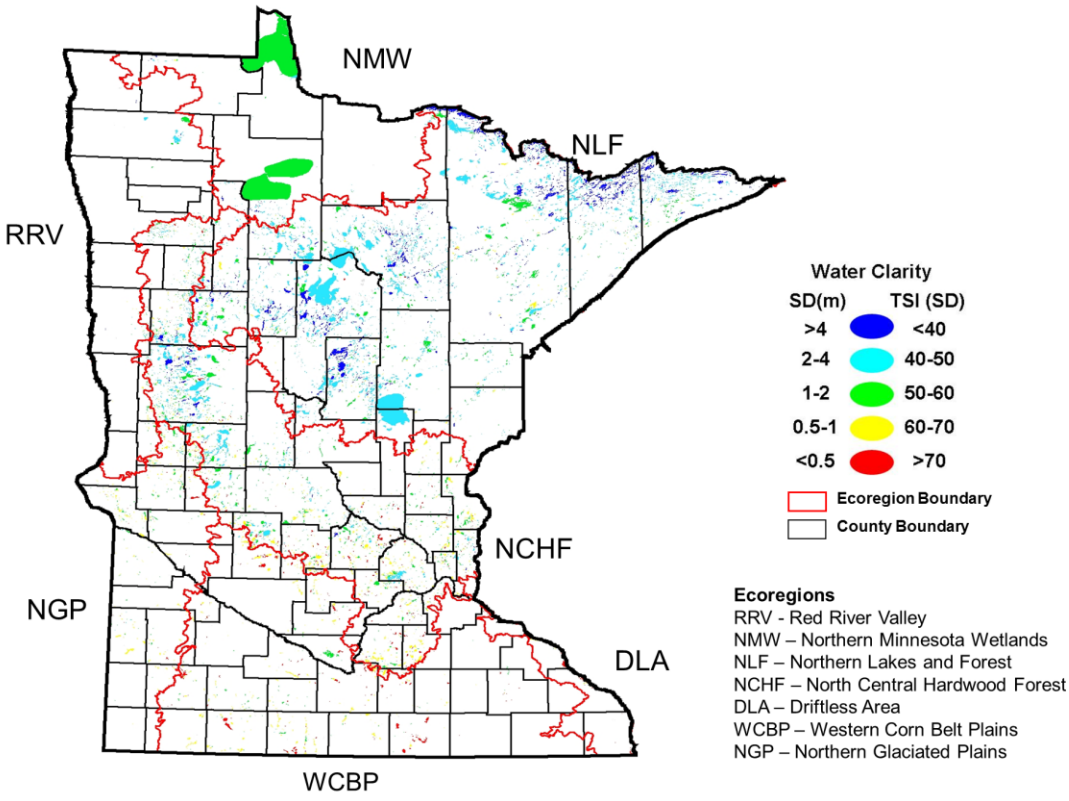

Figure 2.7 Minnesota 2005 lake clarity with county and ecoregion boundaries.

Water clarity in Minnesota tends to be low in the south and southwest and higher in the north and northeast (Fig. 2.7). At the statewide level water clarity has remained stable between 1985 and 2005 (Fig. 2.8) with mean water clarity of 2.25 m. One interesting discovery from the data is that many of the clearest lakes are abandoned iron ore mine pits that have filled with water. The increase in lakes with water clarity around 15 m in the 2005 time period (Fig. 2.8) needs further investigation, but could be due to changes in some mine operations.

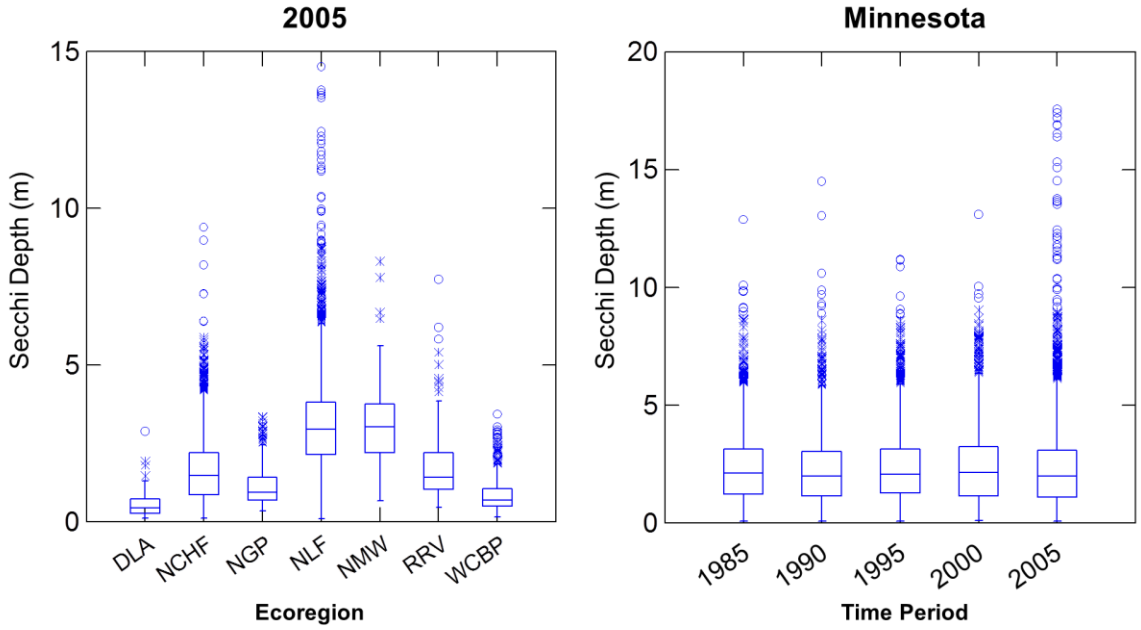

Figure 2.8 Boxplots of 2005 Minnesota lake clarity by ecoregion and statewide for 1985 - 2005.

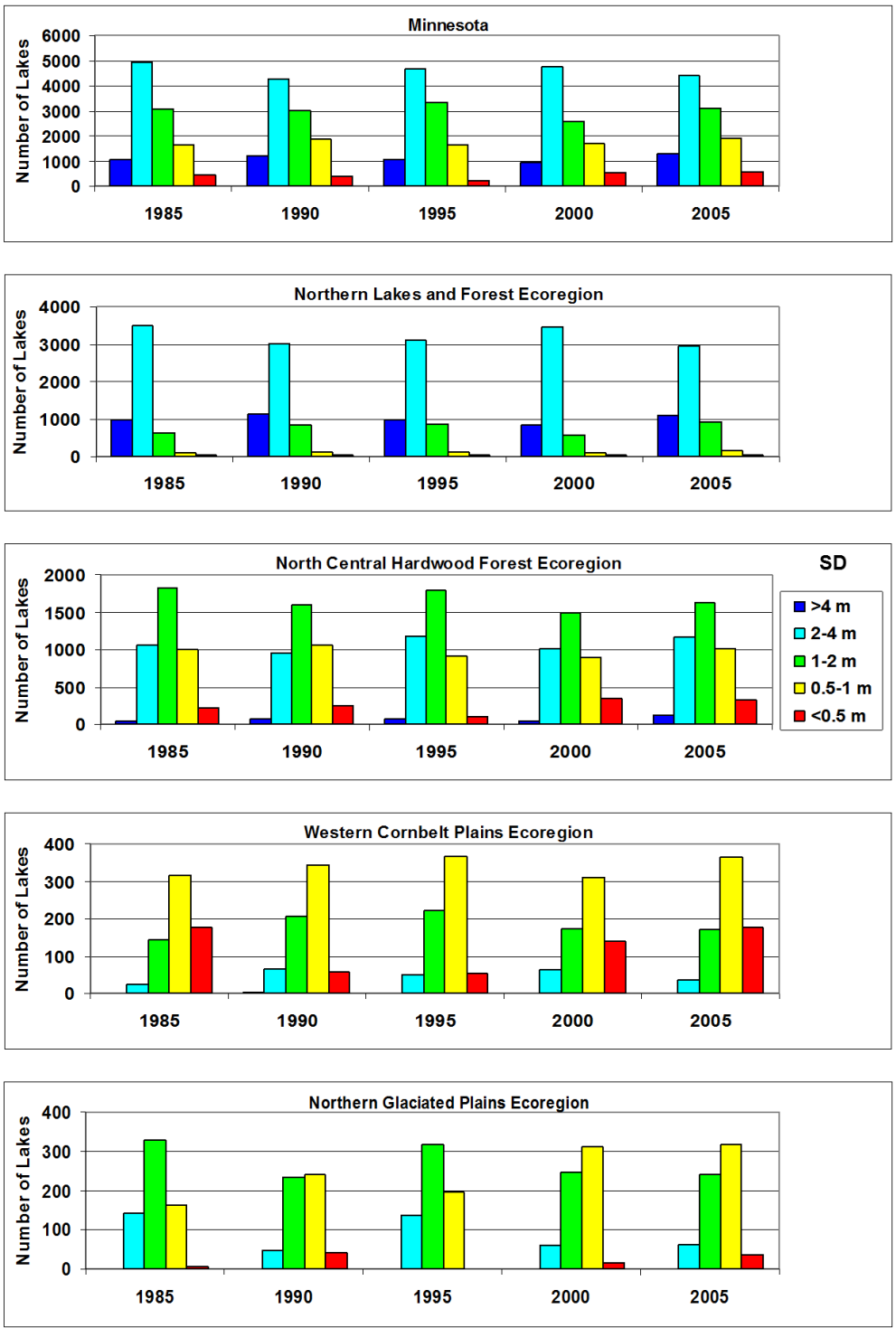

Figure 2.9 Lake clarity distribution statewide and by ecoregion.

Ecoregions. Lakes in Minnesota span seven natural ecoregions which differ in vegetation, soils, geology, climate, hydrology, and land use. We used the EPA Level III Ecoregions of Minnesota for analysis (Minnesota Land Management Information Center, 2006). That the distribution of water clarity differs among the ecoregions is apparent from the boxplots for 2005 in Fig. 2.8. Water clarity distributions at the statewide level and for the four ecoregions that include most (96%) of Minnesota's lakes are shown in Fig. 2.9. The Northern Lakes and Forest Ecoregion (NLF), which has 46% of the state's lakes, has results concentrated in the higher water clarity classes and an average $SD_{Landsat}$ of 3.09 m. The North Central Hardwood Forests Ecoregion (NCHF), which has 38% of the state's lakes, has a wide range of water clarity and an average $SD_{Landsat}$ of 1.58 m. Lakes in the Western Corn Belt Plaines Ecoregion (WCBP), which has 7% of the state's lakes, generally have lower water clarity (average $SD_{Landsat}$ of 0.95 m). The Northern Glaciated Plains Ecoregion, with 6% of the lakes, also has low water clarity (average of 1.27 m).

Over the 1985-2005 period, average water clarity remained relatively stable in lakes of the NLF and NCHF ecoregions but declined slightly in the WCBP, where the highest average clarity (1.07 m) occurred in 1990 and the lowest (0.85 m) occurred in 2005. There also appears to be a trend of declining water clarity in the NGP ecoregion where the highest average water clarity (1.50 m) occurred in 1985 and the lowest (1.12 m) in 2005.

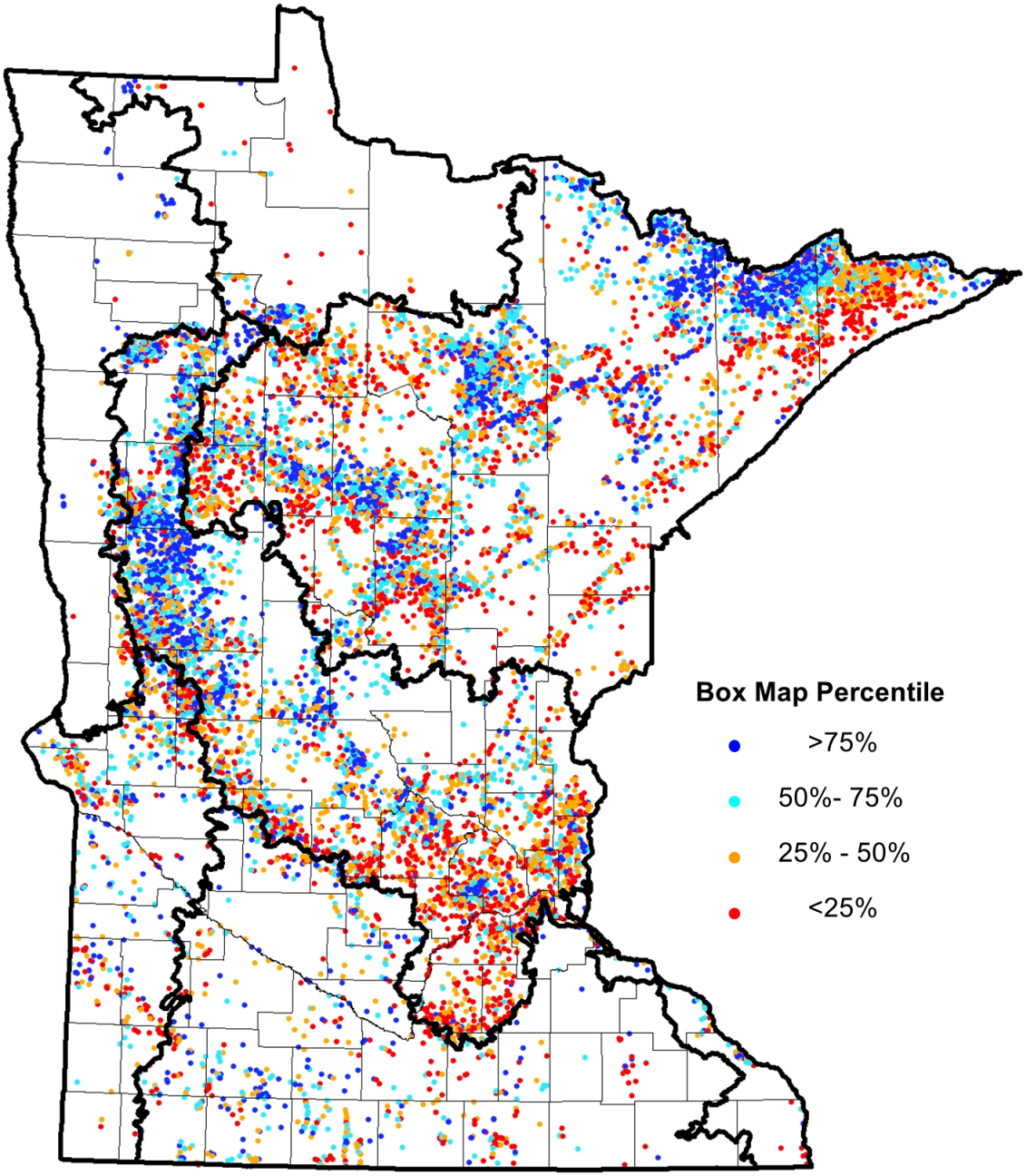

Figure 2.10 Minnesota lake clarity 2005 quartile distribution within each ecoregion.

Individual Lakes. Water clarity is a good indicator of user perception of water quality in lakes (Heiskary et al., 1988) and usually reflects the amount of phytoplankton

or sediment present. Although lakes in Minnesota generally are more eutrophic (and less clear) in the south and less eutrophic (and clearer) in the north, at the regional and sub-regional levels conditions are quite variable. Fig. 2.10 shows the quartile distribution of water clarity within each ecoregion. While there is some clustering of lakes within higher and lower water clarity quartiles, lakes from the opposite quartiles are distributed throughout the ecoregions and state. The range of water clarity conditions throughout the state and even within ecoregions thus in most cases is large. The wide range of water clarity likely reflects both natural characteristics (e.g., depth, area and watershed) and effects of anthropogenic characteristics (i.e., land use and management practices).

Comparison with other states. The above results contrast to the findings by Peckham and Lillesand (2006) who analyzed Landsat-estimated water clarity for 2,467 Wisconsin lakes and found increasing water clarity in Wisconsin lakes at the statewide level and in some ecoregions. At the statewide level they reported a significant increase in mean water clarity of 0.75 m from 1980 to 2000. The NLF ecoregion in Wisconsin had a mean water clarity increase of 0.81m, and the NCHF ecoregion had an increase of 0.80 m.

Our results indicate that water clarity has been stable statewide in Minnesota and also within the NLF and NCHF ecoregions. It is not certain why there should be differences between the Minnesota and Wisconsin assessments, but different assessment designs could be a contributing factor. The methods we used are similar to the methods Peckham and Lillesand (2006) used for their 1990 and 2000 water clarity assessments, but their 1980 assessment was conducted using different methods and Landsat MSS

imagery. It is uncertain whether the MSS assessment is entirely consistent with later TM-based assessments. Other differences between the two studies include the time frames of analysis – ten-year intervals (1980 to 2000) in Wisconsin versus five-year intervals (1985 to 2005) in Minnesota, and the lakes assessed for temporal trends in Wisconsin were limited to those assessed in the MSS study (around 30% of the lakes in the later assessments).

2.4 Conclusions

For effective environmental management, it is essential to have accurate long-term water quality information on a broad regional and spatial scale. Development and evaluation of a Minnesota statewide 20-year water clarity census of over 10,500 lakes has demonstrated that satellite imagery can provide an accurate method to obtain comprehensive spatial and temporal coverage of a key water quality characteristic. Although traditional monitoring programs are important, they largely rely on volunteers or agencies that target lakes of interest (i.e., are not randomly selected). Using data from such programs to extrapolate to larger regional assessments likely will lead to biased conclusions. However, by using the data from these programs to calibrate Landsat imagery, the entire population can be reliably assessed.

The Landsat water clarity database is being used in several research efforts where available field data were sparse. For example, Lindon et al. (2005) used it to target lakes in Cass and Crow Wing Counties that were large (>200 hectares), lacked water quality data and were more eutrophic than typical for the area for additional monitoring. It was

used in west central Minnesota for nutrient criteria research to target shallow lakes that represented a range of trophic status but lacked data (Heiskary, 2005). The database was also used by Baker et al. (2004) to correlate water clarity to common loon populations. The comprehensive water clarity database can also be used in conjunction with morphometric, land-use and demographic data to analyze spatial patterns and temporal trends in lake clarity throughout the state and develop better understanding of the factors that affect these patterns and trends. Results of such analyses will aid local and state agencies in making informed decisions about development policy and improve the management of lake resources.

This study also demonstrates the significance of the Landsat program of continuous collection and archiving of moderate resolution imagery as a historical record of an important water quality variable. The current state of the Landsat program is unfortunate with Landsat 5 imaging operations currently suspended, Landsat 7 operating (SLC off) past its expected life time and no replacement is expected for another year, which could result in a data gap. However, with recent technological advances, there also is great potential for an enhanced Landsat system that could improve monitoring of water resources. A new system with higher frequency of image acquisition, improved spectral bands, and improved atmospheric correction and radiometric calibration capabilities could enable the development of a universal equation that could minimize the need for calibration with field data. Even if these advances do not happen, there already is a massive 40-year archive of Landsat imagery available for regional assessments of water clarity.

Although assessment of water clarity is important, it is also important to make the results easily available to lake managers, government agencies and the public. The availability of such information is essential for a well-informed public and a prerequisite for effective environmental management. To make the data available we have created "LakeBrowser," a MapServer application, at http://water.umn.edu/, where data for individual lakes, counties, and ecoregions can be accessed.

Chapter 3

Geospatial and Temporal Analysis of a 20-year Landsat Water Clarity Census of Minnesota's 10,000 Lakes

A large 20-year database on water clarity for all Minnesota lakes ≥ 8 ha (20 ac) was analyzed statistically for geospatial distributions and temporal trends. The database includes statewide water clarity estimates (expressed in terms of Secchi depth) for more than 10,500 lakes using Landsat imagery for time periods centered around 1985, 1990, 1995, 2000 and 2005. Water in Minnesota lakes is less clear (more turbid) in the south and southwest and clearer in the north and northeast. This pattern is evident at the levels of individual lakes and ecoregions. Temporal trends in water clarity were detected in ~11percent of Minnesota's lakes: 4.6% had improving clarity and 6.2% had decreasing clarity. Ecoregions in southern and western Minnesota, where agriculture is the predominant land use, had a higher percentage of lakes with decreasing clarity than the rest of the state, and small and shallow lakes had a higher percentage of decreasing clarity trends than large and deep lakes. The mean water clarity statewide remained stable from 1985 to 2005; however, decreasing water clarity trends were detected in ecoregions dominated by agricultural land use. Deep lakes had higher clarity than shallow lakes for all lakes and also for lakes grouped by land cover. Lakes with lower watershed to lake area ratios had higher water clarity than lakes with higher ratios. Water clarity decreased as the percentage of agriculture and/or urban area increased at the ecoregion, county,

minor watershed and catchment levels. This pattern also held when lakes were grouped by depth classes.

3.1 Introduction

The state of Minnesota, U.S.A. the "Land of 10,000 Lakes," has approximately 12,000 lakes that are four hectares (ha) or larger in area. They vary greatly at local, regional and statewide scales by size, depth, ecology, and water quality. The wide diversity of lakes allows for many recreational and tourism opportunities but makes their management challenging.

In addition to natural variations in landscapes that affect watershed hydrology, urban and agricultural land cover in a watershed affects the spatial and temporal patterns of runoff and significantly affects lake water quality. Numerous studies have identified patterns and evaluated the effects of land use characteristics on water quality. These studies typically have been conducted on lake or stream watersheds and measured or modeled the effects of land uses (e.g., Tong and Chen, 2002) or land use change (e.g., Choi et al., 2003; Mattikalli and Richards, 1996; Wilson and Weng, 2009) on water quality. Other studies conducted at local to regional scales have compared lake conditions and land use in different watersheds and linked land use with water quality differences (e.g., Gove et al., 2001). Heiskary and Wilson (1989) used the ecoregion framework of Omernik et al. (1987), which recognizes distinct regional patterns of geology, vegetation, hydrology and land use, to characterize water quality differences in four of Minnesota's ecoregions. These findings were used to help define reasonable water quality goals for

each ecoregion, and they led to the development of lake water quality standards in Minnesota. The water quality data used to define these standards were selected largely on the basis of interest of volunteers or local or state agencies and thus targeted recreational lakes that tend to be larger than average; i.e., the lakes were not randomly selected (Chapter 2 (Olmanson et al., 2008)). Therefore, biases may occur when these data are extrapolated to the larger population of Minnesota lakes (Peterson et al., 1999; Soranno et al., 2011; Wagner et al., 2008).

Landsat imagery has proven to be a cost-effective source to assemble comprehensive information for regional lake assessments (e.g., Kloiber et al., 2002), and we used it to develop a water clarity database for all lakes in the state ≥ 8 ha (20 ac) in area over a 20-year timeframe. The database, which was documented by Chapter 2 (Olmanson et al., 2008), includes water clarity measurements on more than 10,500 lakes for time periods centered around 1985, 1990, 1995, 2000 and 2005.

This paper describes the results of statistical analyses of the database for geospatial and temporal trends of water clarity over the 20-year period, as well as trends related to land cover/use and lake morphometry. To conduct the analyses we grouped the lakes by general physical and chemical characteristics, such as area, depth and alkalinity, and linked their water clarity values to land cover variables at the ecoregion, county, minor watershed and catchment levels.

3.2 Methods

3.2.1 Landsat Water Clarity Data

The water clarity database was developed using over 100 Landsat images from the Landsat 4 Multispectral Scanner (MSS), Landsat 5 Thematic Mapper (TM), and Landsat 7 Enhanced Thematic Mapper plus (ETM+). The database includes statewide assessments of over 10,500 lakes for five time periods centered around 1985, 1990, 1995, 2000 and 2005; its development and accuracy were described by Chapter 2 (Olmanson et al., 2008), and the data can be accessed at water.umn.edu. Because clear images for the late summer index period were not available over the entire state in most years, the nominal time periods generally include results from multiple years (e.g., 1994, 1995 and 1996 for the "1995" time period). The database is in a geographic information system (GIS) format that can be used to create maps (Figure 3.1) and conduct statistical analysis and summaries at different geographic delineations (Table 3.1).

3.2.2 Land Cover Data

Land cover data used for this project are from an online map (http://land.umn.edu) for the state of Minnesota for the year 2000 derived by multitemporal, multispectral supervised image classification of satellite imagery acquired by the Landsat TM and Landsat ETM+ satellites. The map has seven land cover classes: urban, agriculture, grassland, forest, water, wetland and shrubland, and is a product of NASA-sponsored "eforest" research project of the University of Minnesota Remote Sensing and Geospatial Analysis Laboratory. The land cover classification scheme was modeled after the Upper

Midwest Gap Analysis Program Image Processing Protocol (Lillesand et al., 1998). This scheme identifies the land cover types of the Upper Midwest, is compatible with existing national systems, and provides a realistic classification hierarchy for the Landsat TM and ETM+ sensors. Furthermore, these classes are consistent with earlier classifications, thus allowing year-to-year comparisons. In addition, impervious surface area of the urban/developed class was mapped as a continuous variable from 0 to 100 percent. The overall accuracy of the statewide land cover map was 88 percent and the agreement r^2 between estimated and measured percent impervious surface area was 0.86 with standard error 11.7. For further information and access to the data see http://land.umn.edu/.

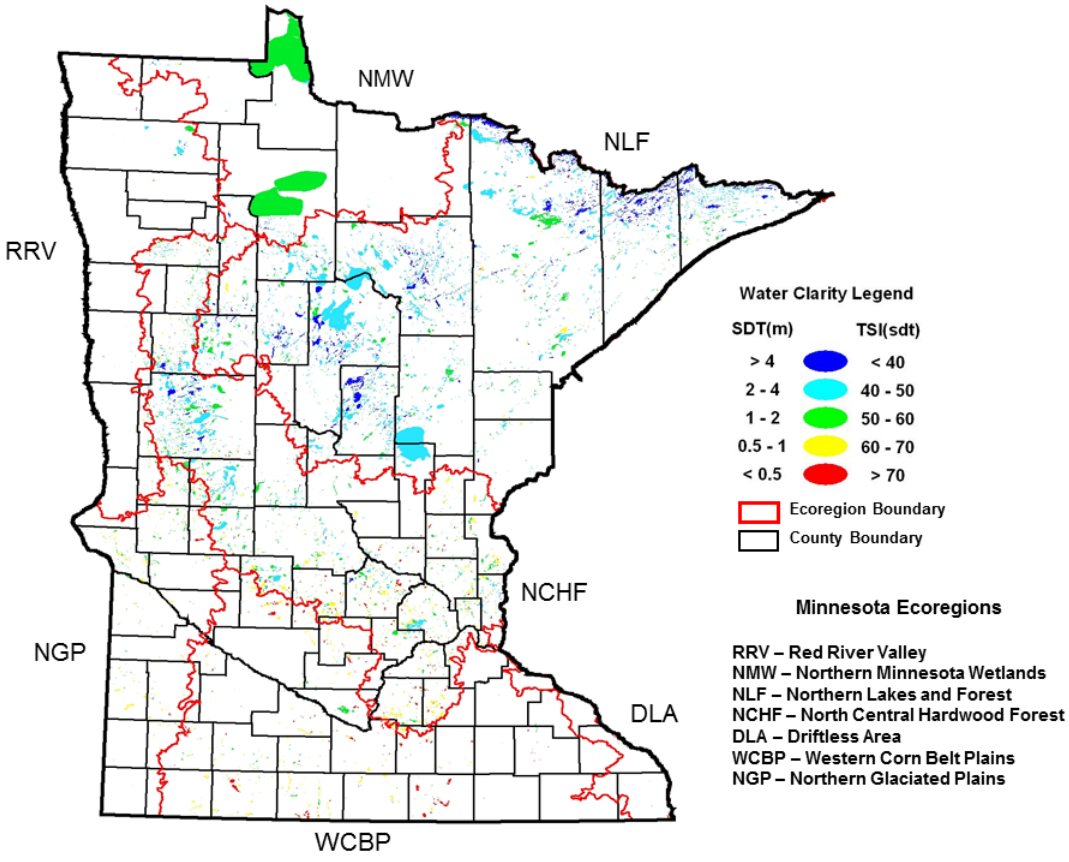

Figure 3.1 2005 Minnesota lake water clarity map with county and ecoregion boundaries.

Table 3.1 Minnesota Landsat water clarity database summary for the state and by ecoregion.

Minnesota	**1985**	**1990**	**1995**	**2000**	**2005**
Minimum	0.08	0.07	0.08	0.12	0.09
Q1	1.24	1.15	1.28	1.15	1.09
Median	2.13	2.00	2.07	2.15	2.00
Mean	2.26	2.21	2.27	2.25	2.25
Q3	3.13	3.04	3.13	3.23	3.10
Maximum	12.88	14.44	11.18	13.10	17.56
Number (n)	11,136	10,732	10,988	10,516	11,241
STDV	1.26	1.36	1.27	1.29	1.51
NLF	**1985**	**1990**	**1995**	**2000**	**2005**
Minimum	0.08	0.14	0.15	0.15	0.09
Q1	2.39	2.15	2.17	2.49	2.13
Median	3.11	2.94	3.00	3.14	2.95
Mean	3.13	3.05	3.03	3.12	3.10
Q3	3.77	3.75	3.77	3.74	3.82
Maximum	12.88	14.49	11.16	13.10	17.56
Number (n)	5,243	5,149	5,123	4,980	5,151
STDV	1.10	1.29	1.20	1.09	1.52
NCHF	**1985**	**1990**	**1995**	**2000**	**2005**
Minimum	0.14	0.09	0.14	0.12	0.11
Q1	0.90	0.79	0.99	0.78	0.86
Median	1.46	1.41	1.55	1.42	1.47
Mean	1.54	1.51	1.68	1.54	1.64
Q3	2.03	2.00	2.14	2.08	2.19
Maximum	6.90	8.90	9.62	6.51	9.39
Number (n)	4,147	3,920	4,075	3,790	4,226
STDV	0.80	0.91	0.91	0.90	1.01
WCBP	**1985**	**1990**	**1995**	**2000**	**2005**
Minimum	0.14	0.07	0.15	0.15	0.15
Q1	0.48	0.62	0.64	0.54	0.50
Median	0.66	0.82	0.81	0.76	0.69
Mean	0.81	1.07	1.04	0.96	0.85
Q3	1.01	1.43	1.37	1.23	1.04
Maximum	4.02	4.29	3.92	3.04	3.42
Number (n)	658	673	695	685	746
STDV	0.50	0.61	0.56	0.58	0.53
NGP	**1985**	**1990**	**1995**	**2000**	**2005**
Minimum	0.34	0.29	0.51	0.38	0.33
Q1	0.98	0.62	0.92	0.71	0.68
Median	1.34	0.98	1.29	0.95	0.93
Mean	1.50	1.13	1.45	1.15	1.12
Q3	1.92	1.52	1.84	1.52	1.41
Maximum	4.32	4.01	3.49	3.25	3.35
Number (n)	639	565	650	631	656
STDV	0.63	0.60	0.64	0.54	0.59
RRV	**1985**	**1990**	**1995**	**2000**	**2005**
Minimum	0.65	0.32	0.52	0.35	0.45
Q1	1.29	0.71	1.15	0.71	1.03
Median	1.77	1.15	1.63	1.32	1.43
Mean	1.88	1.29	1.88	1.37	1.91
Q3	2.24	1.74	2.28	1.63	2.20
Maximum	9.85	4.93	11.18	4.93	17.40
Number (n)	212	198	207	196	211
STDV	0.92	0.68	1.17	0.83	1.85
NMW	**1985**	**1990**	**1995**	**2000**	**2005**
Minimum	0.58	0.60	0.66	0.76	0.67
Q1	1.99	1.82	2.18	2.56	2.18
Median	2.63	2.81	3.10	3.16	3.02
Mean	2.63	2.61	2.90	3.05	3.09
Q3	3.25	3.34	3.60	3.62	3.75
Maximum	5.79	6.09	7.12	5.67	8.31
Number (n)	180	182	187	179	196
STDV	0.88	1.05	1.01	0.88	1.22
DLA	**1985**	**1990**	**1995**	**2000**	**2005**
Minimum	0.19	0.14	0.08	0.20	0.11
Q1	0.54	0.50	0.30	0.44	0.25
Median	0.71	0.75	0.39	0.71	0.43
Mean	0.85	1.02	0.53	1.03	0.60
Q3	0.97	1.24	0.57	1.47	0.72
Maximum	2.74	3.74	2.93	4.51	2.88
Number (n)	57	45	51	55	55
STDV	0.63	0.60	0.64	0.54	0.59

3.2.3 Lake Classification by Morphometric and Chemical Characteristics

Although each lake is unique in the totality of its biological, chemical, and morphometric characteristics, a variety of general patterns show these characteristics influence lake responses to watershed impacts. To differentiate in-lake characteristics from watershed influences we grouped the lakes by general physical and chemical characteristics using a tripartite classification system (area, depth and alkalinity; Table 3.2) described by Osgood et al. (2002). Surface area could be calculated using lake polygons from the analysis of satellite images, but measured data were needed for lake depth and alkalinity. These characteristics are available for only a subset of Minnesota's lakes. We extracted these data from a subset of 4,265 "survey lakes" sampled by the Minnesota Department of Natural Resources (MDNR). The MDNR has measured maximum depth for 4,167 lakes and calculated mean depth for 1,139 lakes. We estimated mean depth (when not available) from maximum depth data using a regression relationship between the two variables reported by Osgood et al. (2002).

Table 3.2 Lake classification criteria.

Number	Size (Hectare)	Mean Depth (m)	Alkalinity (mg/l CaCO3)
1	Small <40	Shallow <2	Low <50
2	Medium 40 - 200	Medium (2-5)	Medium 50 - 100
3	Large >200	Deep >5	High >100

e.g., Lake Class 111 would be a small shallow lake with low alkalinity.

Alkalinity data were available for 1,390 lakes. We developed a map of lake alkalinity across the state using the kriging algorithm in ArcMap and all available alkalinity data. Alkalinity in Minnesota has a distinct pattern with low alkalinity in

northeast Minnesota and high values in the southwest (Figure 3.2). Alkalinity values for lakes without measured values were extracted from the alkalinity map.

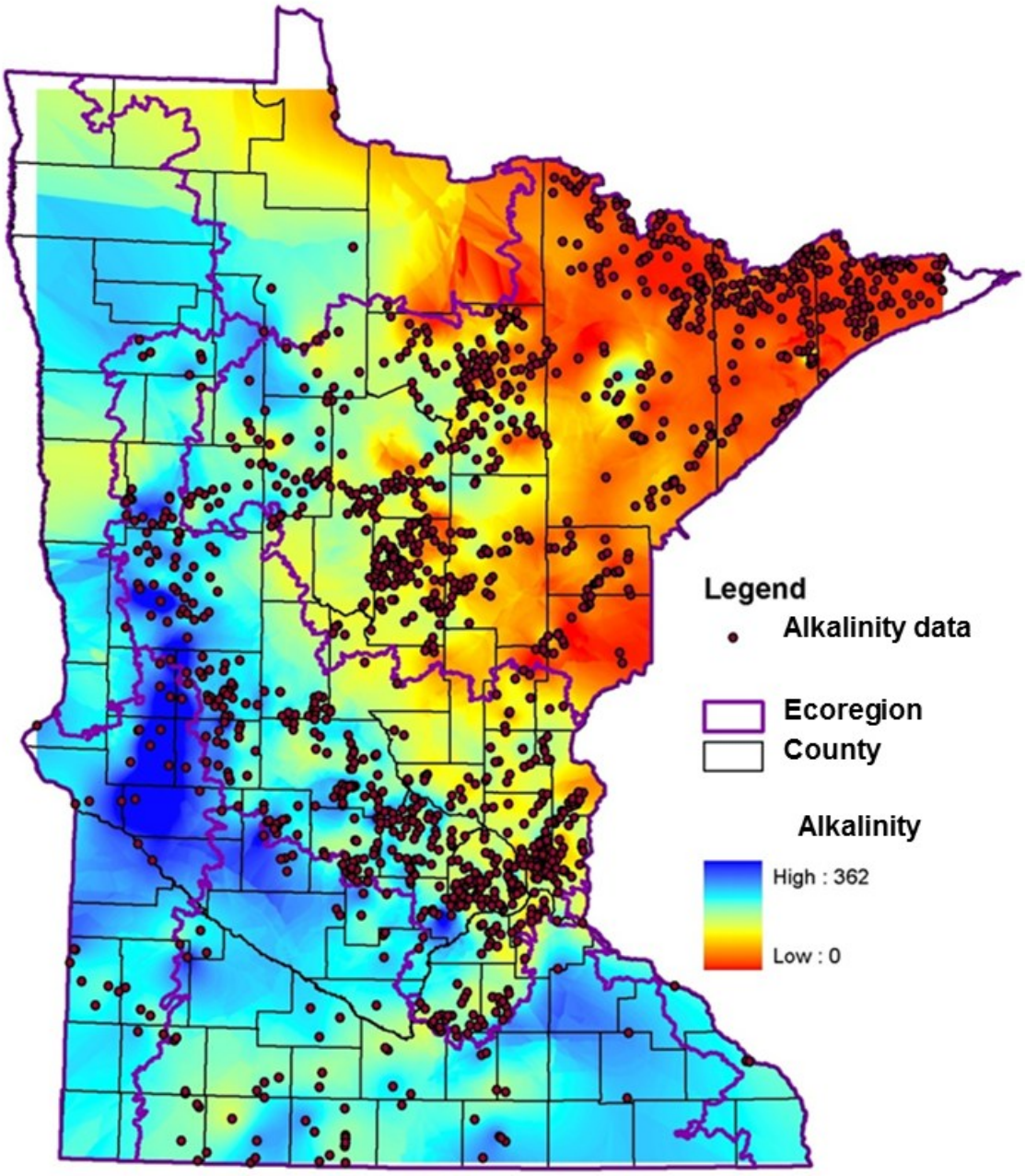

Figure 3.2 Minnesota lake alkalinity surface interpolated using kriging from U.S. EPA Storet alkalinity data.

The above operations yielded 4,167 survey lakes with surface area, mean depth, and alkalinity data. For statistical analyses the survey lakes were screened to eliminate complex, multi-basin lakes, for which the depth data may not adequately represent each basin, which left 3,357 single basin lakes that were used for further analysis. The lakes were grouped into 27 classes with the ranges presented in Table 3.2.

3.2.4 Geographic Delineations

We used the EPA Level-III ecoregions of the conterminous United States (LMIC/MPCA version) (Omernik, 1987) as one basis for our geospatial and temporal analyses. In Minnesota there are seven ecoregions (Figure 3.1), each of which is different in terms of its aggregate land use, geology, soils, vegetation, climate, wildlife, and hydrologic characteristics. We also used county, minor watershed, catchment delineations and individual lakes at the state-wide level and within ecoregions, to investigate geospatial and temporal trends. The smallest delineated drainage areas mapped by the MNDNR, called "catchments," have been delineated topographically within major and minor watershed boundaries. The hydrologic watersheds for some lakes contain many catchments (and may include additional lakes). Therefore, we selected only the 1,018 hydrologic lake watersheds that are headwater catchments and linked land cover information to each of these lakes. Additional information about the MDNR catchments is found at http://deli.dnr.state.mn.us/metadata/wshd_lev08py3.html

3.2.5 Statistical Analysis

To compile the data needed for analysis, we used Esri ArcMap to calculate lake areas from the lake polygons, tabulate land cover area for each catchment and ecoregion and link each lake to its catchment and ecoregion. Microsoft Excel was used to calculate land cover percentages for each catchment and categorize catchments by statewide land cover quintiles. To investigate water clarity trends of individual lakes we used Excel's LINEST function to calculate the least squares linear regression statistic for 9,647 lakes with data for all five time periods (1985 to 2005). To determine how trends varied by lake type, we linked each lake to the "wetland type" from Bulletin 25 (MDNR, 1968), which classifies lakes according to the U.S. Fish and Wildlife Service's Circular 39 (U.S. FWS, 1971). JMP 9.0 was used for analysis of variance (ANOVA) of the classes and to summarize the data statistically.

3.3 Results and Discussion

Geospatial and temporal analyses were conducted on three separate data sets: (1) the full water clarity database of the lakes in the state for five time periods, (2) survey lakes with known morphometric and chemical characteristics, and (3) a subset of the headwater catchment survey lakes in conjunction with land cover data for the 2000 time period. The latter dataset, although only a subset of the entire database, is still large (> 1000 lakes) and has the advantage of allowing for determination of watershed to lake ratios and comparisons of the responses of different type of lakes to extent of development and differences in land cover.

3.3.1 Spatial and Temporal Analyses: All Lakes

Spatial and temporal trends: General Statewide. At the statewide level we found the following spatial and temporal trends for water clarity in Minnesota lakes (Tables 3.1 and 3.3 and Figure 3.1). (1) Lake clarity consistently was lower in the south and southwest and higher in the north and northeast. (2) The statewide average value for water clarity remained stable between 1985 and 2005 at 2.25 m. (3) Many of the clearest lakes are abandoned iron mine pits in the Northern Lakes and Forest (NLF) ecoregion that have filled with water. (4) Mean water clarity in the NLF and North Central Hardwood Forest (NCHF) ecoregions in central and northern Minnesota remained stable from 1985 to 2005, but decreasing water clarity trends were detected in the Western Corn Belt Plains (WCBP) and Northern Glaciated Plains (NGP) ecoregions in southern Minnesota, where agriculture is the predominant land use. These findings are similar to those reported by Chapter 2 (Olmanson et al., 2008).

Table 3.3 Water clarity (m) statistics ecoregion 1985 to 2005 by ecoregion.

Ecoregion	State Lakes %	Typical Range	Mean	Range	STDV
NLF	47	2.27 – 3.77	3.09	0.1	0.04
NCHF	37	0.86 – 2.09	1.58	0.17	0.07
WCBP	5.9	0.56 – 1.22	0.95	0.26	0.11
NGP	5.7	0.78 – 1.64	1.27	0.38	0.19
RRV	1.9	0.98 – 2.02	1.67	0.62	0.31
NMW	1.6	2.15 – 3.51	2.86	0.48	0.23
DLA	0.5	0.41 – 0.99	0.81	0.5	0.23

Spatial and temporal trends: Within Ecoregions. Minnesota's seven ecoregions differ in terms of their aggregate land use, geology, soils, vegetation, climate, wildlife, and hydrologic characteristics, and significant differences also occur in lake clarity among the ecoregions (Tables 3.1 and 3.3 and Figure 3.3). The observed pattern is fairly consistent for the five time periods (1985-2005). The NLF and Northern Minnesota Wetlands (NMW), which have land cover dominated by forest, lakes and wetlands (Figure 3.4), generally have the best water clarity in the state. The Northern Glacial Plains NGP, Red River Valley (RRV) and WCBP generally have low water clarity and are dominated by agricultural land cover.

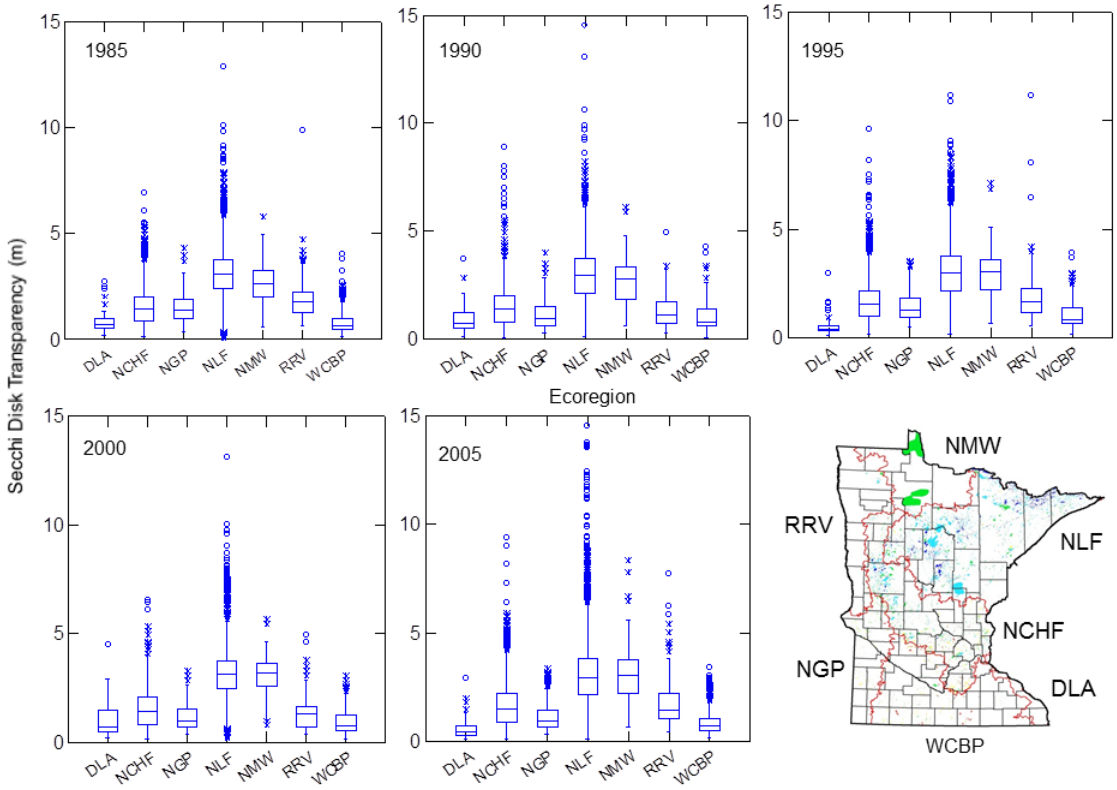

Figure 3.3 Minnesota water clarity boxplots 1985-2005 by ecoregion.

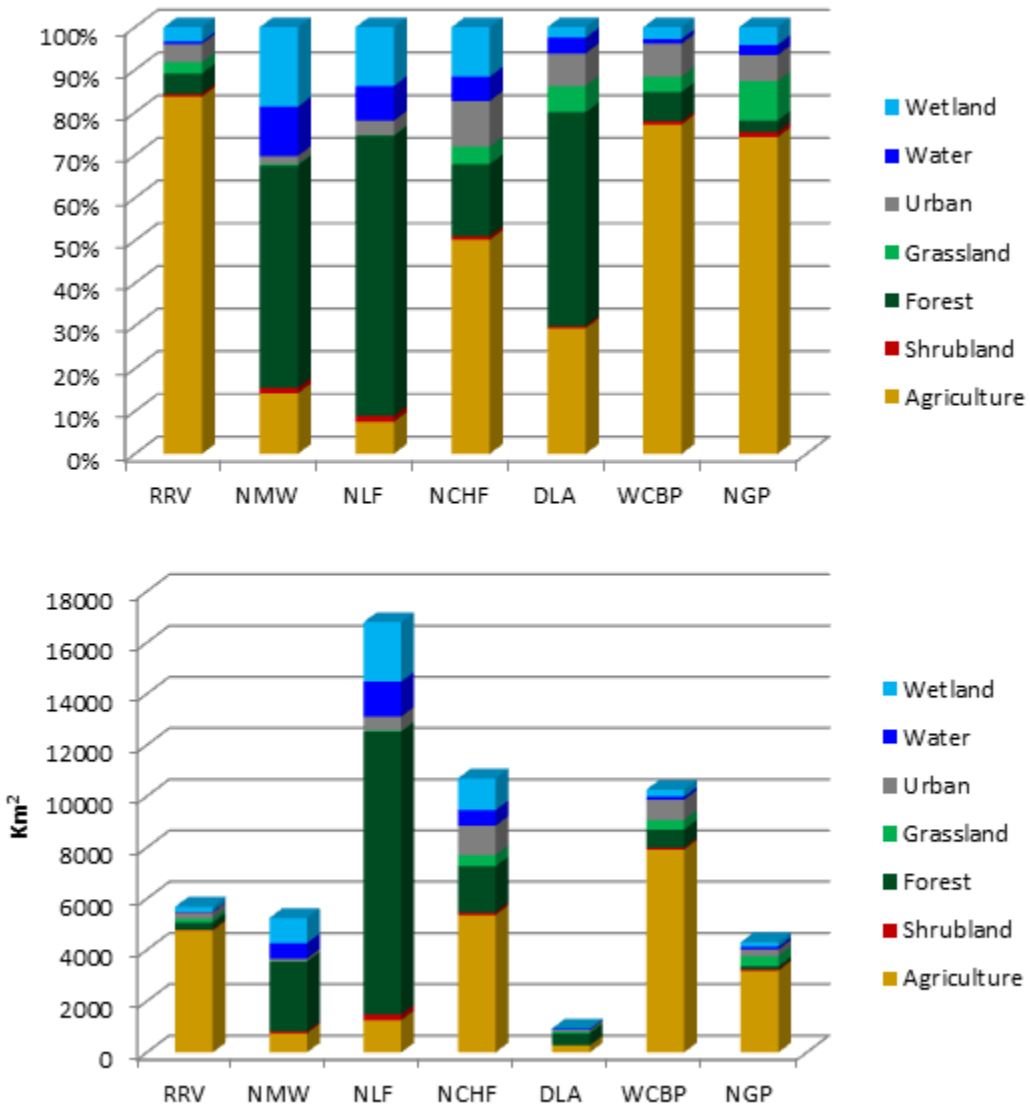

Figure 3.4 2000 land cover distribution by ecoregion.

Water clarity in lakes of the NLF ecoregion typically is high; the 25th-75th percentile values for means of individual lakes from all time periods (hereafter referred to as the "typical range") are 2.27-3.77 m, and the grand average for all lakes over the five

measurement periods is 3.09 m. Using available SD data from 447 lakes, Heiskary and Wilson (1989) found similar results with a typical range of 1.8-3.9 m. In contrast, Heiskary and Wilson (2005) used SD data from 32 "reference lakes" (lakes that are minimally impacted and considered representative for their ecoregion) and found a slightly higher typical range of 2.4-4.6 m. Slightly differences in typical ranges for subsets (available SD data and reference lakes) of the whole database are to be expected especially since the reference lakes represent minimally impacted lakes. Average water clarity remained fairly stable from 1985 to 2005 (range of 0.10 m and standard deviation (STDV) of 0.04 m). The NLF is a particularly lake-rich region (containing 47 percent of the state's lakes) dominated by forests (66%) and hilly land interspersed with wetlands, bogs, lakes and ponds. The lakes in this ecoregion are used mainly for recreation.

Lakes in the North Central Hardwood Forest (NCHF) ecoregion exhibit a wide range of water clarity (typical range of 0.86-2.09 m). Heiskary and Wilson (1989) found similar results with typical range of 0.8-2.2 m using available data from 491 lakes, and Heiskary and Wilson (2005) found a slightly higher typical range of 1.5-3.2 m for 43 reference lakes. The overall average water clarity remained stable between 1985 and 2005 (mean = 1.58 m; range = 0.17 m; STDV = 0.07 m). This ecoregion has 37% of the state's lakes and is a transitional area with mixed land cover (Figure 3.4) and a terrain that varies from rolling hills to plains. Agriculture encompasses approximately 50% of the land in the NCHF, but there also are large areas of forest (17%), wetlands (12%) and grasslands (4%). This ecoregion includes the Twin Cities metropolitan area and thus has

the highest proportion (11%) of urban and suburban land among the state's ecoregions. Many of its lakes have been developed for residential and recreational purposes.

Water clarity in the Western Corn Belt Plains (WCBP) ecoregion generally is low, with a typical range of 0.56-1.22 m and an overall average of 0.95 m. Heiskary and Wilson (1989) found an even lower typical range (0.3-0.9 m) for 47 lakes with available SD data, but Heiskary and Wilson (2005) found a typical range for 16 reference lakes closer to our results (0.5-1.0 m). The average water clarity showed some variability between 1985 and 2005 (range of 0.26 m and STDV of 0.11 m). There also was a trend of declining water clarity (slope = −0.044; r^2 = 0.91 for 1990 to 2005); the highest mean water clarity was 1.07 m in 1990, and the lowest was 0.85 m in 2005. This ecoregion has 5.9% of the state's lakes and is characterized by nearly level to gently rolling terrain that is dominated by agriculture (77% of the total land area).

The water clarity in the Northern Glaciated Plains (NGP) ecoregion is generally low with a typical range of 0.78-1.64 m and grand average of 1.27 m. Heiskary and Wilson (1989) found a lower typical range (0.3-1.2 m) for 15 lakes with available SDdata, and Heiskary and Wilson (2005) obtained a lower typical range (0.4-0.8 m) for 13 reference lakes. This finding may reflect difficulties in finding minimally impacted reference lakes in this ecoregion. The average water clarity was more variable temporally than that in the other ecoregions (range = 0.38 m; STDV = 0.19 m), and there was a strong trend of declining water clarity (slope = −0.085; r^2 = 0.45). The highest mean clarity (1.5 m) occurred in 1985 and the lowest (1.12 m) in 2005. This ecoregion has 5.7% of the state's lakes and is similar to the WCBP in that it is characterized by flat to

gently rolling terrain dominated by agriculture (74%), but it has more wetland (4%) and grassland (9%).

In aggregate, the three remaining ecoregions account for only 4% of the state's lakes. The Red River Valley (RRV) ecoregion (< 2% of the state's lakes) is a flat plain left by glacial Lake Agassiz. The average water clarity was more variable than that of the other ecoregions: means of ~1.9 m in 1985, 1995 and 2005 and ~1.3 m in 1990 and 2000; Table 3.1) with a typical range of 0.98 to 2.02 m and an overall average of 1.67 m. The range of the water clarity data in this ecoregion was 0.62 m (STDV = 0.31 m). The Northern Minnesota Wetlands (NMW) ecoregion has < 1.6% of the state's lakes but does include a few of the state's largest lakes: Lower Red Lake, Upper Red Lake, and Lake of the Woods. The latter two are plagued by excessive algal blooms, but aside from these exceptions, this ecoregion has good water clarity and a trend of increasing clarity (Tables 3.2 and 3.3 and Figure 3.3). The Driftless Area (DLA) ecoregion has only 0.5% of the state's lakes, and most of them are man-made reservoirs or backwater areas of the Mississippi River and its tributaries. The ecoregion is characterized by steep slopes that drain to the Mississippi River and is named for its lack of recent glacial activity. The mean water clarity of the lakes is low and variable (Tables 3.2 and 3.3 and Figure 3.3).

Spatial and temporal trends: Individual Lakes. Although there is a general pattern of lakes being more eutrophic and thus low in clarity in southern Minnesota and clearer in the north, at the local level clarity is quite variable (Figure 3.1). The range and variability of water clarity throughout the state and at the local and ecoregion level is

striking and likely reflects both natural characteristics (e.g., depth and watershed size) and effects of anthropogenic characteristics (i.e., land use and management practices).

Trends were identified in terms of an increase or decrease in water clarity by a factor of two (i.e., a doubling or halving SD) over the 20-year record. The water clarity data were log transformed to normalize the response throughout the range of SD values, and using the above criterion, we found that 1,039 (10.8% of Minnesota's lakes had trends in clarity. Of this total, 440 lakes (4.6%) had increasing clarity trends, and 599 lakes (6.2%) had decreasing clarity trends (Figure 3.5). On a statewide basis, lakes with increasing and decreasing water clarity trends are spread throughout the state (Figure 3.5a), but there is some clustering of lakes with increasing and decreasing water clarity (e.g., abandoned iron mine pits in NLF ecoregion are dominated by increasing water clarity; Shallow lakes along Lake Superior's north shore are dominated by decreasing water clarity). Smaller lakes (< 60 ha) had a greater fraction of lakes (58%) with decreasing water clarity than larger lakes (> 60 ha; 53%) (Figure 3.5b). Lake "type" information was available for 88% of the lakes identified as having trends. Lakes identified as shallow "type 2", "type 3" and "type 4" wetlands (MDNR 1968) had higher percentages (100, 79, and 70%, respectively) of decreasing water clarity than increasing water clarity than the deeper "type 5" wetlands (52%) (Figure 3.5c). These trends suggest that smaller and shallower lakes are more susceptible to decreasing water clarity potentially due to changes in land use than larger and deeper lakes, which agrees with a long history of studies on lake eutrophication (e.g., Vollenweider, 1972; 1975). Although land cover data is currently not available for each time period, future studies would

benefit from having historic (~1975) to present statewide land cover maps at 5 year intervals to quantify impact of specific changes in land cover.

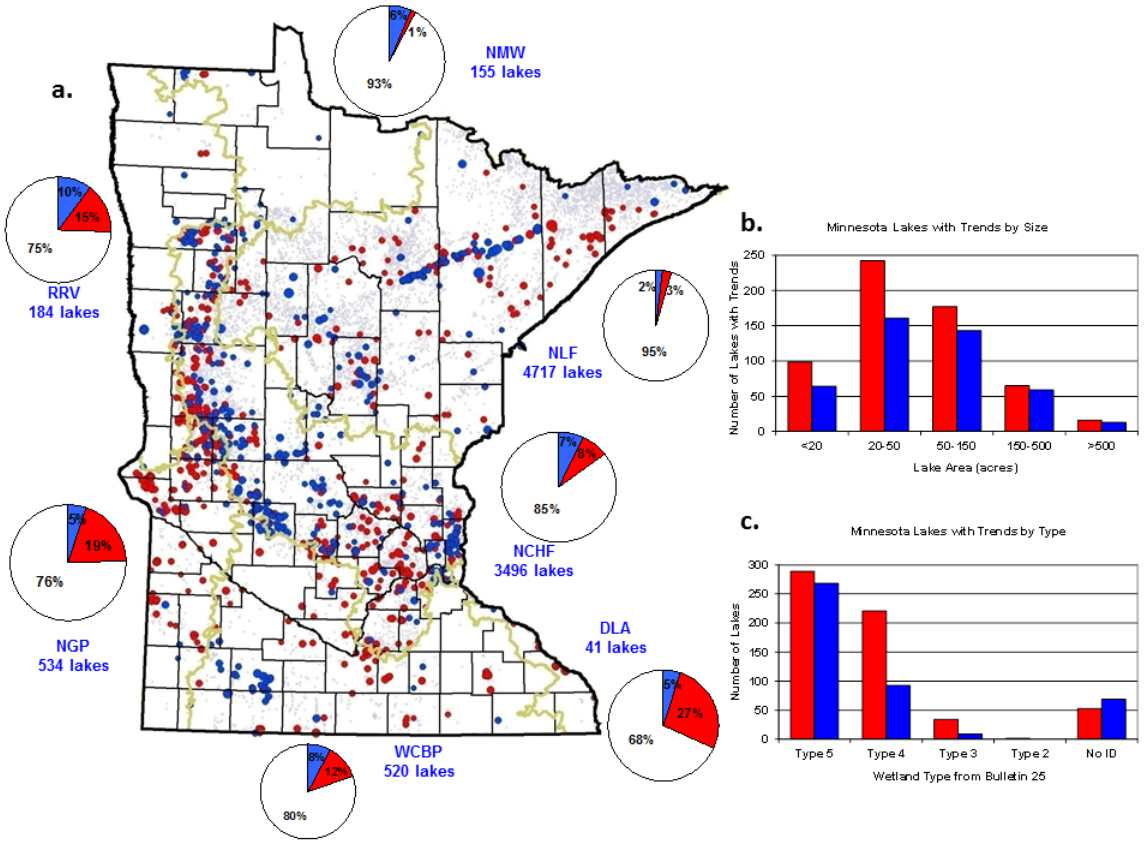

Figure 3.5 a. Map of water clarity trends. The blue dots indicate lakes with improving water clarity and the red dots indicate lakes with decreasing water clarity, the size of the dot indicates the magnitude of the trend. The pie charts show the percentage of lakes in each ecoregion with increasing water clarity trends in blue and decreasing water clarity trends in red. b. Trends by lake size. c. Trends by lake type.

At the ecoregion level 20-32% of the lakes in the RRV, NGP, WCBP and DLA had trends, and a much larger portion of lakes had decreasing clarity than increasing clarity (Figure 3.5a). These ecoregions are dominated by agricultural land use, and the trends may indicate changes in agricultural activity over the study period. The NCHF had

trends in ~15% of its lakes with nearly equal portions of increasing and decreasing water clarity, and less than 5% of the NLF lakes had trends (2.7% decreasing and 2% increasing). The NMW ecoregion had increasing water clarity in 6.5% of its lakes and decreasing clarity in 1.3%. The latter two ecoregions have lower percentages of agricultural and urban land use than the other ecoregions, which may account for the relative stability. The relatively large fraction of NMW lakes with improved water clarity may be attributable to the relatively small dataset or climatic changes over the study period.

3.3.2 Spatial and Temporal Analyses: Survey Lakes

For the survey lakes we explored how well this subset represents the state's lakes as a whole, how the lake classes are distributed throughout the state and how water clarity varies with depth, lake area, and alkalinity.

To determine whether the survey lakes are representative of all Minnesota lakes we compared the size class distributions of all lakes (Figure 3.6) in the state and the survey lakes (Figure 3.7). It is apparent that small lakes, which constitute ~70% of Minnesota lakes, are underrepresented in the survey lakes; only 40% of these lakes are small. Also, lakes from the NLF ecoregion are better represented in the survey lakes than lakes in other ecoregions (Table 3.4 and Figure 3.7). This analysis indicates that the survey lakes are not a representative sample of all Minnesota lakes. This would bias our results if we were extrapolating to the larger population (Peterson et al., 1999). Insofar as we are only comparing different types of lakes within this dataset, the survey lake

database actually is better for our purpose because the lake area (Figure 3.7) and depth classes (Figure 3.8) are fairly equally represented. As for lake class distribution, lakes of all size classes and shallow lakes are well distributed throughout the state while medium and deep lakes occur more in central and northern Minnesota (Figure 3.9).

Table 3.4 Number of Minnesota vs. Survey Lakes by ecoregion.

Lakes	Minnesota	DLA	NCHF	NGP	NLF	NMW	RRV	WCBP
# Minnesota	12193	101	4466	690	5671	215	215	835
# Survey Lakes	3357	4	900	70	2209	22	29	123
% lakes surveyed	27.5	4.0	20.2	10.1	39.0	10.2	13.5	14.7

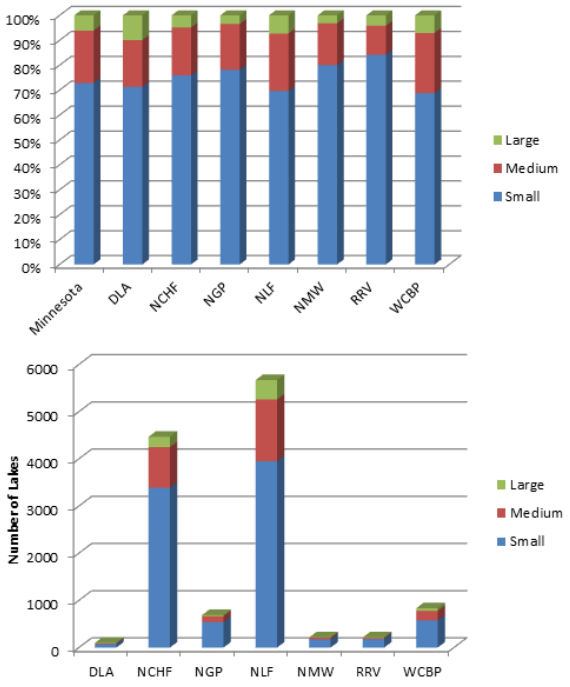

Figure 3.6 Distribution of Minnesota lakes by lake size class and ecoregion.

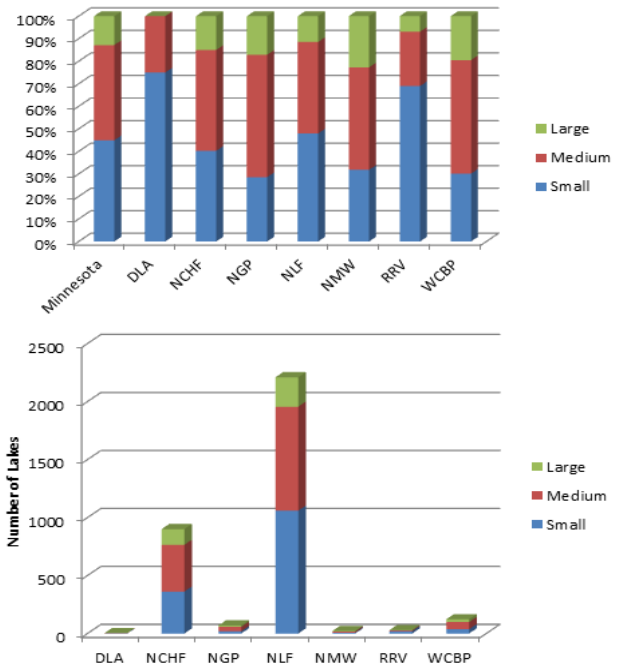

Figure 3.7 Distribution of survey lakes by lake size class and ecoregion.

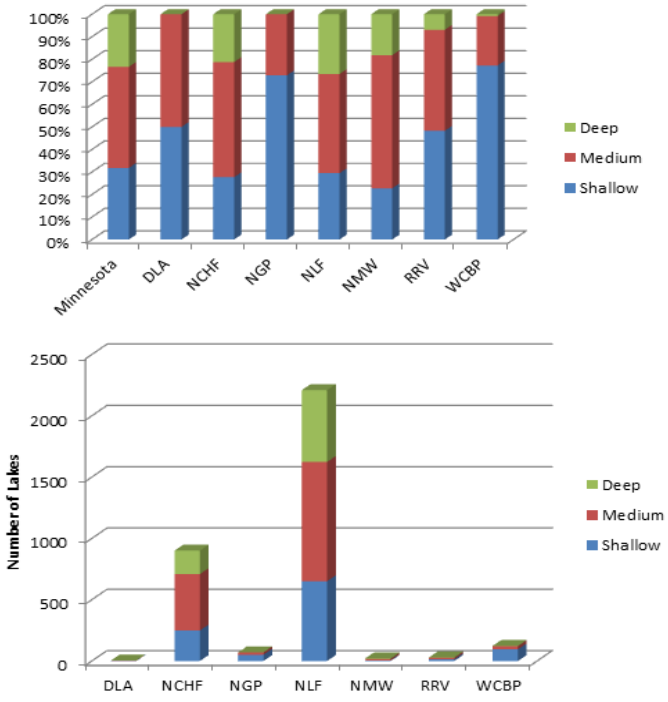

Figure 3.8 Distribution of survey lakes by lake depth class and ecoregion.

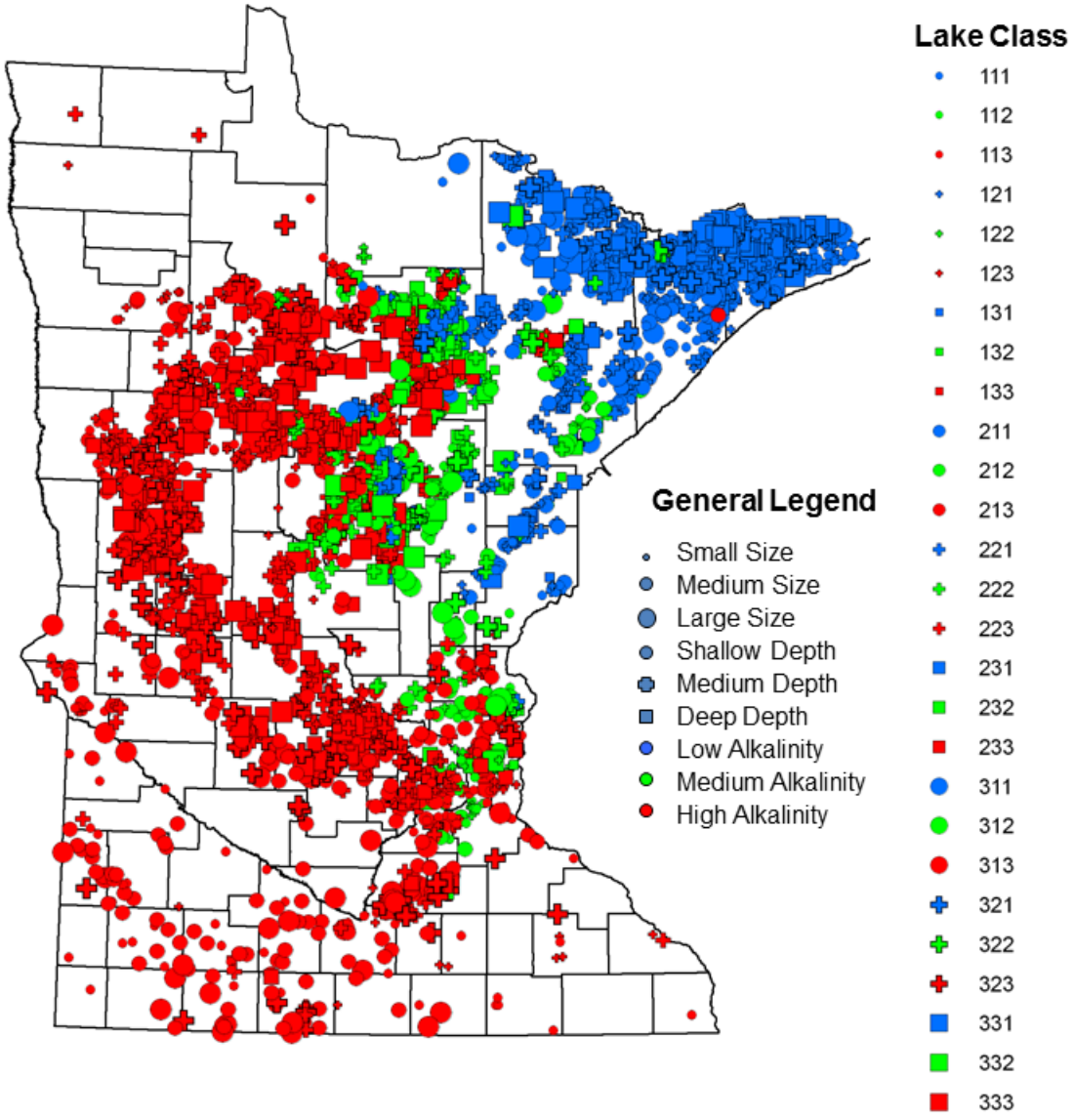

Figure 3.9 Lake class distribution map.

We examined the tripartite (area, depth and alkalinity) classification system at the state wide and ecoregion level to determine whether these variables contributed to differences in water clarity. To distinguish general patterns we focused on values in the typical range (25^{th}-75^{th} percentile). At the statewide level, some significance differences

in water clarity were associated with the depth, size, and alkalinity classes (Figure 3.10). Clarity generally was lower in shallow lakes than deep lakes. To a lesser degree, clarity was lower in large lakes than small lakes, and it appears to be higher in low-alkalinity lakes than high-alkalinity lakes. At the ecoregion level, the patterns hold for depth and size but not for alkalinity. For example, boxplots of water clarity for the NLF ecoregion (Figure 3.11) show similar distributions for all alkalinity classes, and the highest alkalinity class had slightly higher water clarity. The clarity differences for alkalinity classes at the statewide level thus appear to be an artifact of geographic trends in alkalinity. As Figure 3.9 shows, the majority of low-alkalinity lakes occur in the NLF ecoregion, which also has the highest water clarity. Therefore, alkalinity can be ignored as a factor related to water clarity, reducing the number of classes to nine. Because depth has a much stronger influence on clarity than lake area, we further simplified our analysis to the three depth classes. At the ecoregion level, the lowest water clarities occur in the shallowest lakes and highest occurs in the deepest lakes (Figure 3.12). Depth has long been recognized as a factor contributing to distinct differences in nutrient levels in Minnesota lakes (Heiskary and Wilson,1988) and has been used as a factor for developing nutrient criteria for Minnesota lakes; Heiskary and Lindon (2005) recommended that the MPCA use separate nutrient criteria for shallow lake management.

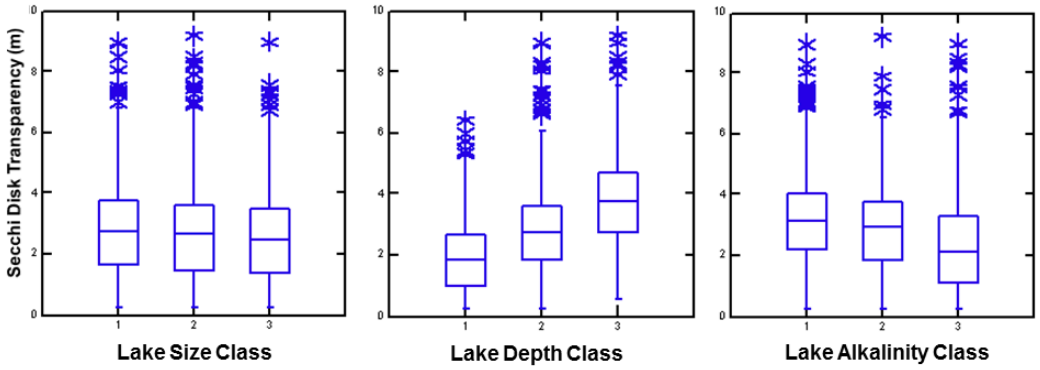

Figure 3.10 Minnesota 2000 Landsat water clarity boxplots by lake class.

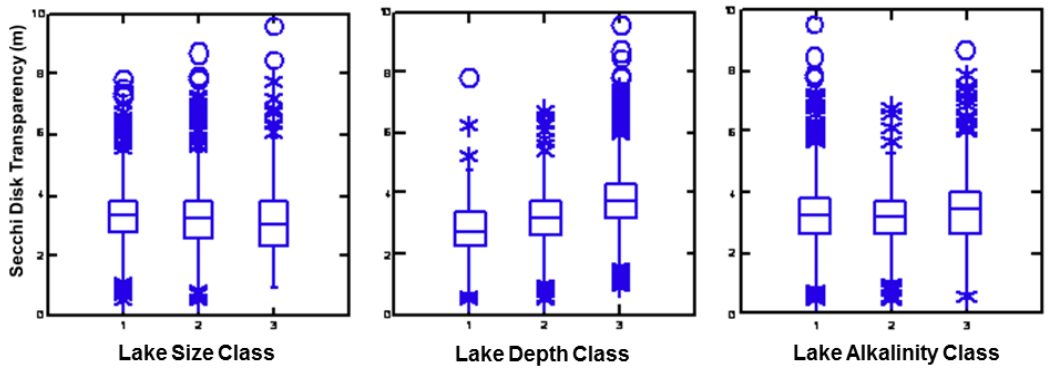

Figure 3.11 Northern Lakes and Forest Ecoregion 2000 Landsat water clarity boxplots by lake class.

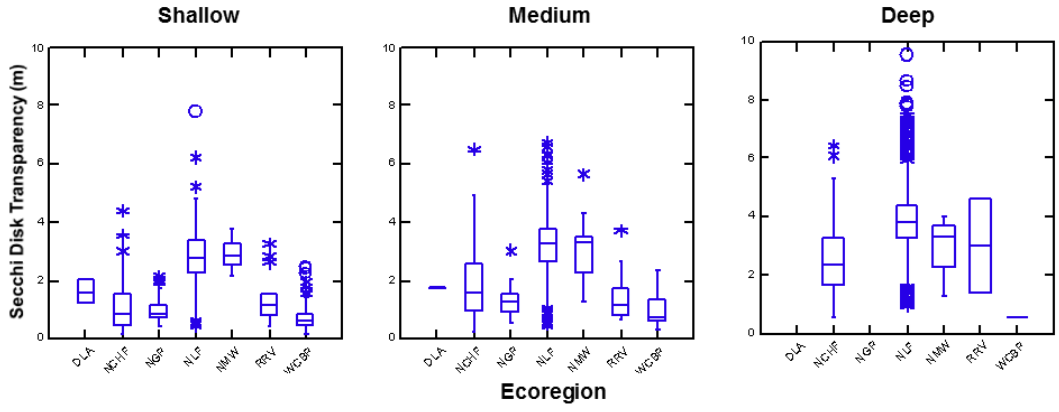

Figure 3.12 2000 Landsat water clarity boxplots by lake depth class and ecoregion.

3.3.3 Water clarity-watershed land use relationships

Aquatic scientists have long regarded lakes as reflections of their watersheds—that is, water quality in lakes depends not only on in-lake factors like depth but also on the loadings of nutrients and other materials they receive from their watersheds or catchments (Horne and Goldman, 1994). We investigated how land use affects water clarity at different geographic delineations (county, minor watershed and catchment). At the county level strong relationships were found between water clarity and land cover classes. The relationships between the countywide average water clarity and the percentage of developed land (urban plus agriculture) and forest land in the county yielded r^2 values of 0.75 and 0.78, respectively. As the geographic delineation decreased in size to minor watersheds and then to catchments, the variability increased and the strength of the relationship decreased (e.g., $r^2 = 0.53$ and 0.43, respectively, for forest) (Figure 3.13). This finding can be attributed to the "law of averages," where the average water clarity of a large number of lakes (with many contributing factors) at the county level reduces the variability. As the delineations decrease in size, the number of lakes reduces (to only one at the catchment level). Because in this analysis we accounted only for land cover, other unaccounted for factors (e.g., depth and watershed size) increase the variability.

To decrease the variability we focused on survey lakes with known morphometric characteristic at the catchment level. Headwater catchments (lake watersheds) linked with land cover were examined, and results are presented in boxplots representing the typical range within lake depth classes.

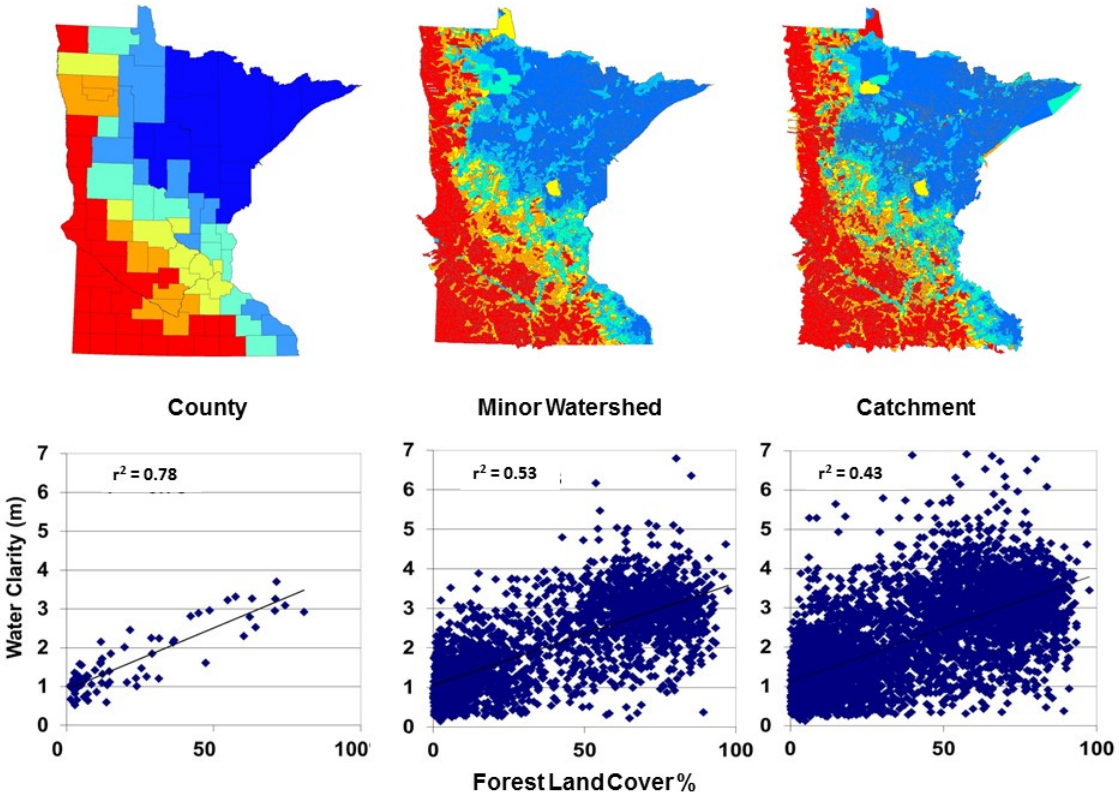

Figure 3.13 Forest land cover vs. average water clarity at the county, minor watershed and catchment levels.

For the headwater catchments (lake watersheds) we found significant differences in water clarity using one-way ANOVA for classes of lakes with different intensities of land cover in their catchments. Lakes with watersheds having more urban (Figure 3.14a) and agriculture (Figure 3.14b) land or the sum of these categories (Figure 3.14c) were associated with decreased water clarity. The pattern described earlier with regard to depth also holds: shallow lakes had lower water clarity than deep lakes with similar land cover. Urban and agricultural land uses have long been recognized as significant contributors to water quality degradation. Many studies have used empirical relationships or models to

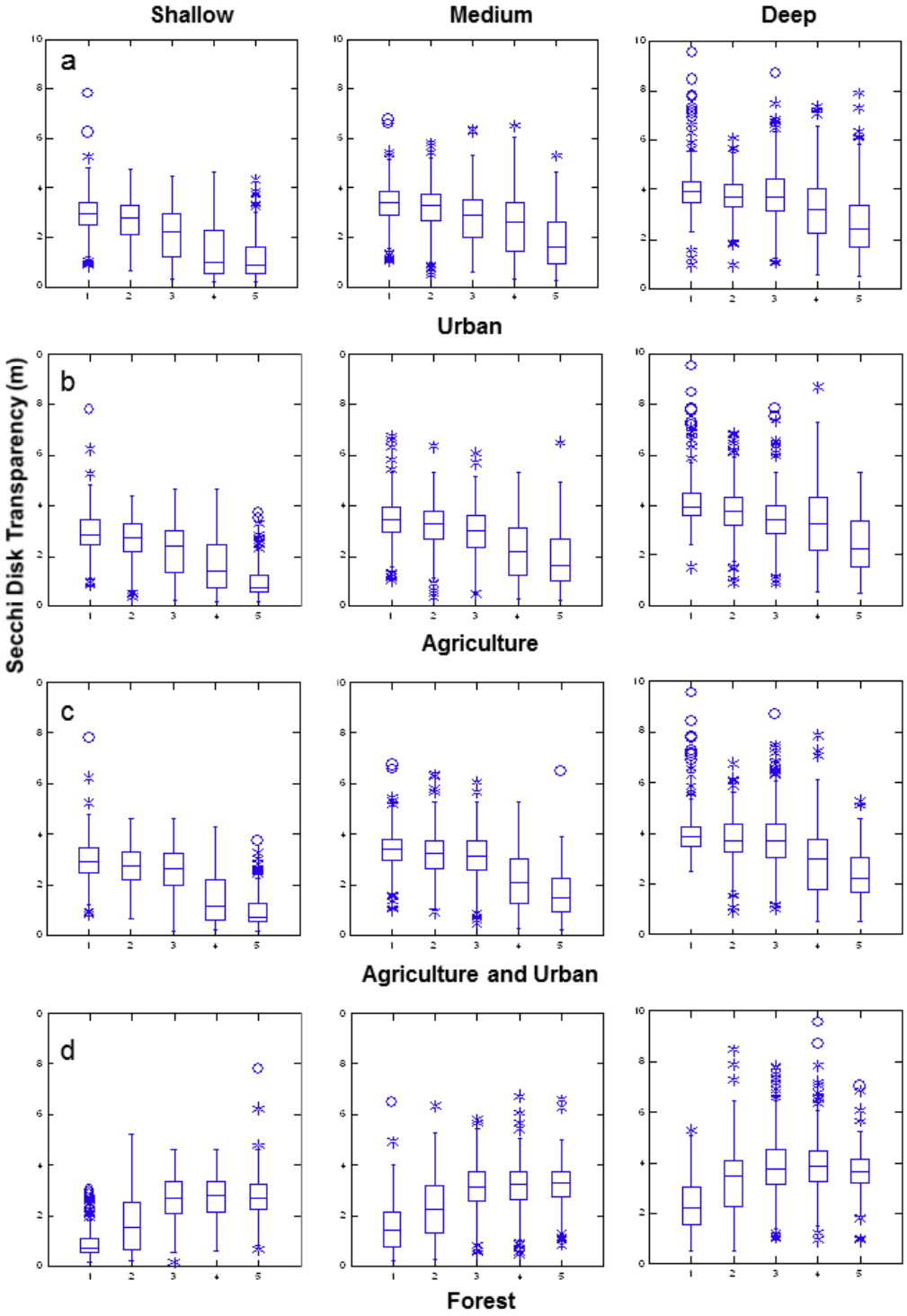

Figure 3.14 2000 Landsat water clarity boxplots by lake depth class and land cover percentage quintiles (a.urban; b. agriculture; c. Developed (Urban and agriculture); d. Forest) from low (1) to high percentage (5).

quantify these impacts (e.g., Brezonik and Stadelmann, 2002; Tong and Chen, 2002; Mattikalli and Richards, 1996; Leone et al., 2008). In contrast, increasing forest cover up to 45% is associated with improving water clarity (Figure 3.14d). These finding are consistent with other reports in the literature. For example, Detenbeck et al. (1993) used a geographic information system (GIS) to link water quality to land cover variables for 33 lake watersheds in Minnesota and found that forest was associated with better water quality and agriculture was associated with lower water quality. Ramstack et al. (2004) used sediment cores from 55 Minnesota lakes to compare water quality of pre-settlement (circa 1750 and 1800) with post-settlement (1800 to present) and found changes were significantly correlated with percentages of the watershed area that is developed (urban or agriculture). For the forested areas of northeastern Minnesota water quality has changed little since 1800.

For the headwater catchments we also found significant differences in water clarity for watershed to lake area ratio classes (1-10:1, 11-55:1 and 56-113:1), on average lakes with larger watersheds in relation to lake area have a larger potential for nutrient loading and lower water clarity than lakes with low watershed to lake area ratios.

Although depth, watershed to lake area ratio and land use are major contributing factors for water clarity, many other factors also affect water clarity but were not readily available for statewide analysis. Kloiber (2006) found that soil factors such as organic matter or percentage of clay contributed over half of the explanatory power of regression models to estimate nonpoint source pollution. Another important factor missing in our analysis is agricultural animals (in pastures and feed operations). Arbuckle and Downing

(2001) and Berka et al. (2001) found that surplus nutrients from animals in agricultural areas should be accounted for in water quality studies since they can significantly impact water quality. Other variables that can have large effects on water clarity but would be difficult to quantify at a statewide scale include aquatic vegetation and rough fish, such as the common carp.

3.4 Conclusions

Using a 20-year database of water clarity of over 10,000 lakes created from Landsat imagery, we were able to conduct a comprehensive statistical analysis of the spatial distributions and temporal trends of water clarity in Minnesota. At the statewide level our analysis indicated that lakes are less clear (more turbid) in the south and southwest and clearer in the north and northeast. These trends can largely be attributed to differences in land cover and use. As the percentage of developed (agriculture and urban) land uses increase in the lake watershed, water clarity generally decreases. The mean water clarity statewide remained stable from 1985 to 2005, but decreasing water clarity trends were detected in ecoregions dominated by agricultural land use. For individual lakes, temporal trends were detected in ~11percent of Minnesota's lakes: 4.6% had improving clarity and 6.2% had decreasing clarity. Ecoregions in southern and western Minnesota, where agriculture is the predominant land use, had a higher percentage of lakes with decreasing clarity than the rest of the state. By grouping lakes into depth classes we found that on average deep lakes had higher clarity than shallow lakes with comparable land cover at the catchment level. Lakes with lower watershed to lake area

ratios on average have higher water clarity than lakes with higher watershed to lake area ratios. We also found that small and shallow lakes were more susceptible to degradation and had a higher percentage of decreasing clarity trends than large and deep lakes.

Chapter 4

Evaluation of medium to low resolution satellite imagery for regional lake water quality assessments[2]

This study evaluates currently available imagery from Landsat, MERIS, MODIS and AWiFS sensors for their usefulness in regional-scale measurements of lake water clarity and chlorophyll for comprehensive lake management and scientific studies (e.g., modeling). Images from these systems were collected nearly concurrently and processed using methods similar to those developed previously for regional assessments of lake water clarity using Landsat imagery. We tested both atmospherically corrected and uncorrected imagery products; the uncorrected products performed as well as or better than the atmospherically corrected products in empirical relationships to estimate water clarity and chlorophyll. MODIS and MERIS systems, which have large swath widths and high temporal coverage are well suited for regional assessments of large lakes, but their low spatial resolution limits the number of lakes that can be assessed. Landsat imagery allows all lakes $\geq$ 4 ha (more than 12,000 in Minnesota) to be assessed, but its low spectral resolution limits assessments to water clarity. The MERIS system, with spectral and spatial resolution suitable for large (>150 ha) lakes, was the only system with a spectral band set that measured key absorption and scattering characteristics of phytoplankton that could be used reliably for regional chlorophyll assessments. Although none of the currently available systems is ideal, the study yielded a better definition of the

[2] Reprinted in slightly revised form from: Olmanson, L.G., Brezonik, P.L. & Bauer, M.E. (2011). Evaluation of medium to low resolution satellite imagery for regional lake water quality assessments. *Water Resources Research,* 47, W09515, by permission of American Geophysical Union.

spectral, spatial, and temporal characteristics of the ideal system for regional-scale water quality remote sensing that may be realized in upcoming satellite systems.

4.1 Introduction

The state of Minnesota, U.S.A., the "Land of 10,000 Lakes," has more than 12,000 lakes that are four hectares (ha) or larger in area. These highly cherished recreational and aesthetic resources are important for the state's economy and tourism. Of the lakes that have been studied to date, 26 percent have been found to be impaired by anthropogenic eutrophication (P. Anderson, Minnesota Pollution Control Agency, pers. com., 2010). In 2008 Minnesota voters passed the Clean Water, Land and Legacy Amendment to the Minnesota Constitution, which dedicates part of the state's sales tax to protect, enhance, and restore its lakes. Long-term water quality information is needed on a broad regional scale to meet that goal. Although monitoring of lakes by conventional methods has increased in recent years, a large majority is not monitored regularly, and most have not been monitored at all.

To help fill this gap, remote sensing methods have been embraced. Historical and recent statewide assessments have been conducted using Landsat imagery to measure water clarity of all lakes ~8 ha and larger. Chapter 2 (Olmanson et al., 2008) documented a series of such assessments that include more than 10,500 lakes at approximately five-year intervals for the period 1985-2005, and assessments were completed more recently for 1975 using Landsat multispectral scanner (MSS) imagery and 2008 using Landsat Thematic Mapper (TM) and Enhanced Thematic Mapper plus (ETM+) imagery. These

assessments have demonstrated strong relationships between the spectral-radiometric responses of Landsat TM, ETM+ and MSS data and in situ observations of water clarity measured in terms of Secchi disk transparency (SD). Data for all lakes and years are available at http://water.umn.edu/, and a web-based mapping tool called "Lake Browser" enables searches and displays of results for individual lakes. This database is used routinely by scientists, teachers, agencies, and the public for research, education, water management and recreational purposes.

Minnesota water management agencies plan to continue monitoring water resources using remote sensing, but the current Landsat satellites, 5 and 7, which are far beyond their expected service lives, could fail at any time. The next Landsat mission is not scheduled to be launched until 2013. Moreover, the relatively coarse spectral characteristics of the Landsat sensors effectively limit their use to assessment of water clarity. Therefore, it is prudent to consider alternative systems that could be used for regional assessments of lake water quality.

On a broad scale, the quality of inland and coastal surface waters is of great concern globally because so much of the world's population relies on these resources for employment, recreation, sustenance, drinking water and overall wellbeing. Remote sensing, along with tactical in situ sampling and monitoring, could play a useful role in helping to predict, alleviate and even prevent future water catastrophes (GEO, 2007 and Wood et al., 2011). Lakes, as well as oceans, have an important role in the global carbon cycle, but lakes have been largely ignored in carbon-climate models (Tranvik et al., 2009 and Battin et al., 2009). Thus, there is interest in extending the satellite-based capabilities

that have been developed to monitor chlorophyll and other water quality characteristics in the oceans to inland waters. Unfortunately, the methods used for open ocean ("Case I") waters are not effective in optically complex inland and coastal ("Case II") waters (GEO, 2007, Gitelson et al., 2009 and Moore et al., 1999).

Many challenges must be overcome if remote sensing techniques are to be used to assess water quality in inland and coastal waters on a routine basis. These include the development of appropriate atmospheric correction methods, evaluation of existing sensors and development of better ones, and development of algorithms to extract water quality information from raw sensor data (GEO, 2007). With numerous lakes of diverse size and varying water quality conditions spread across seven ecoregions and with proactive water quality monitoring programs of local and state agencies, Minnesota has the appropriate characteristics for studies to address these challenges.

In this paper we evaluate three alternative satellite systems and compare them with the Landsat: (1) MERIS (Medium Resolution Imaging Spectrometer) on the Envisat satellite, (2) MODIS (Moderate Resolution Imaging Spectroradiometer) on the Terra and Aqua satellites, and (3) AWiFS (Advanced Wide Field Sensor) sensor on the Indian IRS-2 satellite. Table 4.1 provides a summary of the systems. These systems have potential for use in regional assessments of surface waters because they collect images on a regular basis and their data are available at low or no cost. Two of the systems have improved spectral band sets, which should allow reliable assessment of additional water quality variables beyond water clarity. All three systems have lower spatial resolution than

Landsat, however, which limits assessments to water bodies larger in area than can be assessed with Landsat.

Table 4.1 Characteristics of the satellites and sensors studied.

Satellite/sensor	Spatial and Temporal Characteristics			Number of Spectral Bands				
	Resolution (m)	Frequency (days)	Swath (km)	Visible	Near IR	Mid IR	Thermal	Total
Landsat 7/ETM*	30	16	185	3	1	2	1	7
Landsat 5/TM	30	16	185	3	1	2	1	7
IRS-2/AWiFS	56	5	740	2	1	1		4
Envisat/MERIS	300	3	1,150	12	3			15
Aqua & Terra/MODIS	250	1	2,330	1	1			2
Aqua & Terra/MODIS	500	1	2,330	3	2	2		7**
Aqua & Terra/MODIS	1,000	1	2,330	10	8	2	16	36**

*Additional 15 m pan band

** Includes lower resolution bands

Our objectives were to: (1) evaluate the accuracy of these systems and their atmospherically corrected data products to measure important water quality variables on a regional scale, and (2) determine the minimum size and number of lakes that can be assessed with each system. Our overall goal was to develop reliable and inexpensive techniques for synoptic measurements of key indicators of lake water quality that can be used to complement data obtained by conventional ground-based methods. This is not a replacement for ground-based measurements but a way of obtaining measurements on lakes that have not been monitored and more synoptic measurements of complex lake systems, which can be difficult to monitor using ground-based methods. The work was conducted using images collected nearly concurrently and processed by methods similar

to those developed for regional assessments of water clarity from Landsat imagery (Chapter 2 (Olmanson et al., 2008)).

MODIS and MERIS imagery have been used routinely for global-scale assessments of oceanic chl *a*, but only a few previous studies have examined their usefulness for coastal waters and lakes; e.g., for MODIS, Chen et al. (2007) and Werdell et al. (2009), for MERIS, Alikas et al. (2008), Giardino et al. (2005), Matthews et al. (2010), Moses et al. (2009), and Odermatt et al. (2008, 2010). These studies indicate that the sensors have good potential for monitoring chl *a*, total suspended matter (TSM) and colored dissolved organic matter (CDOM). Also, there have been relatively few studies comparing different sensor systems; one is Reinart and Kutser (2006) which compares SeaWiFS, MODIS, MERIS and Hyperion for detecting cyanobacteria blooms in the Baltic Sea. Each study involved only a coastal area or one or a few lakes, however, and many used semi-analytical methods that require ground-based measurements of the inherent optical properties of each lake for proper model calibration. Such methods are not practical for regional assessments of hundreds to thousands of lakes. In contrast, our approach examines the capabilities and limitations of these sensors to measure water quality characteristics of large numbers of lakes across large regions.

4.2 Background Information

4.2.1 Satellite Imagery

Landsat satellites have collected imagery routinely throughout the world for four decades. The archive of Landsat imagery was invaluable in producing historical lake

water clarity assessments in Minnesota (Chapter 2 (Olmanson et al., 2008), Wisconsin (Chipman et al., 2004, Peckham and Lillesand, 2006) and for Lake Simcoe (Guan et al., 2011). The assessments were limited to water clarity (defined in terms of Secchi disk transparency) because the coarse spectral resolution of Landsat's bands does not permit unequivocal predictions of variables like chlorophyll. Landsat's relatively high spatial resolution (Table 4.1) allows lakes as small as ~4 ha to be assessed, but its repeat cycle of 16 days (eight days, as long as both Landsat 5 and 7 remain operational) imposes major limitations on intra-seasonal monitoring, especially in areas with frequent cloud cover.

Launched in 2002 on Envisat, the Medium Resolution Imaging Spectrometer (MERIS) sensor has 15 spectral bands with 300 m spatial resolution that can be programmed by ground control. MERIS has a three-day repeat cycle, and Minnesota is covered approximately two of every three days because of overlapping swaths. Its primary water resources application has been to monitor chlorophyll concentrations in the oceans in relation to the marine component of the global carbon cycle.

Launched in 1999 and 2002, the Moderate Resolution Imaging Spectroradiometer (MODIS) sensors on the Terra and Aqua satellites have 36 spectral bands with varying spatial resolution (Table 4.1). The satellites provide a twice daily repeat cycle with a wide swath. Because of its many bands and daily coverage, MODIS plays a key role in improving our understanding of landscape, oceanic and atmospheric dynamics. Like MERIS, it is used routinely to monitor chlorophyll concentrations in the oceans.

The Advanced Wide Field Sensor (AWiFS) on the Indian IRS-2 satellite was launched in 2003. It has only four spectral bands (Table 4.1) but does provide good spatial resolution (56 m) and a five-day repeat cycle. Its larger geographic coverage and higher temporal frequency (compared to Landsat) are potentially beneficial for routine water quality monitoring.

4.2.2 Inferring water quality characteristics from satellite imagery

Two related water quality characteristics of inland lakes that are measurable by satellite imagery are trophic state and water clarity. Trophic state typically is evaluated in terms of total phosphorus (TP) and chlorophyll *a* (chl *a*) concentrations and Secchi disk transparency (or Secchi depth, SD). Water clarity variables include turbidity, suspended solids, and Secchi depth. Except for TP, these variables have optical properties that can be inferred from multispectral satellite imagery. In many lakes TP is the limiting factor for chlorophyll, and in the late summer in Minnesota it is strongly correlated with chlorophyll and water clarity. Kutser et al. (1995) used these relationships to map TP, but because the relationship between TP and radiance or reflectance is only indirect, the correlation essentially is spurious. Mapping or prediction of non-optical water quality characteristics based on such indirect relationships is not appropriate. The most commonly measured variable in lakes, SD is a good indicator of phytoplankton abundance (or chlorophyll levels) in many lakes, but other constituents such as humic color and turbidity from suspended organic and inorganic particles also can affect SD measurements (e.g., Brezonik, 1978; Preisendorfer, 1986). These other constituents also have optical properties and can potentially be inferred from satellite imagery. Thus, it is

important to understand the conditions that affect lake water clarity and develop sensors that can differentiate among the clarity-influencing factors.

Two types of methods are used to estimate water quality characteristics from remote sensing data: empirical and semi-analytical. Empirical methods use in situ data on the characteristic of interest to calibrate a predetermined fixed model or regression analysis to determine the "best-fit" model using radiance data from available bands and band combinations. If each image is calibrated individually with in situ data spread throughout the image or study area, atmospheric correction or normalization of the image brightness data is unnecessary (Song et al., 2001) because atmospheric correction typically amounts to relative changes in pixel values that do not affect correlations with ground-based data. When multiple image dates are compared without field calibration, however, atmospheric correction is essential for accurate classifications (Keller, 2001, Song et al., 2001, and Kloiber et al., 2002a).

Semi-analytical methods use models of radiative transfer through the atmosphere and water. To work properly these methods require accurate atmospheric correction (Keller, 2001, Moses et al., 2009) and radiation field measurements of inherent optical properties (IOP) for the entire range of conditions in the water bodies being assessed. The latter requirement usually limits applications to one or a few lakes because changes in water quality can alter the IOP and invalidate calibrations, which leads to erroneous results (Odermatt et al., 2010). Radiation field data are not readily available for Minnesota lakes, and development of IOP to characterize the diverse conditions in Minnesota's lakes would be a daunting challenge. Moreover, the lack of IOP data for

most lakes renders the semi-analytical approach infeasible for large scale regional assessments.

4.3 Methods

4.3.1 Imagery

Landsat. Landsat 7 ETM+ reference imagery, used as a basis for comparison with the other imagery, was acquired on 25 August 2008, path 27 rows 26-30 (Figure 4.1), with the "scan line corrector" off (SLC off). Chapter 2 (Olmanson et al., 2008) found that such imagery worked as well for water clarity assessment as earlier (intact) ETM+ imagery because only a representative sample of pixels is needed from each lake. This Landsat image was clear throughout Minnesota and includes spectral-radiometric data for > 6,000 lakes with a good representation of water quality conditions statewide. The image covers parts of three major ecoregions: the Western Corn Belt Plains, an agriculturally dominated ecoregion with eutrophic lakes, the North Central Hardwood Forest, a transitional ecoregion that includes metropolitan Minneapolis and St. Paul, and the Northern Lakes and Forest ecoregion, which is dominated by lakes, wetlands and forested land and contains the clearest lakes in the state.

MERIS. We tested three MERIS products acquired on 25 August 2008: (1) L1, calibrated top of the atmosphere (TOA) radiance, (2) L2, surface radiance/reflectance, and (3) water-leaving reflectance (MERIS C2) that we derived from L1 using the Case 2 Regional Processor version 1.4.1 neural network algorithms in the BEAM version 4.7 image processing software (BEAM, 2010; Doerffer and Schiller, 2008a, b). We used the

first two products as acquired. These images were mostly clear throughout the state (Figure 4.2).

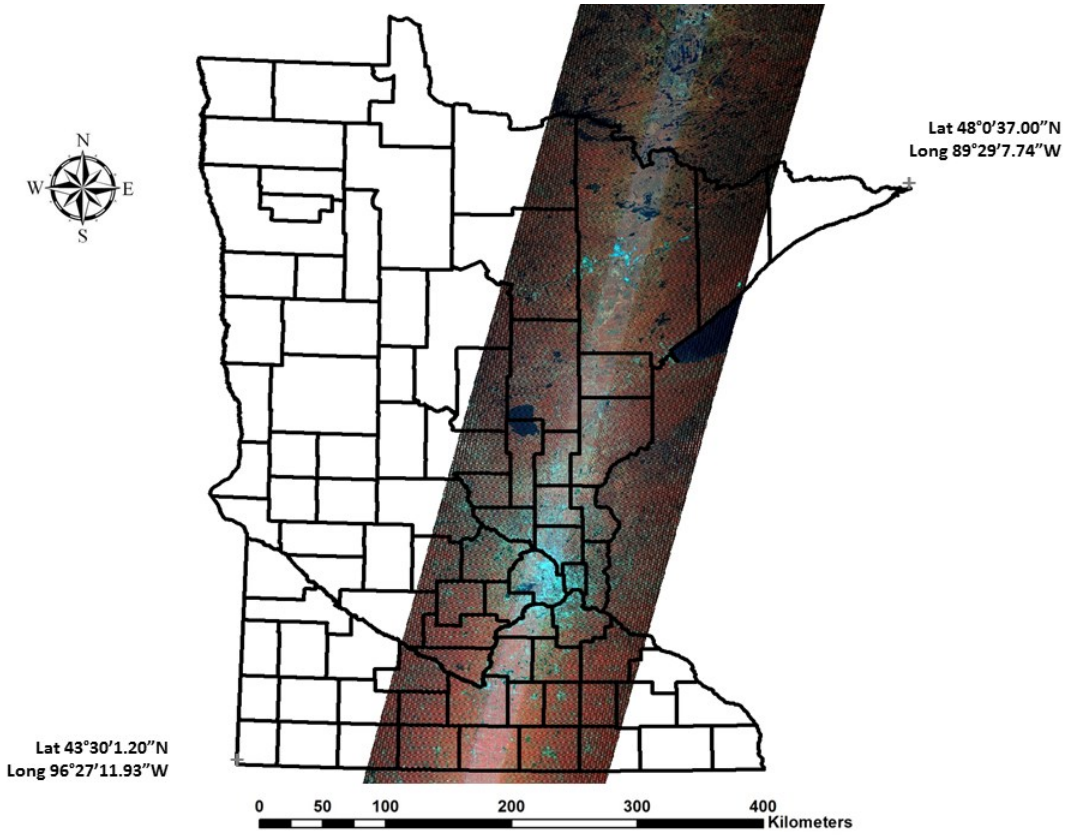

Figure 4.1 Landsat ETM+ with SLC off, Path 27 Rows 26 through 30, 25 August 2008.

The dark pixel method usually used for atmospheric correction on Case I waters, which assumes a zero near infrared (NIR) water-leaving radiance, fails in Case II waters because there is significant water-leaving radiance in both the visible and NIR. If one assumes that the NIR signal is caused solely by atmospheric contributions and extrapolates these measurements to correct visible bands, essential components of the signal are removed (Moore et al., 1999). The standard atmospherically corrected MERIS

L2 surface radiance/reflectance products thus use different procedures for Case I and Case II waters. Case I waters are processed by conventional methods (Gordon and Wang, 1994), and Case II waters are processed using the "bright pixel" atmospheric correction method, which assumes significant water-leaving radiance exists in both the visible and NIR, and uses an iterative process to separate the atmosphere contribution from the water-leaving radiance. The conventional atmospheric correction method (Gordon and Wang, 1994) then is used with the derived atmospheric scattering to retrieve water-leaving radiance/reflectance for all wavelengths (Moore et al., 1999).

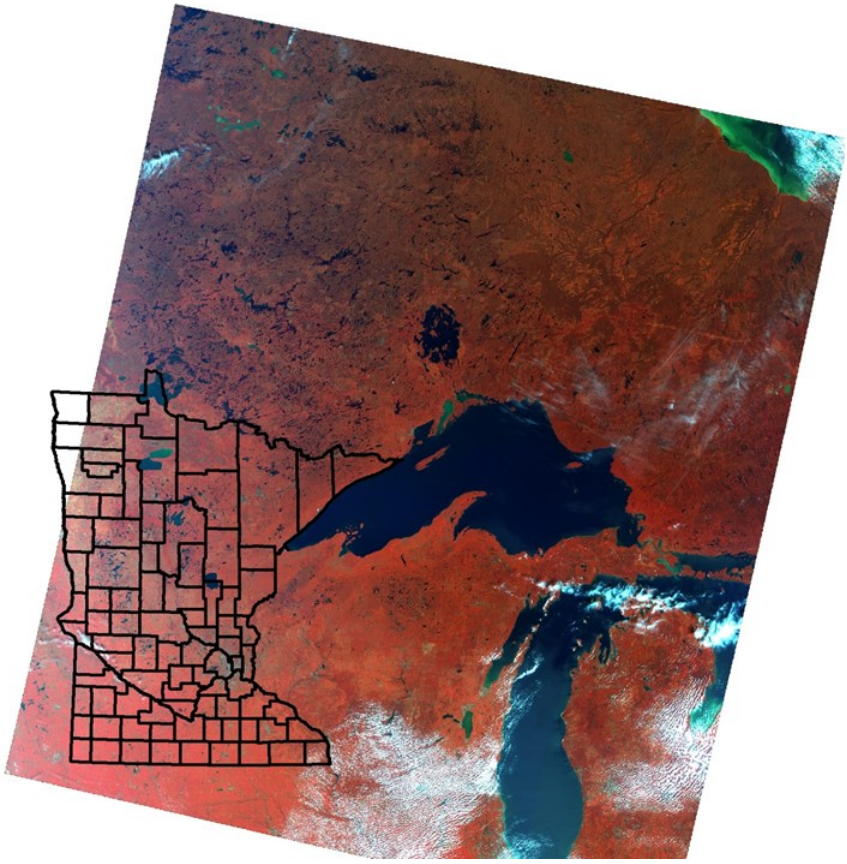

Figure 4.2 MERIS L1 TOA calibrated radiance, 25 August 2008.

The other atmospherically corrected MERIS product we tested (MERIS C2) was developed specifically for Case II waters. Water leaving radiance/reflectance was retrieved for 12 wavebands using relationships between TOA radiances from the L1 product and water-leaving radiance simulated by radiative transfer solutions (BEAM, 2010 and Doerffer and Schiller, 2008a, b).

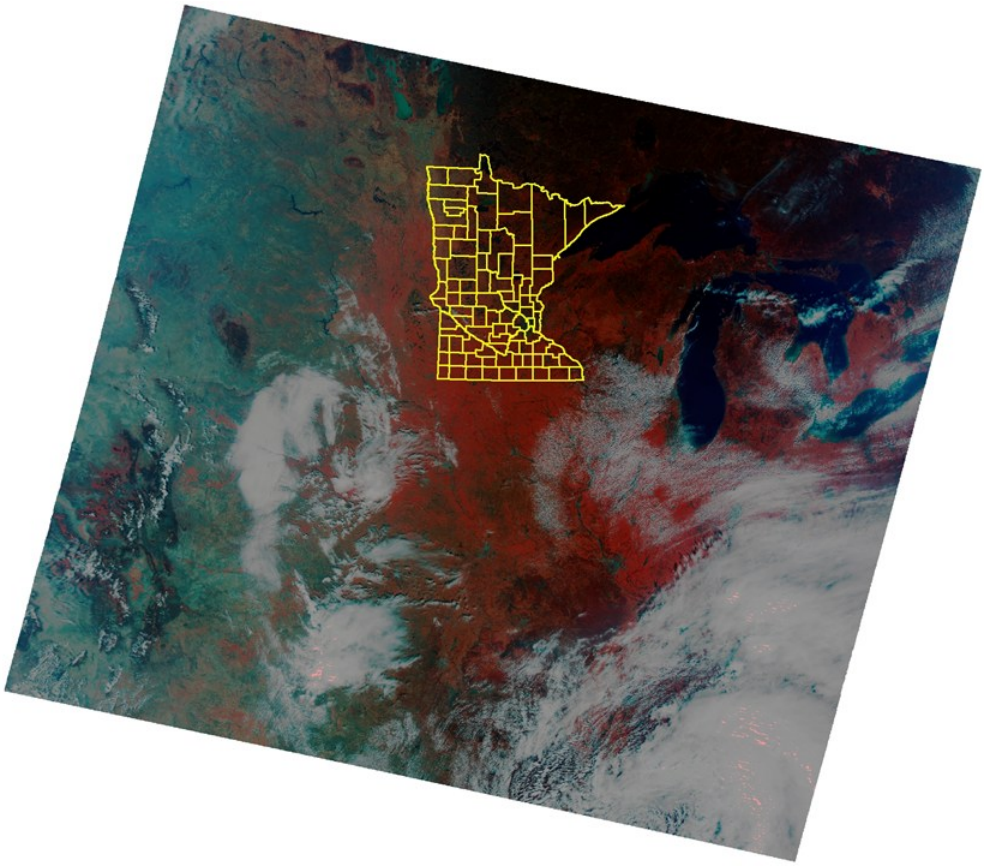

Figure 4.3 MODIS Terra 500 m calibrated radiance, 25 August 2008.

MODIS. We tested four MODIS products: (1) 250 m and (2) 500 m MOD02 Level 1B calibrated radiances, (3) 500 m MOD09 8-day composite surface reflectance products, all from the Terra satellite, and (4) 1,000 m MOD02 Level 1B calibrated

radiances from the Aqua satellite for 25 August 2008. These images also were mostly clear throughout Minnesota (Figure 4.3). The atmospheric correction method used for MOD09 surface reflectance was designed for land features and uses gas and aerosol information derived from MODIS data. It also corrects for adjacency effects, which is the atmospheric scattering of light from contrasting (relatively bright) neighboring surfaces. This method has the benefit of using bands in the middle or shortwave infrared (SWIR), where the dark pixel assumption is generally valid over surface waters, which may improve the correction in these areas (Shi and Wang, 2009).

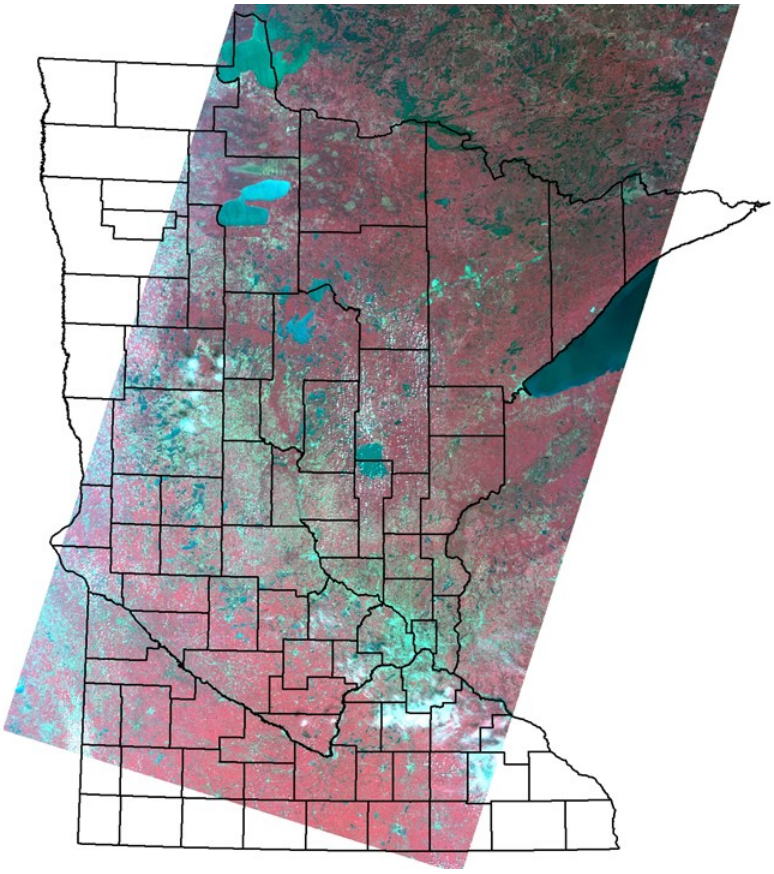

Figure 4.4 AWiFS, 26 August 2008.

AWiFS. No AWiFS image was available for 25 August 2008, the date of the Landsat, MERIS and MODIS images. An AWiFS image was available for 26 August 2008 (Figure 4.4), but it had more cloud and haze cover than those from the previous day, making comparison with the other images difficult. For accurate water quality assessments, it is essential to use imagery without cloud cover or haze, which affect spectral-radiometric responses and cause erroneous results that are difficult or impossible to remedy. Other late summer AWiFS images from 2008 also were not clear, and the August 26 AWiFS image thus was used with caution.

4.3.2 Water quality data

The Minnesota Pollution Control Agency (MPCA) provided water quality data for image calibration based largely on volunteer efforts of a Citizen Lake Monitoring Program (CLMP) and routine monitoring activities of the MPCA and many local management agencies. Chlorophyll *a* corrected for pheophytin was measured by several laboratories in the state using standard procedures: APHA-10200h (Greenberg et al., 1992), ASTM D3731-87 (ASTM, 1994), and USEPA-445 (U.S. EPA, 1992). To calibrate the imagery we used water clarity data (Secchi depth, SD) and chl *a* data collected within $\pm$3 days of the image acquisition date. Ideally, calibration data would be collected at the same time as the image acquisition, but for historical assessments this generally is not the case. Several studies (Chipman et al., 2004, Kloiber et al., 2002b, and Chapter 2 (Olmanson et al., 2008)) have shown that good results can be obtained with data collected within a few days of the imagery and that the larger number of ground observations with the longer time window offsets some of the possible loss of correlation. In these past

studies, model parameter values did not change significantly with a wider time window. We concluded that measurements taken within a few (±3) days of image acquisition would provide adequate relationships Although chlorophyll and water clarity exhibit strong seasonal patterns in temperate lakes, large and rapid fluctuations usually do not occur during the relatively stable late summer (Stadelmann et al., 2001). There were 545 SD and 298 chl *a* measurements collected statewide within the above time frame.

4.3.3 Image Processing and Classification

The basic image classification procedures used were described by Olmanson et al. (2001) and Kloiber et al. (2002a). Modifications were made to account for the different sources of imagery or when experience and advances in software and computer hardware enabled simpler or improved image processing procedures. We used Leica Geosystems ERDAS Imagine, Brockmann Consult's BEAM toolbox, MODIS Swath Reprojection Tool, MODIS Reprojection Tool and Esri ArcGIS for image processing. Acquiring a representative sample for each lake from the image was a primary objective. Image samples generally were near the center of each lake, where reflectance from aquatic vegetation, the shoreline, or the lake bottom did not affect the spectral-radiometric response.

Initial image preprocessing included reprojection to UTM Zone 15 NAD 83 using the appropriate reprojection tool for each image. The MERIS C2 water-leaving radiance/reflectance product was derived from MERIS L1 data using Case 2 Regional Processor algorithms (BEAM, 2010 and Doerffer and Schiller, 2008a, b).

The atmospheric correction method for the MERIS L2 product yielded many water pixels throughout the image with apparent negative reflectance in most of the visible and NIR bands. Because removing these pixels would have left very few lakes that could be assessed, the imagery was rescaled by adding the lowest negative value for each band plus one to the data. We imported each imagery product into ERDAS Imagine, clipped areas covered with clouds, and checked for haze by inspecting the image using several RGB band combinations to highlight haze. Areas with high levels of haze were excluded.

Once image preprocessing was complete, a "water-only" image was produced by performing an unsupervised classification method based on ISODATA clustering. Because water features have spectral characteristics distinct from terrestrial features, water pixels were grouped into one or a few distinct classes that could be easily identified. We then masked out terrestrial features to create a water-only image, performed an unsupervised classification on this image, and generated spectral signatures of each class. We used these signatures, along with the location where the pixels occur, to differentiate four classes of pixels: (1) open water, (2) shallow water (where sediment and/or macrophytes affect spectral response), (3) those exhibiting adjacency effects and (4) erroneous values. The last three classes tend to have high spatial variability compared to open water pixels. Based on this analysis, we removed the affected pixels.

Next, the spectral-radiometric data from the "open water" images were obtained to develop relationships with measured water quality data. For this purpose, we used a lake polygon layer with 12,049 polygons delineating lakes or lake basins (Olmanson et

al., 2001) to help automate the process. The signature editor in ERDAS Imagine was used to extract spectral data from the images for all the lakes. Using a histogram analysis procedure (Chipman et al., 2004, and Olmanson et al., 2001), we calculated the mean band values from the middle 50% of the pixels and imported these values into Microsoft Excel. To avoid reliance on samples with only a few pixels, lakes with fewer than six (three remaining) pixels were removed. Ratios and differences for all band combinations were calculated, and field data were linked to the appropriate lake sample.

To develop models to estimate SD and chl *a* from the imagery products, we performed forward step-wise regressions of the band data sets using the JMP 8.0 statistical software package by SAS Institute, Inc. Raw and log-transformed values of each water quality variable were the dependent variables and single bands, band ratios and band differences were the independent variables. From these results, we used the two independent variables that contributed most to the regression fit and applied them in a second multiple regression using the general form:

(WQ var) or ln(WQ var) = a(band or combination) + b(band or combination) + c

where a, b and c are coefficients fit to the calibration data by the regression analysis, ln(WQ var) is the natural logarithm (ln) of the water quality variable for a given lake, and "band or combination" is the image brightness, radiance or reflectance value for the selected lake pixels in the best fit band, band ratios or band differences, respectively. The models developed for each variable and each image product were applied to each pixel to create pixel-level chl *a* and SD maps.

For comparisons between chl *a* and SD maps, we converted the results to their corresponding trophic-state indices using the formulas (Carlson, 1977):

$$TSI(\text{chl } a) = 9.81\ln(\text{chl } a) + 30.6$$

$$TSI(SD) = 60 - 14.41\ln(SD)$$

These equations essentially convert SD and chl *a* data to a common (TSI) scale based on a best-fit hyperbolic relationship between the two variables.

4.4 Results and Discussion

4.4.1 Spectral Characteristics of the Sensors

For accurate estimation of water quality characteristics like chl *a* using remote sensing, it is important to have sensors with well positioned spectral bands. Figure 4.5 shows reflectance spectra of 15 Minnesota lakes from ground-based spectral-radiometric measurements with the visible and near infrared spectral band positions of Landsat, MERIS and MODIS superimposed. The 15 lakes include a broad range of chl *a* and humic color concentrations (Menken et al., 2006), reflecting the diversity of lakes in Minnesota. The broad spectral bands of Landsat TM and ETM+ and the MODIS 250 and 500 m bands do not discriminate the absorption and scattering characteristics of phytoplankton and thus are not as well suited for chlorophyll measurements. In contrast, the relatively narrow MERIS bands are centered to measure the absorption and scattering characteristics of chlorophyll, and the MODIS 1000 m bands also measure many of the absorption and scattering characteristics of chlorophyll. Several other ground-based field studies have used spectroradiometers to explore relationships between chl *a* and water-

leaving reflectance of lakes (e.g., Dall'Olmo and Gitelson, 2005, Gitelson et al., 2008, Gons, 1999, and Schalles et al., 1998) and identified spectral features potentially useful for developing accurate predictive equations for chl *a* under a wide range of biophysical and optical conditions. The position and width of spectral bands is fundamental to how well water-leaving reflectance can be characterized and used to estimate variables like chl *a* and CDOM.

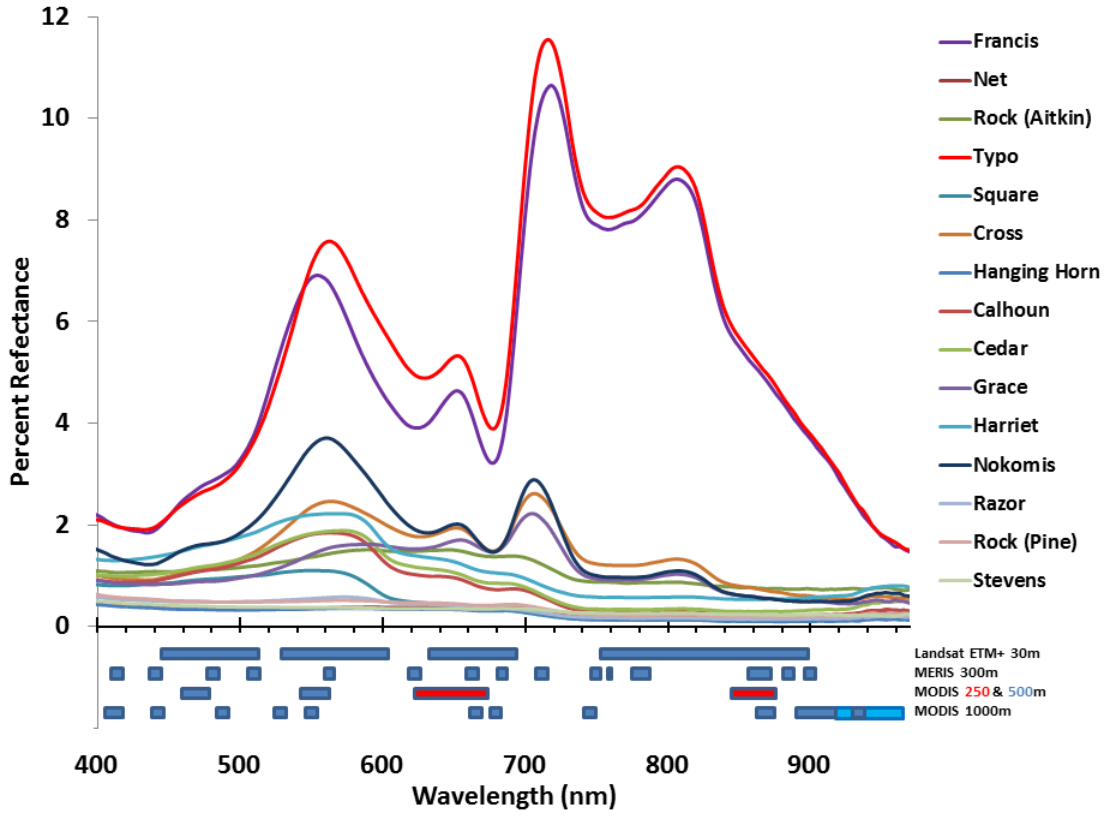

Figure 4.5 Reflectance spectra of 15 Minnesota lakes with Landsat, MERIS and MODIS band locations indicated; spectra plotted from data used in Menken et al. (2006).

To evaluate how well the MERIS band set accurately represents the reflectance spectra of lakes, we calculated mean values of reflectance from the hyperspectral plots in

Figure 4.5 over the range of each MERIS band, plotted the results at the center wavelength of each band, and drew smooth curves through the data points (Figure 4.6). The resulting "MERIS-simulated" reflectance spectra accurately represent most of the spectral characteristics of lakes shown in the hyperspectral reflectance spectra (Figure 4.5), which suggests that MERIS is well suited for assessing a variety of optically related water quality characteristics.

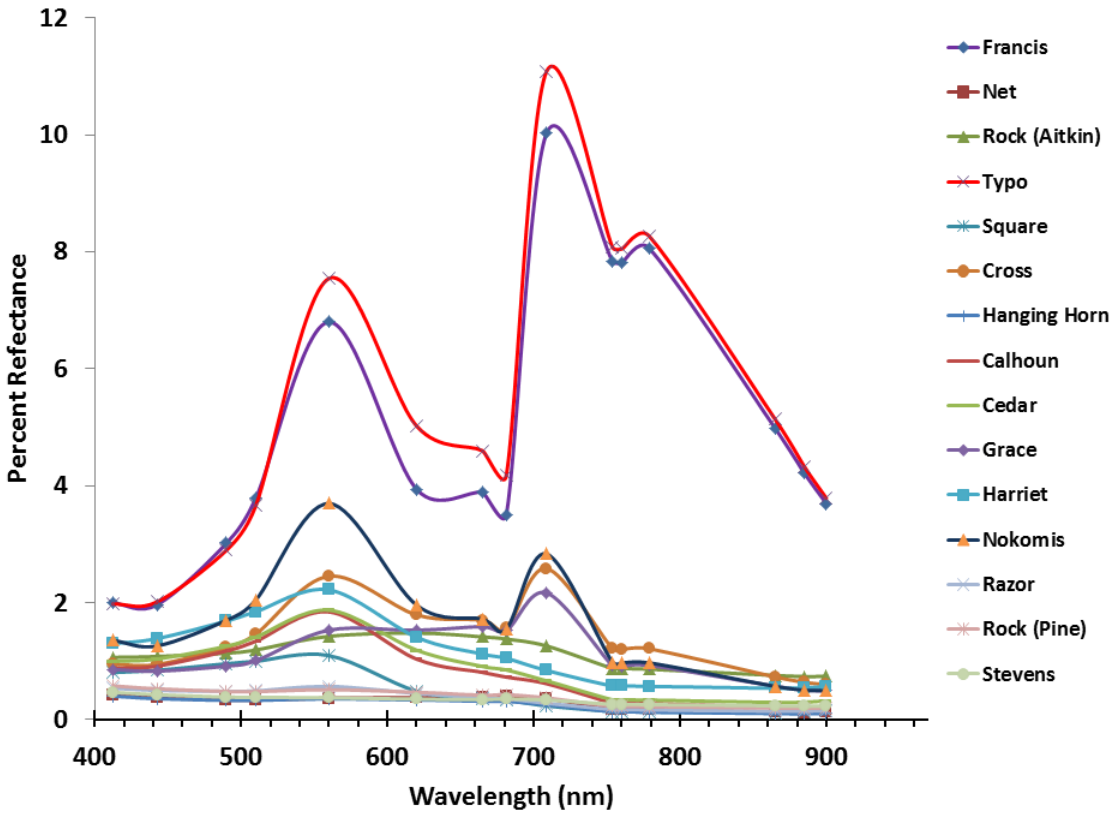

Figure 4.6 Reflectance spectra of 15 Minnesota lakes using simulated MERIS band set calculated from Menken et al. (2006) hyperspectral reflectance data.

4.4.2 Model Development

Several models developed by regression analysis from the image products showed strong relationships between both log transformed and non-transformed values of SD and chl *a* and the spectral-radiometric responses of data from the Landsat, MERIS and MODIS sensors. The non-transformed in situ data were not normally distributed (Figure 4.7), but the log transformed data were or were nearly so (Figure 4.8). They thus met the assumptions of regression and produced models with improved fits in the important chl *a* range of 0-20 μg/L. Therefore, models based on log-transformed data were used for image comparisons.

Table 4.2 summarizes the calibration model statistics for SD and chl *a* for the Landsat, MERIS and MODIS imagery products that we examined and includes the ranges for the two variables (which differed for each product), the bands used in the best-fit relationship, adjusted R^2, RMSE, and number of data points for each model. It is apparent that some products yielded better results than others. Adjusted R^2 values ranged from 0.50 (MERIS C2) to 0.83 (Landsat ETM and MERIS L1) for SD and from 0.41 (MERIS C2) to 0.85 (MERIS L1) for chl *a*.

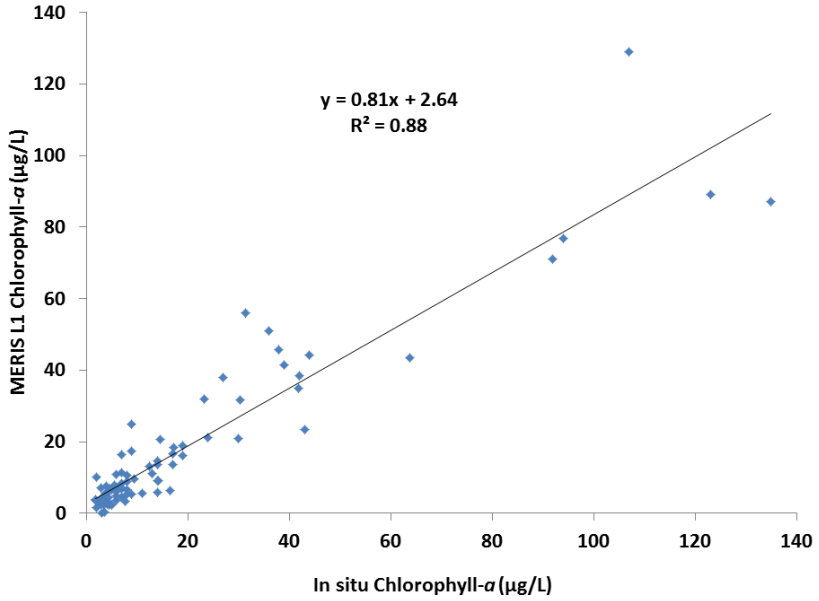

Figure 4.7 Scatter plot of MERIS L1 inferred Chl *a* using non-transformed model vs. in situ Chl *a* (note the non-normal distribution of chlorophyll data).

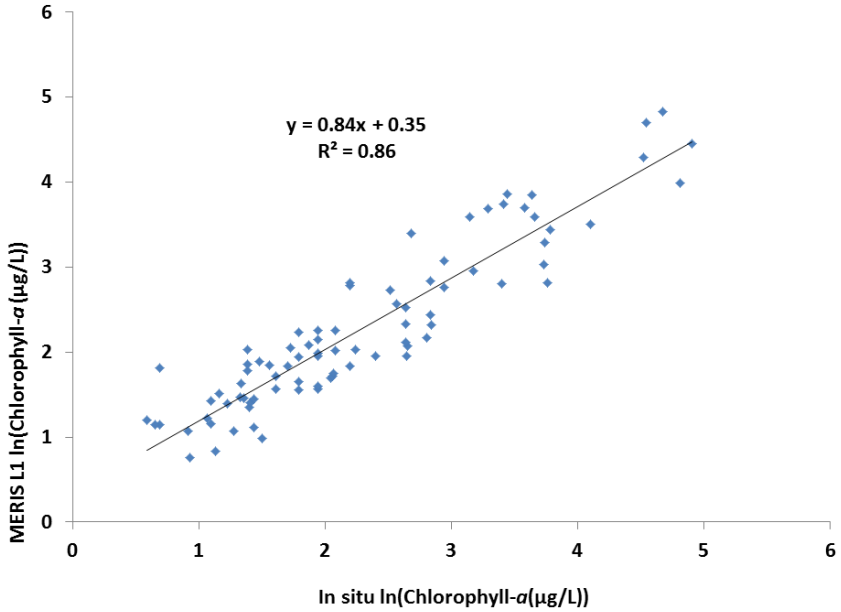

Figure 4.8 Scatter plot of MERIS L1 inferred ln(Chl a) using log transformed model vs. in situ ln(Chl a) (note the near normal distribution of log transformed chlorophyll data).

Table 4.2 Image processing calibration model statistics for Landsat, MERIS and MODIS data (8/25/2008 images).

	Secchi Disk Transparency (m)					Chl- a (µg/L)				
Imagery Product	**N**	**Range**	**Best fit bands**	**[a]R^2**	**RMSE**	**N**	**Range**	**Best fit bands**	**[a]R^2**	**RMSE**
Landsat ETM+ SLC off	280	0.1-9.8	TM1/TM3, TM1	0.83	0.347	177	1-540	TM1/TM3, TM3-TM4	0.79	0.626
MERIS TOA radiance L1	229	0.3-7.6	490/665, 708-754	0.83	0.270	90	2-135	708/754, 510/665	0.85	0.408
MERIS Surface rad/Reflec L2	140	0.1-6.6	665-681, 510/665	0.77	0.312	56	2-123	708/754, 510/665	0.76	0.478
MERIS C2 Water leaving reflec	186	0.1-6.6	490-560, 620/681	0.50	0.578	75	2-135	412-560, 708/754	0.41	0.879
MODIS 250 m radiance L1B	305	0.1-9.8	MO1	0.65	0.449	123	2-272	MO1	0.57	0.740
MODIS 500 m radiance L1B	110	0.1-6.6	MO1/MO3, MO4	0.75	0.294	42	2-75	MO1/MO3, MO5/MO6	0.79	0.403
MODIS 1000 m radiance L1B	7	1.7-3.1	667/678	0.77	0.106	6	3-17	667-678	0.61	0.441
MODIS 8-day surface reflec	110	0.1-6.6	MO1/MO3, MO3-MO7	0.75	0.279	47	2-272	MO1/MO3, MO3/MO6	0.78	0.449

[a]Adjusted R^2

Table 4.3 Size and number of Minnesota lakes assessed with Landsat, MERIS and MODIS data.

Imagery Product[a]	Spatial Resolution (m)	No. of Lakes	Lake Size (ha[b])
Landsat ETM+ SLC off	30	~10,500	4
MERIS TOA radiance L1	300	896	150
MERIS Surface rad/reflec L2	300	471	300
MERIS C2 Water leaving reflec	300	664	250
MODIS 250 m radiance L1B	250	1257	125
MODIS 500 m radiance L1B	500	385	400
MODIS 1000 m radiance L1B	1000	57	1000
MODIS 8-day surface reflec	500	385	400

[a]8/25/2008 images except MODIS 8-day which was an 8-day composite.

[b]Greater than fifty percent of lakes around this size assessed using this imagery.

The range in spatial resolution of the sensors (30-1000 m) resulted in a wide range in the lake size (area) that could be assessed with each sensor. This, in turn, had a large effect on the number of Minnesota lakes that each sensor could assess (Table 4.3). By far, Landsat ETM+ has the finest spatial resolution, enabling us to assess lakes as small as 4 ha (> 10,000 Minnesota lakes) with its data. For the other sensors/imagery products (excluding AWiFS which is discussed below), minimum lake size ranged from 125 to 1,000 ha, and the corresponding numbers of lakes amenable to assessment ranged from 1,257 to 57 respectively.

Because we tested systems with different spectral characteristics, models developed for one system may not be applicable to other systems. Several band combinations had strong relationships with in situ data; our goal, however, is not to recommend an "overall best model" for regional assessment but only to describe the model that worked best for each type of imagery with the available field data.

Landsat. The broad spectral bands of Landsat TM and ETM+ do not discriminate the absorption and scattering characteristics of chl *a* and thus are not well suited for its measurement. Although Landsat cannot distinguish reliably between phytoplankton and other constituents that affect water clarity, strong correlations of Landsat radiance values with both chl *a* and SD were expected because water clarity in Minnesota's lakes is strongly correlated with phytoplankton concentrations (Figure 4.9). In such lakes, Landsat probably can be used for reasonable estimates of either chl *a* or water clarity if calibration data are available; 177 chl *a* and 290 SD measurements were available within ±3 days of the 25 August 2008 Landsat image. The fit between Landsat radiance and chl

a was strong (adjusted $R^2 = 0.79$; Table 4.2), and that for SD even stronger (adjusted $R^2 = 0.83$). Chl *a* and SD maps (not shown) were very similar when the results were normalized and plotted in terms of TSI values, suggesting that Landsat images can be calibrated using chlorophyll data, but there may not be any more information than if calibrated with SD data.

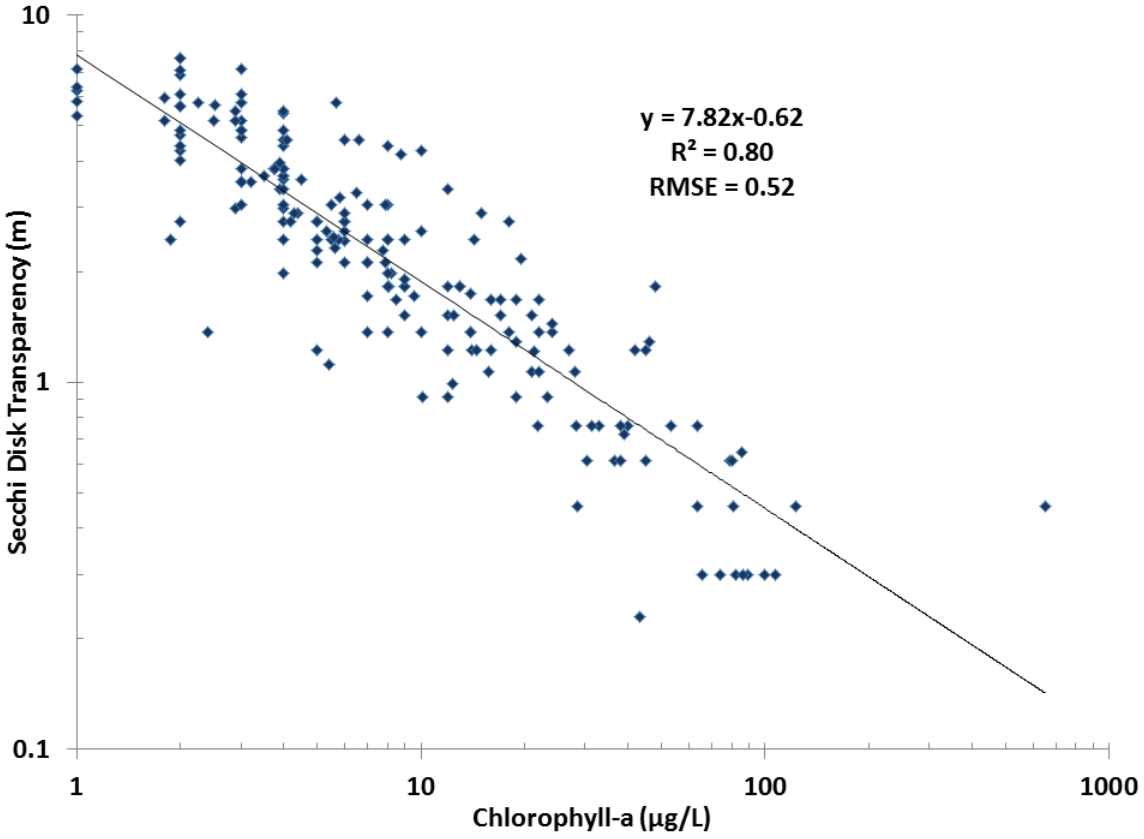

Figure 4.9 Plot of in situ calibration data for SD vs. chl *a*.

MERIS. The fit between MERIS L1 calibrated radiance and chl *a* was the strongest among the sensors and products we tested (adjusted $R^2 = 0.85$), and the fit between MERIS L1 data and SD also was strong (adjusted $R^2 = 0.83$). The chl *a* and SD

maps (not shown) showed some differences when the results were plotted using the normalized TSI scale, which indicates that the MERIS spectral resolution enables one to distinguish phytoplankton from humic color and non-living suspended solids. We did not have data on these characteristics, however, to test this quantitatively.

The main drawback of MERIS is its coarse spatial resolution (300 m), which limits the lakes that can be assessed reliably to those larger than ~150 ha (depending on shape, depth and extent of aquatic vegetation). This reduced the data available for image calibration to 90 chl *a* and 229 SD measurements; the total number of Minnesota lakes that could be assessed was ~900, or 8.5 percent of those that could be assessed with Landsat.

In addition to higher spectral resolution, MERIS has higher temporal resolution than Landsat (coverage of Minnesota two out of every three days, a result of its large swath and overlap area). High temporal resolution is important because it increases the probability of acquiring clear imagery. For example, up to three years were needed to acquire clear late-summer Landsat imagery for the entire state for some time periods (Chapter 2 (Olmanson et al., 2008)). In this study we were unable to obtain an AWiFS image on August 25 to compare with the other images because the five-day repeat cycle for AWiFS did not provide a fly-over of Minnesota on that date. The wide swath of MERIS allows all of Minnesota along with Wisconsin or North and South Dakota and large portions of Canada to be assessed using one image (Figure 4.2), making MERIS potentially useful for national lake water quality assessments.

It was beyond our scope to determine the best atmospheric correction or normalization technique, but it is reasonable to expect that accurate atmospheric correction will yield more accurate classification results (Song et al., 2001). Accurate atmospheric correction would be essential for satellite-based routine assessments that are not based on concurrent in situ calibration data. The atmospherically corrected products we tested (MERIS L2 and MERIS C2) did not perform as well, however, as the uncorrected MERIS L1 product. We found that the MERIS L2 surface radiance/reflectance product had amplified adjacency effects, and some areas with erroneous pixel values limited the pixels that were suitable for chl *a* and SD predictions. Although this did not have appreciable effects on large lakes, it limited the minimum lake size that could be assessed to ~300 ha, of which there are only ~470 in Minnesota (about half as many as could be assessed with MERIS L1 data). The fit between MERIS L2 and chl *a*, although not as strong as that for MERIS L1, nonetheless was fairly strong (adjusted $R^2 = 0.76$; Table 4.2). The fit between MERIS L2 data and SD also was strong (adjusted $R^2 = 0.77$). The main drawbacks of MERIS L2 data are that (1) the number of lakes that can be assessed is small (only about 4.5 percent of the lakes that can be assessed with Landsat), and (2) the correlation was poorer than with MERIS L1 data.

The MERIS C2 product performed poorly relative to MERIS L1 and L2. Adjacency effects, although not as extensive as with MERIS L2, limited the size of lakes that could be assessed to those larger than ~250 ha (i.e., ~665 in Minnesota, or ~70 percent of the number that could be assessed with MERIS L1 data).The fits between MERIS C2 and chl *a* and SD were poor (adjusted $R^2 = 0.41$ and 0.50, respectively).

Moses et al. (2009) also found that MERIS C2 data performed significantly worse than MERIS L2 data for chl *a* estimations > 35 µg/L in Taganrog Bay and the Azov Sea in Russia. Giardino et al. (2010) found that MERIS C2 reflectance values deviated significantly from in situ reflectance beyond the red wavelengths, and they used an alternative atmospheric correction method for their chlorophyll model.

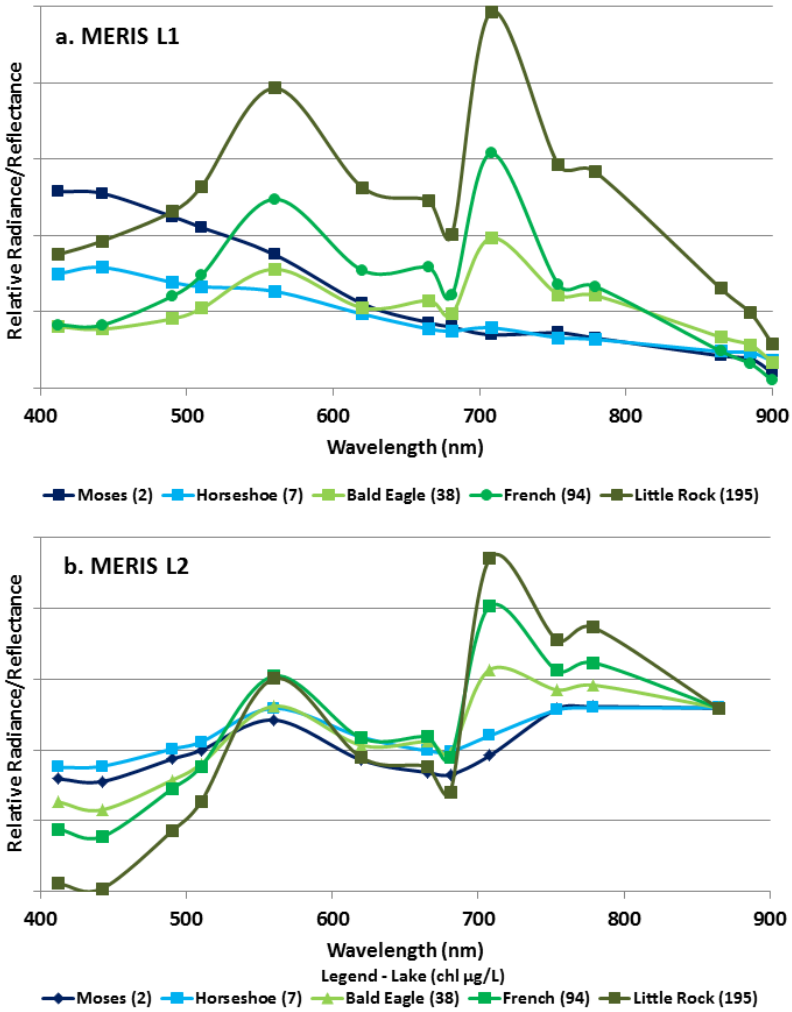

Figure 4.10 Reflectance spectra of lakes with low to high chl *a*: (a) MERIS L1 DOS corrected TOA calibrated radiance of five lakes; (b) MERIS L2 surface radiance/reflectance of five lakes.

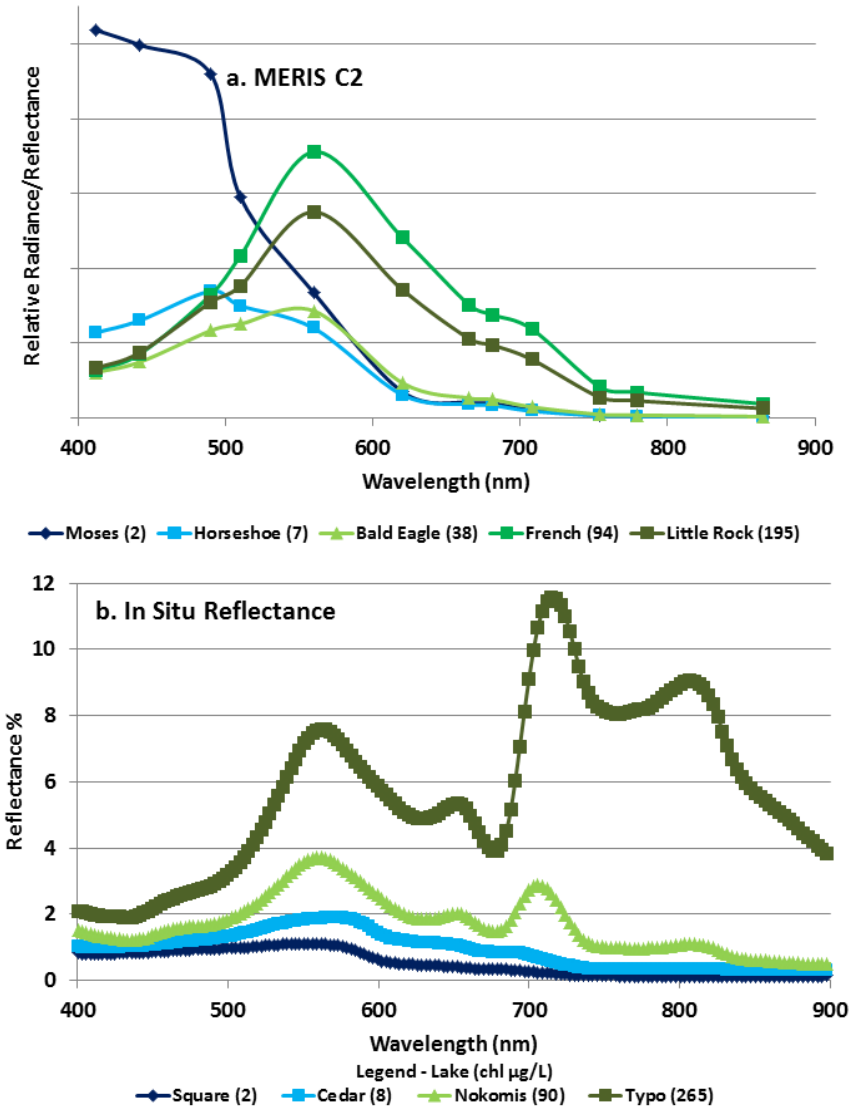

Figure 4.11 Reflectance spectra of lakes with low to high chl *a*: (a) MERIS C2 water-leaving radiance/reflectance of five lakes; (b) Ground-based reflectance measurements of four chlorophyll-dominated lakes from Menken et al. (2006).

To compare the reflectance spectra of lakes from the three MERIS products, dark object subtraction (Song et al., 2001) was performed on the MERIS L1 data for five lakes with chlorophyll concentrations ranging from 2 to 195 µg/L (Figure 4.10a); the MERIS

L2 and C2 reflectance spectra of the same lakes are in Figures 4.10b and 4.11a, respectively. For comparison, Figure 4.11b shows ground-based hyperspectral reflectances (Menken et al., 2006) of four lakes with IOPs dominated by phytoplankton (chlorophyll range from 2 to 265 μg/L). Having an accurately atmospherically corrected product would enable the use of a semi-analytical algorithm or universal equation for routine assessments without the need for simultaneous ground-based calibration data, and this remains an important goal. It is apparent, however, that the MERIS L2 and C2 products do not meet that goal. The MERIS L1 data with a simple dark object subtraction resemble the ground-based data (Figure 4.10a) more closely than the MERIS L2 (corrected for negative values) and C2 products. Many chlorophyll characteristics in the red and near infrared region apparent in the other products are missing in the MERIS C2 results; this is similar to the findings of Giardino et al. (2010).

MODIS. The MODIS 1000 m bands are well suited spectrally for water quality monitoring, but the coarse spatial resolution limits the system to monitoring lakes larger than ~1,000 ha, of which there are only 57 in Minnesota. Only seven SD and three chl *a* measurements were available on these lakes within ±3 days of the image. We expanded the window to ±7 days for chl *a*, which increased the measurements to six, but this still posed limits on model development. Nonetheless, the fits between MODIS 1000 m calibrated radiance data and in situ chl *a* and SD were acceptable (adjusted $R^2 = 0.61$ and 0.77, respectively). Because of the limited amount and range of data available for calibration, these results should be used with caution.

Monitoring a greater number of lakes in Minnesota by MODIS would require use of the 250 and 500 m bands, which are spectrally similar to Landsat TM/ETM+ bands and thus not well suited for chl *a* assessment. With only two spectral bands, the fits between MODIS 250 m calibrated radiance data and chl *a* and SD were relatively poor (adjusted R^2 = 0.57 and 0.65, respectively; Table 4.2). The fits between MODIS 500 m calibrated radiance data (which includes the 250 m bands) and chl *a* and SD were stronger (adjusted R^2 = 0.79 and 0.75, respectively). The atmospherically corrected (500 m) eight-day surface reflectance product of MODIS was intended for land applications, but it performed as well as or better than the MERIS atmospherically corrected products we tested and as well as the MODIS calibrated radiance data. The fits between MODIS surface reflectance data and in situ chl *a* and SD were strong (adjusted R^2 = 0.78 and 0.75, respectively; Table 4.2).

The drawbacks of MODIS for lake assessments are the low spectral resolution of the 250 and 500 m data and the coarse spatial resolution, which limits the lakes that can be assessed reliably to those larger than ~400 ha for the 500 m data (depending on shape, depth and extent of aquatic vegetation). This reduced the number of lakes with data for image calibration to 47 for chl *a* and 110 for SD, and the number that could be assessed was ~400 (3.7 percent of the number that can be assessed with Landsat). The coarse spatial resolution of the 1,000 m bands limits their use to a small number of large lakes in Minnesota (< 1 percent of the total lakes in the state). Nonetheless, MODIS does have the advantage of high temporal resolution, and its wide swath allows all of Minnesota along

with other parts of the central United States and Canada to be assessed using one clear image (Figure 4.3).

AWiFS. Large portions of the 26 August 2008 AWiFS image were not usable because it had more cloud and haze cover than the Landsat, MERIS and MODIS images from the previous day. The lack of blue and thermal bands in AWiFS, which can be used in Landsat images to identify areas affected by haze (Chapter 2 (Olmanson et al., 2008)), reduced our ability to accurately detect areas affected by haze. Although areas with cloud cover were removed from the AWiFS image, areas affected by haze likely remained and probably affected the spectral-radiometric response. The fits between AWiFS and in situ data were poor (R^2 = 0.03 and 0.005 for chl *a* and SD, respectively) —indeed much poorer than would be expected just based on the limited number of available bands. Because we could not make a fair assessment of the accuracy of AWiFS for assessment of chl *a* and SD and because the AWiFS image is not comparable with the other images, the calibrations and other statistics are not reported.

4.5 General Discussion and Conclusions

MODIS and MERIS imagery are well suited for regional assessments of chl *a* and other optically-related water quality characteristics of large inland lakes, but their coarse spatial resolution greatly limits the number of lakes that can be assessed. The spatial resolution of Landsat allows all lakes ≥ 4 ha to be assessed, but its low spectral resolution limits it to assessing water clarity. Similarly, the 56 m spatial resolution of AWiFS allows relatively small lakes to be assessed, but its low spectral resolution and lack of blue and

thermal bands impact the ability to identify haze and may limit its use in water quality assessments.

The positions and widths of the MERIS bands allow the measurement of key spectral-radiometric characteristics of phytoplankton, and this sensor is well suited for chlorophyll assessment of moderately large inland water bodies. The MODIS atmospheric correction algorithm using the SWIR bands performed better than the methods used for MERIS. All the systems tested could be used for regional water clarity assessments, but MERIS is the only sensor with sufficient spectral and spatial resolution suitable for large (>150 ha) lakes that appears to be practical for regional chlorophyll assessment.

Although none of the sensors investigated provides ideal imagery for regional assessments of surface water quality conditions, the characteristics of an ideal system in terms of spectral, spatial and temporal resolution have been identified. With technological advancements, the need for trade-offs between these characteristics is becoming less important, and a system that is ideally suited for regional assessments of inland and coastal waters appears to be technologically feasible. A reasonable goal for such a sensor may be a band set that includes the key bands, acquisition frequency, and swath of the MERIS sensor with moderate spatial resolution of perhaps 30 to100 m, which would enable most lakes to be assessed and still allow for the wider swath desirable for large regional assessments. Daily or near daily imagery greatly increases the probability of acquiring imagery when conditions are clear. A new system with high frequency of image acquisition, spectral bands intended for water (similar to the visible

and near infrared bands of MERIS, which target important spectral characteristics of water, and the shortwave infrared bands of MODIS, which improve atmospheric correction), and accurate radiometric calibration and atmospheric correction capabilities could enable the development of universal equations that could minimize the need for calibration with field data. Many of these characteristics may be realized with the European Space Agency (ESA) Sentinel-2 and Sentinel-3 missions with the first launch scheduled in 2013 (http://www.esa.int/esaLP/SEM097EH1TF_LPgmes_0.html).

Further research is needed to develop and test atmospheric correction procedures for routine operational assessment of inland lakes without the need for ongoing calibrations, but in places like Minnesota with well-developed water quality monitoring programs, the existing image sources, such as Landsat for water clarity assessment of all lakes and MERIS for chlorophyll assessment of larger lakes, can be calibrated with in situ data to provide accurate information on a broad regional scale.

Use of satellite imagery with an improved sensor like that described above as a complement to ground-based sampling could greatly expand the coverage of lakes in national water quality surveys. For example, as part of the series of National Aquatic Resource Surveys coordinated by the U.S. Environmental Protection Agency's (EPA) Office of Water, lakes for sampling are selected based on a statistically representative design. Because of limitations imposed by ground-based sampling, however, only ~1,150 lakes nationwide were included in the 2007 survey (http://water.epa.gov/type/watersheds/monitoring/nationalsurveys.cfm), but use of the

ground survey data for calibration of satellite imagery in future surveys could provide much more comprehensive coverage for some lake characteristics.

Finally, Wood et al. (2011) recently proposed the development of a global hydrologic model with "hyperresolution" (100-1000 m resolution) to monitor and model the world's terrestrial water resources. Satellite imagery was proposed as a key source of observations to obtain much of the data needed for the model, which would quantify such processes as land-atmospheric interactions (e.g., soil moisture, evapotranspiration), water flows, associated biogeochemical fluxes, and water quality. At least some of the water quality components of such a model could be facilitated using the methods described in this paper and an improved satellite sensor such as described above.

Chapter 5

Airborne Hyperspectral Remote Sensing to Assess Spatial Distribution of Water Quality Characteristics in Large Rivers: the Mississippi River and its Tributaries in Minnesota

Aircraft-mounted hyperspectral spectrometers were used to collect imagery with high spatial and spectral resolution for use in measuring optically related water quality characteristics of major rivers of Minnesota. Ground-based sampling undertaken concurrent with image acquisition provided calibration data for chlorophyll, suspended solids, turbidity and other measures of water clarity. Our approach identified the spectral characteristics that distinguish waters dominated by different inherent optical properties (IOPs), and we used those characteristics to develop models to map different water quality characteristics in optically complex waters. For phytoplankton related variables (volatile suspended solids (VSS) and total chlorophyll *a* (chl *a*)), the ratio of the scattering peak at the red edge (~700 nm) with the reflectance troughs caused by chlorophyll absorption at ~670 nm and other plant pigment absorption peaks at 592 and 620 nm all were strong predictors of chl *a* and VSS (r^2 values of 0.75-0.94). The scattering peak at ~700 nm was a strong predictor of variables related to water clarity (total suspended solids (TSS), turbidity and turbidity tube (T-tube)) (r^2 values of 0.77-0.93). For mineral-based variables (nonvolatile suspended solids (NVSS) and the ratio NVSS:TSS), we found that a combination of the TSS and chl *a* relationships described above were strong predictors (r^2 values of 0.73-0.97) and the most robust because this model corrects for the scattering of phytoplankton at ~700 nm. Application of the

methods to quantify spatial variations in water quality for important stretches of the Mississippi River and its tributaries indicate that imaging spectrometry can be used to successfully distinguish and map key water quality variables under complex IOP conditions, particularly to separate and map inorganic suspended sediments independently of chlorophyll levels.

5.1 Introduction

Minnesota has 93,000 miles (150,000 km) of rivers and streams. They are highly important as transportation corridors and recreational resources that contribute significantly to the state's economy and tourism. Of the 17 percent of the state's river and stream miles assessed for the 2010 Impaired Waters List, 40 percent were found to be impaired (P. Anderson, Minnesota Pollution Control Agency, personal communication, 2011). We explored the use of aircraft-mounted remote sensing systems as a cost-effective way to gather information to measure optically related water quality properties of rivers that are relevant to the issue of river water impairment. This paper describes a general approach, as well as specific predictive relationships, that can be used for such measurements.

We have had success previously using multispectral radiance information from Landsat imagery (e.g., Chapter 2 (Olmanson et al., 2008)) to measure lake water clarity. More recently, we have shown that other satellite sensors (MERIS and MODIS) can provide accurate estimates of chlorophyll levels in large and moderately sized lakes (Chapter 4 (Olmanson et al., 2011)). There is little reason to doubt that similar

relationships exist in flowing waters, but compared with lakes, rivers and streams pose a more challenging set of problems in applying remote sensing techniques to assess water quality characteristics. First, conditions in rivers and streams are temporally more dynamic and often spatially more heterogeneous than those in lakes. Second, small rivers and streams may be so shallow that light penetrates to the bottom, such that reflectance from the water is a function of bottom conditions in addition to that of the water itself. Third, the spatial resolution of most satellite sensors, including Landsat, is too coarse for small rivers and streams. Finally, to measure water quality conditions other than clarity, a better set of spectral bands is needed than Landsat provides. Although the MERIS and MODIS satellite sensors provide such bands, their spatial resolution is much coarser than that of Landsat, and they are suitable only for very large rivers or impoundments of large rivers.

Imaging spectrometers, also known as hyperspectral sensors, mounted in small aircraft can collect landscape images with high spatial and spectral resolution. Such systems have been available for over two decades and have been used for mineralogical exploration (e.g., Abrams et al., 1977, Goetz et al., 1985 and Clark et al., 1990), as well as to determine the type, health and condition of vegetation for environmental quality, forestry and agriculture purposes (e.g. Carroll et al., 2008, Gitelson and Merzlyak, 1996, Gitelson et al., 2002, Haboudane et al., 2002, 2004, Shah et al., 2002 and 2004 and Wessman et al., 1988). Several publications have described the application of such systems to measure water quality conditions in lakes (e.g., Ammenberg et al., 2002, Chipman et al., 2009, Moses et al., 2011, Hakvoort et al., 2002 and Hoogenboom et al.,

1998), but only a few publications (e.g., Shafique et al., 2003 and Senay et al., 2001) have focused on potentially more complex river systems. Phytoplankton, mineral suspended sediment, humic color or combinations of these constituents may dominate the optical properties of rivers depending on watershed and flow conditions. Strong relationships were found in these previous studies between chlorophyll concentrations and turbidity or suspended solids concentrations and reflectance data, but none attempted to separate competing inherent optical properties (IOPs).

In this paper we describe the use of aircraft-mounted hyperspectral sensors on three major rivers in Minnesota (the Mississippi, Minnesota, and St. Croix) and some associated floodplain lakes with distinct and competing IOPs. Sufficient information was acquired in three separate aerial data acquisitions to evaluate the usefulness of aircraft-mounted remote sensing as a supplement/complement to conventional ground-based river monitoring programs. For calibration purposes, water samples were collected concurrently with the remote sensing data acquisition, and to obtain a range of conditions for calibrations, we focused our measurements around the confluences of river systems that have different water quality characteristics. Imagery was collected during August of 2004, 2005 and 2007, and each period represented different flow and water quality regimes.

The overall goal was to develop reliable techniques for synoptic measurements of key indicators of river water quality that can be used to complement data obtained by conventional ground-based methods. Our specific objectives were to: (1) identify spectral characteristics that distinguish waters dominated by different IOPs indicative of

important water quality characteristics; (2) develop predictive relationships for these water quality characteristics based on the spectral (reflectance) characteristics (or combinations thereof); (3) determine whether and how accurately chlorophyll *a*, total suspended solids (TSS), and nonvolatile suspended solids (NVSS) can be mapped independently when competing IOPs are dominant and whether the proportion (NVSS/TSS) can be identified and mapped quantifiably; (4) develop an overall approach to measure and map the water quality variables using aircraft-mounted spectrometers; and (5) evaluate the accuracy and usefulness of aircraft-based remote sensing for water quality studies of rivers. The work was conducted using images collected under clear (cloudless) conditions and processed by methods similar to those developed for regional assessments of water clarity and chlorophyll *a* from satellite imagery (Chapter 2, 4 (Olmanson et al., 2008, 2011)).

5.2 Background Information: Major Rivers in Twin Cities Metropolitan Area

The Mississippi River, which originates in Lake Itasca in northern Minnesota, is a moderate sized river (average flow of 11,700 cfs (3163 m^3 s^{-1}), Table 5.1) by river mile 871, where it reaches the Minneapolis-St. Paul (Twin Cities) Metropolitan Area (TCMA). The drainage basin of the Mississippi River above the TCMA (~49,000 km^2 in area) includes much of central and north central Minnesota. Land cover in the basin is mixed, with 37% forest and 21% cropland. In the TCMA (7,700 km^2) the land cover is 40% agricultural row crops, 30% urban and 13% forest. The Minnesota and St. Croix Rivers

are large tributaries that flow into the Mississippi in the TCMA and increase the total river flow on average by more than a factor of two (Table 5.1).

Table 5.1 River discharge for Minnesota, Mississippi and St Croix Rivers in the TCMA.

River	Site	Mean (cfs) Discharge 26,604	August 19, 2004 Discharge (cfs) 9,130	August 15, 2005 Discharge (cfs) 7,370	August 30, 2007 Discharge (cfs) 8,070
Minnesota	Jordan	8810 - 33%	3190 - 35%	1840 - 25%	4160 - 52%
Mississippi	Anoka	11700 - 44%	2770 - 30%	4100 - 56%	1930 - 24%
St. Croix	Stillwater	6094 - 23%	3170 - 35%	1430 - 19%	1980 - 24%

The drainage basin of the Minnesota River covers 42,000 km^2, including large portions of south-central and southwestern Minnesota, as well as small portions of Iowa and South Dakota. The basin has relatively flat to gently rolling hills with highly productive soils and is primarily (75%) row-crop agricultural land. The river carries a high burden of suspended solids from soil and stream bank erosion that is attributed to a combination of artificial drainage and steep slopes due to deep incising of the Minnesota River Valley by Glacial River Warren (Belmont et al., 2011, Gran et al., 2009 and Thorleifson, 1996).

The drainage basin of the St. Croix River covers 20,000 km^2 in eastern Minnesota and northwestern Wisconsin. The basin is the least developed of the three considered here and consists of 50% forest, 15% grassland or pasture, and 15% agricultural row crops. Among the three rivers, the St. Croix tends to have the lowest nutrient and suspended solids concentrations, but it has higher levels of natural colored dissolved organic matter (CDOM).

Aside from their commercial and recreational importance, the rivers play important roles in transporting pollutants downstream. Most of the treated wastewater from the TCMA enters the Mississippi River downstream of a major treatment plant in St. Paul; among other consequences, this leads to high nutrient (nitrogen and phosphorus) concentrations that promote summertime algal blooms in the river and downstream Lake Pepin (Engstrom et al., 2009).

The water chemistry/quality of these rivers is more complex than that of most lakes. Dominance by both phytoplankton, usually measured in terms of chlorophyll *a* concentrations (sometimes called green phase) and inorganic sediment, usually measured in terms of Secchi depth, turbidity, or suspended solids concentrations (sometimes called brown phase), may occur depending on flow and seasonal dynamics. Typically, the Mississippi River accounts for 40-45% of flow and 20% of incoming TSS load; the Minnesota River accounts for 25-30% of flow but 75% of incoming TSS; and the St. Croix River accounts for 25-30% of flow but only 5% of the incoming TSS load (Metropolitan Council, 2004). Water quality conditions in the three rivers are highly diverse, and conditions in the Mississippi River downstream of the confluences with the two tributaries depend on the relative flows of the rivers and the degree to which mixing of the waters has occurred.

Water quality impairment issues occur in the Mississippi River as a consequence of urban and agricultural runoff and inputs of treated municipal wastewater as the river flows through the TCMA. Major concerns exist about the effects of suspended solids and nutrient loadings on Lake Pepin, a natural lake in the main channel of the river ~40 miles

(70 km) downstream of the TCMA (Belmont et al., 2001, Engstrom et al., 2009, Mulla and Sekely, 2009). At a larger scale, there also is concern about nutrient contributions from Minnesota to the total nutrient load of the Mississippi River to the Gulf of Mexico (Goolsby et al., 2001, Rabalais et al., 2002a,b; Turner and Rabalais, 1994.). Under normal conditions Minnesota contributes ~3 percent of the total nitrogen flux and 2 percent of the phosphorus flux delivered to the Gulf of Mexico by the Mississippi River (Alexander et al., 2008).

5.3 Methods

5.3.1 Imagery

Imagery was collected by the Center for Advanced Land Management Information Technologies (CALMIT, University of Nebraska, Lincoln) using AISA (Airborne Imaging Spectrometer for Application) hyperspectral imaging systems in a Piper Saratoga airplane using procedures described by Chipman et al. (2009). The CALMIT system evolved over the course of the study, as new equipment, software and techniques became available. Having different image characteristics complicated our analysis. AISA sensors collect spectral-radiance data and compile imagery in the visible and near infrared portions of the electromagnetic spectrum. They are "push-broom" systems with a global positioning and inertial navigation system that simultaneously record the aircraft position and attitude, along with upwelling radiance and downwelling solar irradiance. These raw data products are used to create geospatially and radiometrically corrected imagery.

During the first acquisition period (August 19, 2004), an AISA-Classic sensor collected hyperspectral imagery in 16 (for 1 and 3 m imagery) or 24 (for 2 m imagery) narrow bands (~5 nm bandwidth) selected by CALMIT to measure key water quality characteristics over six segments (Figure 5.1) that covered ~65 km of the Mississippi River and selected tributaries. A collaborative sampling effort involving crews from the Minnesota Pollution Control Agency, Metropolitan Council, Minnesota Department of Natural Resources, Minnesota Department of Agriculture and the University of Minnesota collected water samples and took in situ measurements at ~39 locations along the river concurrently with the imagery acquisition.

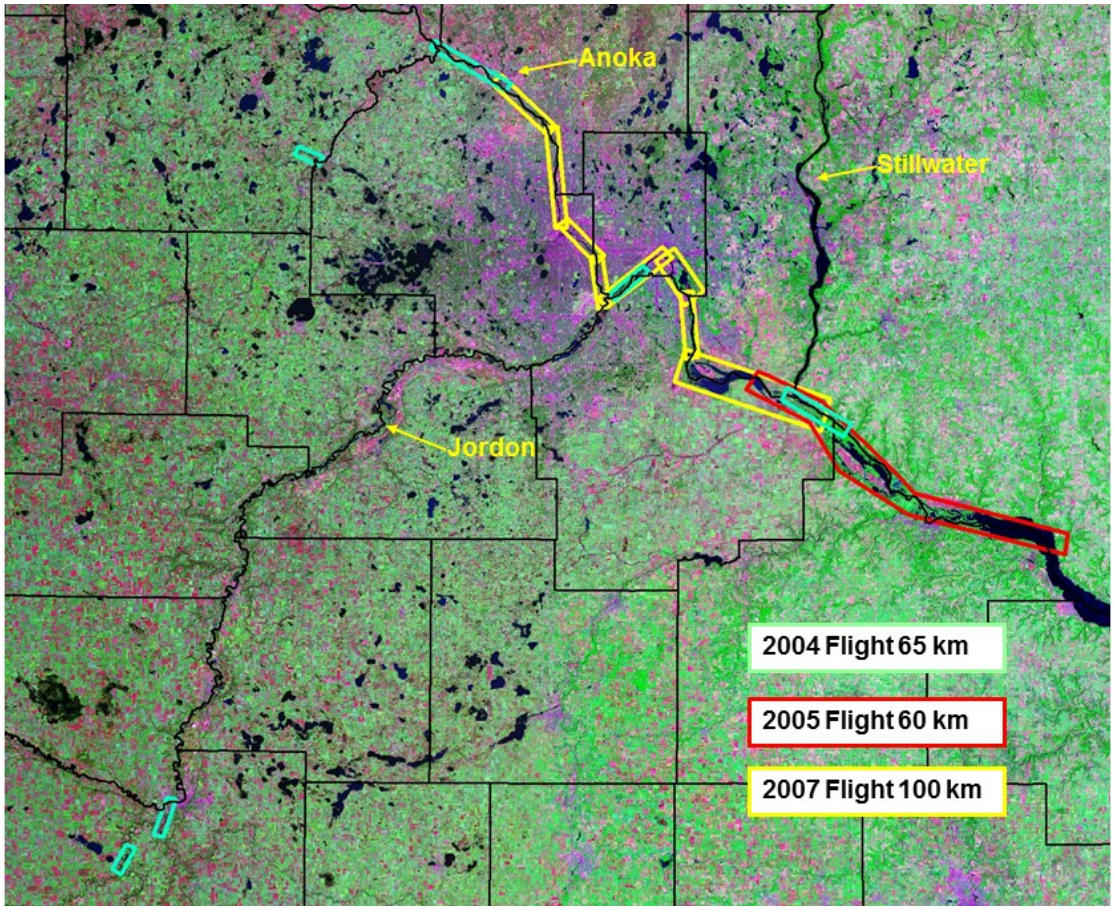

Figure 5.1 Hyperspectral imagery flight lines for 2004, 2005 and 2007.

During the second acquisition (August 15, 2005), an AISA-Eagle hyperspectral imager collected hyperspectra at a spatial resolution of 2 m in 86 contiguous bands: 2.5 nm bandwidth from 435 to 730 nm, 20 nm bandwidth from 730 to 900 nm, and 30 nm from 900 to 960 nm. The hyperspectra were recorded for 10 segments over a 60 km stretch of the Mississippi River from Spring Lake (south of St. Paul) to Lake Pepin (Figure 5.1). Sampling crews from the Minnesota Pollution Control Agency and Metropolitan Council concurrently collected water samples at 26 locations along the river.

The image acquisitions on August 30, 2007 also used an AISA-Eagle hyperspectral imager to collect hyperspectra at 2 m spatial resolution in 97 contiguous bands (2.5 nm bandwidth from 435 to 730 nm and 10 nm bandwidth from 730 to 950 nm) in 12 segments over a 100 km stretch of the Mississippi River from the Rum River northwest of the TCMA to downstream of the St. Croix River (Figure 5.1). Sampling crews from the Minnesota Pollution Control Agency and the Metropolitan Council simultaneously collected water samples from 26 sites.

5.3.2 Water quality measurements

Because of the dynamic nature of rivers, sampling crews were on the river to collect water samples and take in situ measurements as close as possible to the time the aircraft collected imagery. All samples were collected within a few hours of the remote sensing data acquisition and away from mixing zones subject to rapid temporal and spatial changes. Field measurements at each site included water clarity by turbidity tube (Myre and Shaw, 2006) and, if possible, Secchi disk (SD); high flow rates and high

turbidity levels limit the feasibility of SD measurements in some rivers. Samples were collected for turbidity, total suspended solid (TSS), volatile suspended solids (VSS), total chlorophyll *a* (chl *a*) and pheophytin (Pheo) and were analyzed by laboratories of the Metropolitan Council using standard methods: APHA-10200h (Greenberg et al., 1992), ASTM D3731-87 (ASTM, 1994), and USEPA-445 (U.S. EPA, 1992).

5.3.3 Image Processing and Classification

Image classification procedures were based on the methods of Olmanson et al. (2001) and Kloiber et al. (2002a), modified for the hyperspectral nature of the imagery and advances in software and computer hardware that enabled simpler or improved procedures. We used Leica Geosystems ERDAS Imagine and Esri ArcGIS for image processing. Acquiring a representative sample for each sampling site from the image was a primary objective.

Each flight line image was corrected geospatially and radiometrically to "at platform reflectance" using the raw data from the AISA system, but additional image preprocessing was necessary. Although the automated geometric correction process yielded close results, additional geometric correction was performed using ~20 well-distributed ground control points (GCPs) from available orthorectified aerial photography with a positional accuracy (RMSE) on the order of ±1 pixel (1-3 m). Atmospheric correction was conducted on the 2007 images using the FLAASH module in ENVI and standard atmospheric variables for the time and location. Radiometric normalization, necessary for only a few nonconforming images, was accomplished by collecting samples of the spectral data from the overlap area of both ("conforming" and nonconforming")

images representing different land cover and water areas. Regression analyses were performed with the base (conforming) image as the dependent variable and the image needing correction (nonconforming) as the independent variable. The resulting models were used to normalize the nonconforming image to the base image.

Once image preprocessing was complete, a "water-only" image was produced by performing an unsupervised classification method based on ISODATA clustering. Because water has spectral characteristics distinct from terrestrial features, water pixels were grouped into one or a few distinct classes that could be easily identified. We masked out terrestrial features to create a water-only image, performed an unsupervised classification on this image, and generated spectral signatures of each class. We used these signatures, along with the locations where the pixels occurred, to differentiate classes containing open water and shallow water (where bottom sediments and/or macrophytes affected spectral response). These areas tend to have high spatial variability compared to open-water portions of the rivers. Based on this analysis, we removed the affected pixels.

Next, the spectral-radiometric data from the "open water" images were extracted from the areas immediately around the sampling locations to develop relationships with measured water quality data. For this purpose, we used the imagery and the GPS locations of each sample to delineate a polygon in a spectrally-radiometrically similar area around each sample location. These polygons had a minimum of 200 pixels in narrow portions of the rivers or areas with high heterogeneity and up to 1,700 pixels in wider, more homogeneous areas. The signature editor in ERDAS Imagine was used to

extract spectral radiometric data from the polygons. Mean band values from the polygons were imported into Microsoft Excel, ratios and differences for band combinations were calculated, and data from the ground-based measurements and samples were linked to the appropriate imagery samples.

To develop models to predict water quality variables from the imagery products, we performed step-wise forward regressions of the band data sets using the JMP 9 64-bit version statistical software package of SAS Institute, Inc. Because different band sets had been used in each acquisition period, a subset of 18 well-positioned and coinciding or near coinciding bands were used for the 2005 and 2007 data, and 16-18 available coinciding bands were used for the 2004 data. The basis for selection of the bands is described in the results section. Raw and log-transformed values of each water quality variable were the dependent variables and single bands, band ratios and band differences were the independent variables. From these results, we used the one or two independent variables that were consistent for all three datasets and that contributed most to the regression fit and applied them in a second multiple regression, as described by Chapter 4 (Olmanson et al., 2011). The models developed for each variable and each image product were applied to each pixel to create pixel-level water quality maps.

5.4 Results and Discussion

5.4.1 Spectral characteristics of river water

Hyperspectral imagery can provide sufficient information to reconstruct the visible-near IR reflectance spectra of water bodies that in turn can be used to identify the

spectral characteristics (e.g., reflectance peaks and troughs) that distinguish waters dominated by the inherent optical properties (IOPs) indicative of different water quality variables. Figure 5.2 shows characteristic reflectance spectra of samples extracted from the 2007 hyperspectral imagery. Spectra from four locations represent phytoplankton dominated waters: (1) hypereutrophic Lake Conley (chl *a* = 200 µg/L; TSS = 48 mg/L with 42 percent by weight being NVSS), which is a Mississippi River backwater lake upstream of the confluence with the St. Croix River; (2) hypereutrophic Pig's Eye Lake (chl *a* = 230 µg/L; TSS = 51 mg/L with 58 percent by weight being NVSS), a backwater lake used to transport treated wastewater effluent from the Metropolitan Wastewater Treatment Plant (Metro) to the Mississippi River; (3) the Mississippi River upstream of the Rum River at river mile 872 (chl *a* = 78 µg/L; TSS = 13 mg/L with ~60% NVSS); and (4) the Mississippi River upstream of the Minnesota River at river mile 848 (chl *a* = 45 µg/L; TSS = 15 mg/L with ~40% NVSS). Flow at the last location was unusually low at the time of sampling because of flow restrictions at St. Anthony Falls locks and dams (river mile 853.9) in Minneapolis necessitated by a major bridge collapse downstream of the lock and dam. The reflectance spectra of these waters show characteristic absorption by chlorophyll and other plant pigments in the blue (400-500 nm) and red (600-700 nm) wavelengths, which results in low reflectance (i.e., troughs) at ~430 nm (not shown because of noise in that region) and ~670 nm and a phytoplankton scattering peak at ~700 nm.

The Minnesota River and the mixed waters of the Minnesota and Mississippi Rivers at St. Paul (river mile 839) represent sediment-dominated waters with TSS

concentrations of 61 and 45 mg/L (87 and 82% NVSS). Although chl *a* levels were moderately high at these sites (40 and 55 µg/L, respectively), they were not high enough to overcome the dominance by suspended sediment, and their reflectance spectra lack the absorption characteristics (troughs at ~430 and ~670 nm) of chlorophyll and have relatively high reflectances in the green and red region especially from 560 to 700 nm.

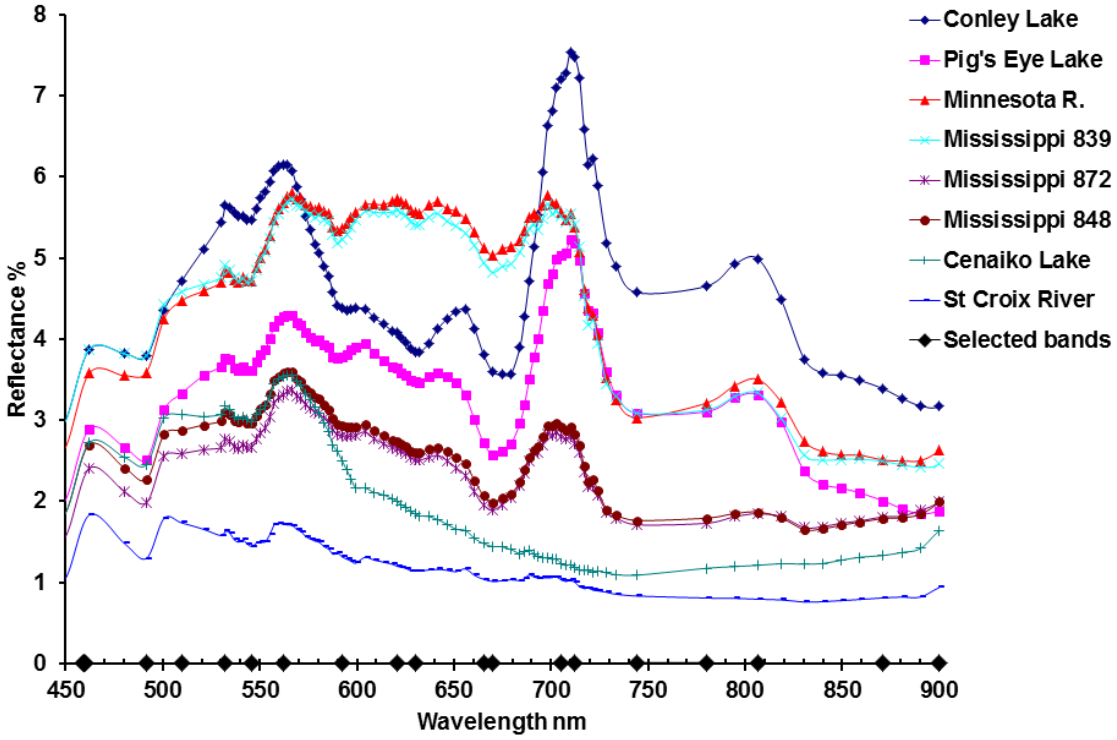

Figure 5.2 Characteristic reflectance spectra extracted from 2007 hyperspectral imagery with 18 selected spectral bands indicated.

Cenaiko Lake, a small, mesotrophic water body located east of the Mississippi River (river mile 865), represents relatively clear water. It had low concentrations of suspended matter (TSS = 3 mg/L; NVSS = 2 mg/L) and low chl *a* (8 µg/L). Although quantitative information is not available on CDOM, the lake water was not visibly stained

brown. Its reflectance spectrum is characterized by a reflectance peak near 570 nm and declining reflectance at higher wavelengths. The lack of the characteristic peaks and troughs caused by chl *a* and the plankton/TSS scattering peak in the red and NIR range is notable. Finally, the St. Croix River with low-to-moderate chl *a* (22 µg/L) and low concentrations of suspended matter (TSS = 2 mg/L; NVSS = 1 mg/L) represents a water body dominated by humic color (CDOM-rich water; color = 30 CPU). It had low reflectance across the entire spectrum, with characteristic absorption by CDOM in the lower wavelengths; very small reflectance peaks are apparent in the spectrum at 570 and 700 nm.

The distinct features of reflectance spectra for waters dominated by different optically-related constituents (chl *a*, inorganic sediment, CDOM) provide insights regarding wavelength bands likely to be useful for predictive models of these characteristics based on multi- or hyper-spectral imagery. Successful models using spectral-radiometric data to estimate water quality variables should use wavelengths that identify key spectral characteristics without interference from competing optical features. For chlorophyll, this means that algorithms commonly used for ocean Case I waters (reflectance in the blue and green reflectance regions) will not work well for inland Case II waters because these waters are influenced by suspended solids and CDOM derived from their watersheds making them optically more complex (Morel and Prieur 1977); i.e., chl *a* is not the only optical property because CDOM and inorganic sediment have overlapping absorption features in the blue region. Successful chlorophyll models for these waters likely will use absorption characteristics from the red wavelengths—the

reflectance trough at ~670 nm and scattering by phytoplankton at the red edge ~700 nm, where absorption by CDOM and suspended solids is minimal (Gitelson, 1992, Moses et al., 2011). The ratio ~700 nm with ~670 nm has been shown to have a strong relationship with chl *a* in a variety of waters (including lakes, estuaries and rivers) over a wide range of concentrations (0.1 to 350 µg/L; Matthews, 2011), and it has been used several times in the literature (Duan et al., 2007, Gitelson et al., 1993, Gons, 1999, Mittenzwey et al., 1992, Menken et al., 2006 and Moses et al., 2009).

Successful models for turbidity and TSS in optically complex waters (where both phytoplankton and inorganic sediment may dominate IOP features) would avoid the absorption characteristics of chlorophyll in the red and CDOM in the blue region and use the scattering peak at the ~700 or band combinations in the NIR and green regions. The scattering peak at ~700 was found to be strongly correlated with TSS by Härmä et al. (2001), Kallio et al. (2001) and Koponenen et al. (2007) and for turbidity by Senay et al. (2001) and the difference (710-740) by Shafique et al. (2003). The scattering peak at ~700 by itself also was found to work well for NVSS by Ammenberg et al. (2002).

CDOM models should use the absorption characteristics of CDOM in the blue wavelengths, but because chlorophyll and suspended matter also affect spectral reflectance in these wavelengths, the algorithm would need to separate the effects of CDOM from the effects of chlorophyll and suspended material.

5.4.2 Model Development

Having different band sets and radiometric characteristics and corrections for each set of image acquisitions complicated our analysis. Therefore, a subset of 18 well-

positioned (Figure 5.2) and coincident bands were used for the 2005 and 2007 data, and 16 to18 bands were used for the 2004 data. Because some key spectral bands were missing in the 1-m data and some atmospheric differences were found in the images outside the TCMA for 2004, only the 2- and 3-m data from the TCMA for this year were included in the analysis. The bands selected for analysis were derived from the spectral characteristics of the data (Figure 5.2) and bands used successfully by others from the literature, as reviewed by Mathews (2011).

Several models developed from the images showed strong relationships between log transformed and non-transformed water quality data (T-tube, turbidity, TSS, VSS, NVSS and chl *a*) and reflectance values from the hyperspectral data; see Table 5.2 for a statistical summary for the models, including ranges of the variables, bands in the best-fit relationships (consistent for all three data sets), R^2, RMSE, and number of data points. The non-transformed water quality data were not normally distributed for some variables, especially chl *a*, but the log transformed data were or were nearly so, thus meeting the assumptions of regression. Chapter 2 (Olmanson et al., 2011) also found that they produced models with improved fit in the important chl *a* range of 0-20 μg/L. Therefore, models based on log-transformed data were used for map development.

Table 5.2 Calibration statistics for water quality models.

		2004				2005				2007			
LN of variable	**Bands**	**N**	**Range**	**r^2**	**RMSE**	**N**	**Range**	**r^2**	**RMSE**	**N**	**Range**	**r^2**	**RMSE**
T Tube (cm)	705	24	8-120	0.91	0.25	19	7-95	0.77	0.24	19	12-160	0.80	0.24
Turbidity (NTU)	705	25	2-25	0.88	0.29	20	2-50	0.77	0.29	19	3-46	0.92	0.23
TSS (mg/L)	705	25	4-80	0.83	0.28	20	4-95	0.77	0.32	19	2-61	0.93	0.25
NVSS (mg/L)	705 & 705/670	25	3-63	0.95[a]	0.24	20	0-60	0.85[a]	0.27	19	1-53	0.97[a]	0.22
VSS (mg/L)	705/670	25	1-17	0.80	0.26	20	4-81	0.94	0.17	19	1-28	0.73	0.25
Chl *a* (µg/L)	705/670, 705/620	25	14-210	0.75, 0.76	0.43-0.38	20	31-830	0.93, 0.91	0.21-0.21	19	8-230	0.83, 0.92	0.32, 0.21
NVSS/TSS (%)	705 & 705/620	25	50-83	0.80[a]	0.05	20	0-83	0.73[a]	0.1	19	30-87	0.91[a]	0.06

[a] R^2

Chl a, the most common water quality variable derived from high spectral resolution remote sensing, had strong relationships with the ratio ~700:~670 nm for all three datasets, as also was found to be the case in several previous studies (see previous discussion). The strength of this relationship is due to the interaction to strong absorption of water and backscattering by phytoplankton that causes a peak ~700 nm in phytoplankton dominated waters and the chl *a* absorption maximum near 670 nm. For this dataset even with a complex combination of IOP features, the 705:670 ratio was strongly correlated with chl *a*, with r^2 of 0.73-0.93 for the three years of data. Two models that also used the peak at ~700 and other plant pigment absorption features seen in Figure 5.2 worked even better: 705:592 (r^2 of 0.85-0.93) and 705:620 r^2 of 0.77-0.93). The RMSE values reported for the predictive equations in Table 5.2 indicate that chl *a* can be estimated with an accuracy of ~21% (based on the 2005 and 2007 data). Some of the uncertainty reflected in the RMSE values likely arises from uncertainties in the chl *a* analyses themselves, as well as from differences between the water mass sampled by the ground crews and that "sampled" by the imagery (caused by differences in the timing of the two sampling methods).

TSS includes both organic and inorganic solids with potentially a variety of different combinations of IOP features. Remote sensing algorithms for TSS reported in the literature (Doxaran et al., 2005, Gitelson et al., 1993, and Koponen et al., 2007) thus are less consistent and apparently more condition-specific dependent on the dominant optical features. For our dataset strong relationships were found between TSS and reflectance in the band centered at 705 nm (r^2 of 0.77-0.88). This model avoids the

absorption characteristics of chlorophyll but uses the well-known scattering ~700 nm of suspended material (including plankton) in water. As discussed earlier, other workers have found that the reflectance peak at ~700 works well for TSS (Härmä et al., 2001, Kallio et al., 2001 and Koponenen et al., 2007).

VSS, the mass of combustible (organic) suspended material that presumably is plankton and microbial detritus, is generally correlated with chl *a*. The relationships between VSS and band ratios that worked well for chl *a* also were strong (705:592, r^2 = 0.80-0.95; 705:620, r^2 = 0.78-0.95; 705:670, r^2 = 0.73-0. 94). NVSS, the mass of inorganic suspended material, had strong relationships with reflectance in the band centered at 705 nm (r^2 values of 0.73-0.96). As discussed previously, this peak was found to be strongly correlated to NVSS by Ammenberg et al. (2002); however, this relationship could be condition-specific, depending on the dominant IOPs, and may not be robust in waters with low inorganic sediments. Therefore, for a more robust model we used the band centered at 705 nm, which worked well for TSS, and the band ratio 705:670, which worked well for chl *a*. This model corrects for the scattering caused by chlorophyll ~700 nm and had even higher R^2 values (0.85-0.97). The RMSE values reported for the predictive equations in Table 5.2 indicate that NVSS can be estimated with an accuracy of ~22-27%.

The ratio NVSS:TSS (the fraction of TSS that is inorganic or mineral) could be useful to identify the dominant IOP (planktonic- versus mineral-based turbidity) in river waters. The predictive model for this ratio that worked best for all datasets used the band centered at 705 nm, which worked well for TSS, and the band ratio 705:620, which

worked well for chl *a*, (R^2 values of 0.73-0.91). The RMSE values reported for the predictive equations in Table 5.2 indicate that NVSS:TSS can be estimated with an accuracy of ~5-10%.

Finally, turbidity and water clarity as measured by t-tube are generally related to TSS. Strong relationships were found for both turbidity (r^2 values 0.77-0.92) and t-tube (r^2 values of 0.73-0.91) with reflectance values for the band centered at 705 nm. These models are similar to the best-fit models for TSS.

5.4.3 Water Quality Maps

Using the water quality models described above, we created pixel-level maps that captured the high spatial heterogeneity of water quality in the river systems we studied. During the first image acquisition (August 19, 2004), flows of the Minnesota and St. Croix Rivers were slightly higher than the flow of the Mississippi River (Table 5.1), and the Minnesota River IOP features were dominated by phytoplankton (green phase). As Figure 5.3 shows, the high phytoplankton waters of the Minnesota River dominated water quality conditions in the Mississippi River downstream the confluence with the Minnesota River during this time. Similarly, Figure 5.4 shows that the phytoplankton (green phase) waters of the Mississippi River were diluted by the relatively clear waters of the St. Croix River downstream of the confluence of those two rivers.

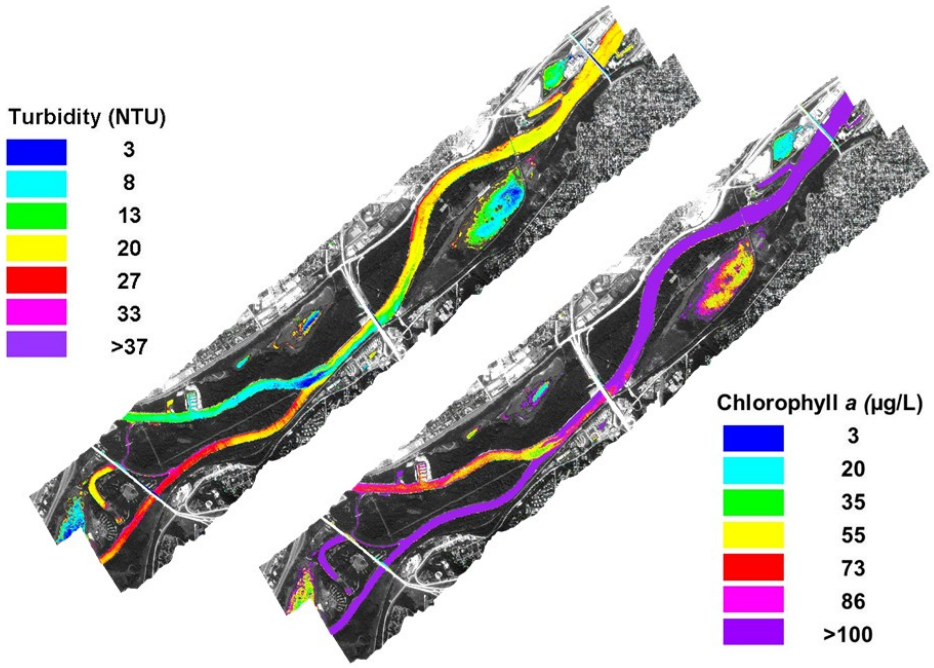

Figure 5.3 Water quality maps (turbidity and chl *a*) for the confluence of the Minnesota River with the Mississippi River, August 19, 2004.

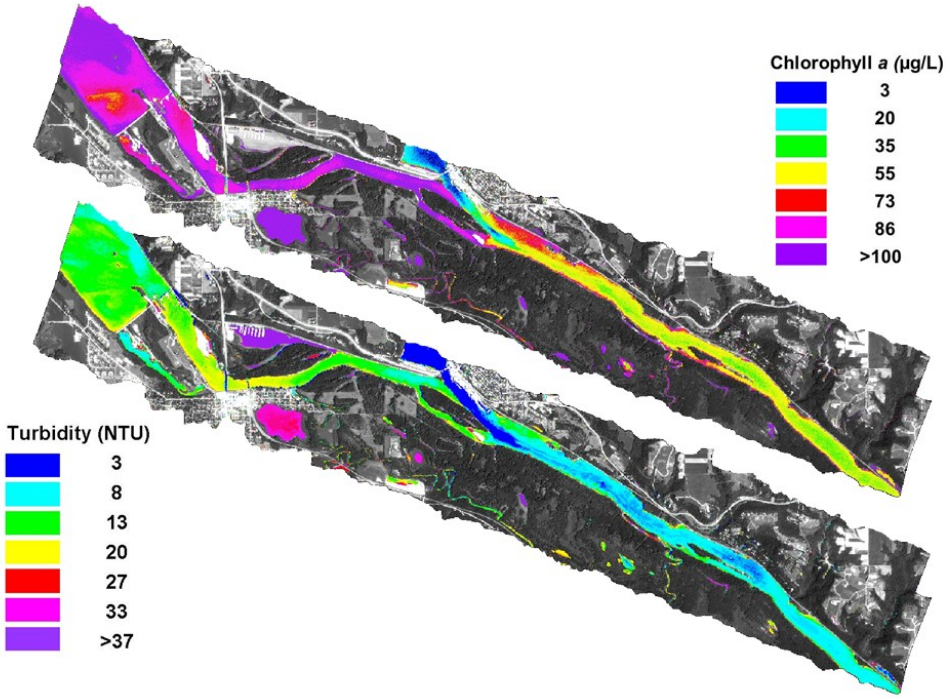

Figure 5.4 Water quality maps (turbidity and chl *a*) for the confluence of the Mississippi River with the St. Croix River, August 19, 2004.

During the second image acquisition (August 15, 2005), the Mississippi River dominated flow (Table 5.1) and water quality conditions, and the main channel had relatively low phytoplankton and sediment levels. However, as Figure 5.5 shows, the backwater areas were dominated by algal blooms. In addition, the figure shows that sediment picked up from the channel around Sturgeon Lake apparently settled as the river flow velocity decreased in the upper part of Lake Pepin, and the low suspended sediment concentrations (clearer water) enabled the development of a large increase in phytoplankton further down-channel in the lake.

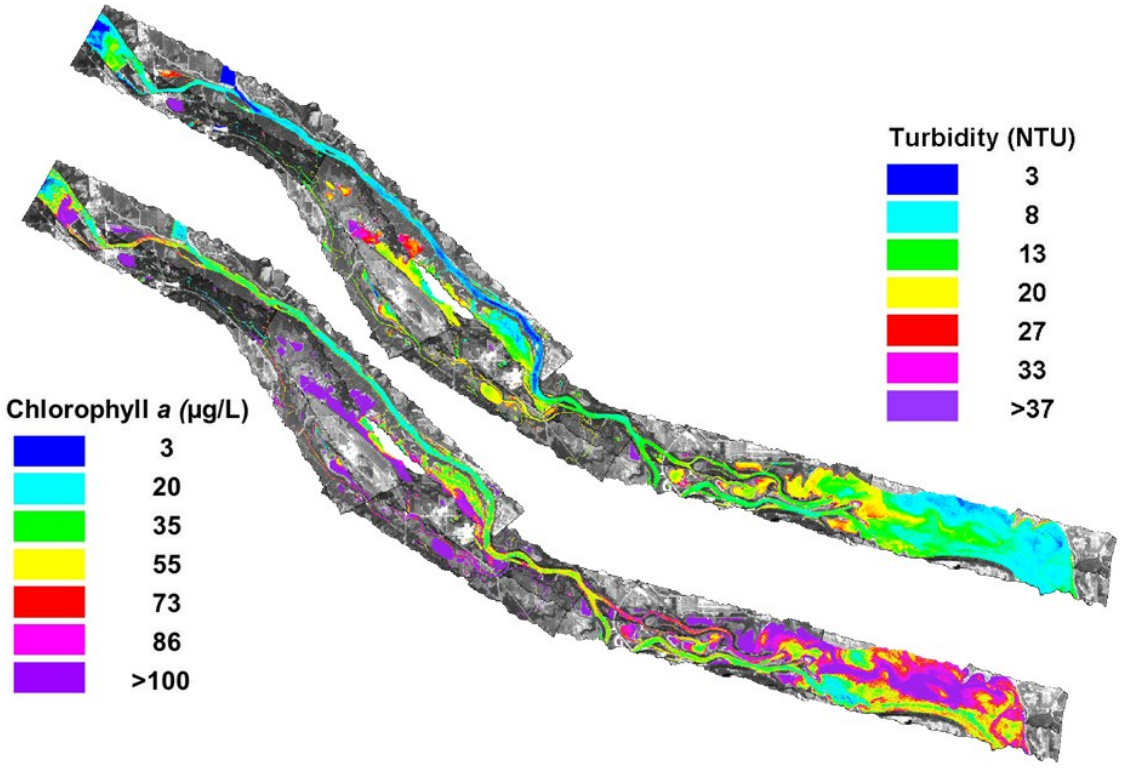

Figure 5.5 Mississippi River Water quality maps (turbidity and chl *a*) from Spring Lake to Lake Pepin and the confluence with the St. Croix River, August 15, 2005.

During the acquisition period on August 30, 2007, the larger flow from the Minnesota River (brown phase) dominated conditions in the Mississippi River downstream of the confluence (Figure 5.6) because flow upstream in the Mississippi (green phase) was restricted by St. Anthony Falls locks and dams. Further downstream the relatively clear waters of the St. Croix River diluted these conditions in the stretch of the river downstream of its entry to the Mississippi (Figure 5.7).

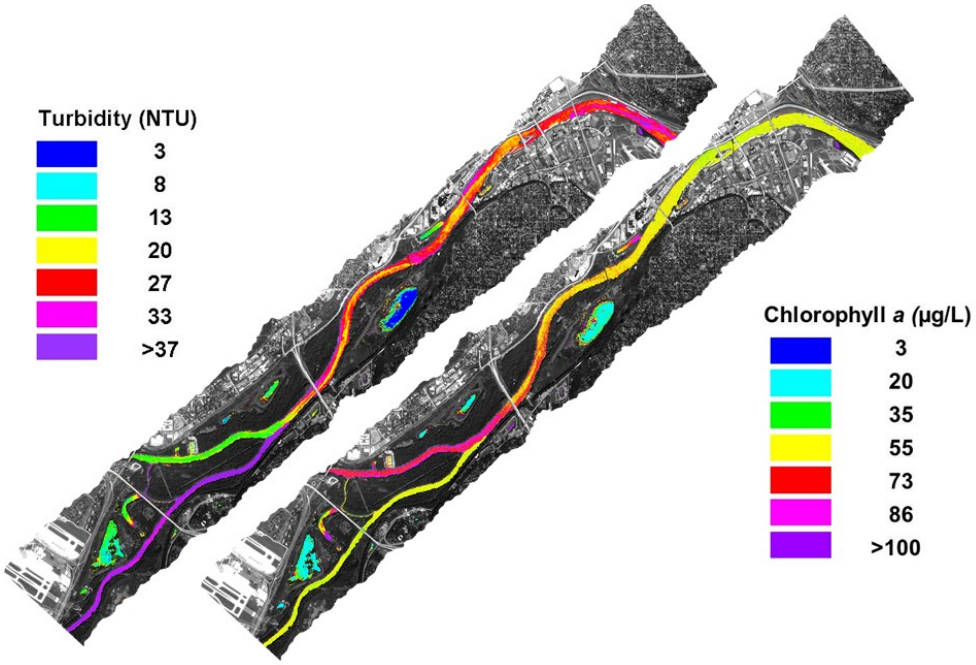

Figure 5.6 Water quality maps (turbidity and chl *a*) for the confluence of the Minnesota River with the Mississippi River, August 30, 2007.

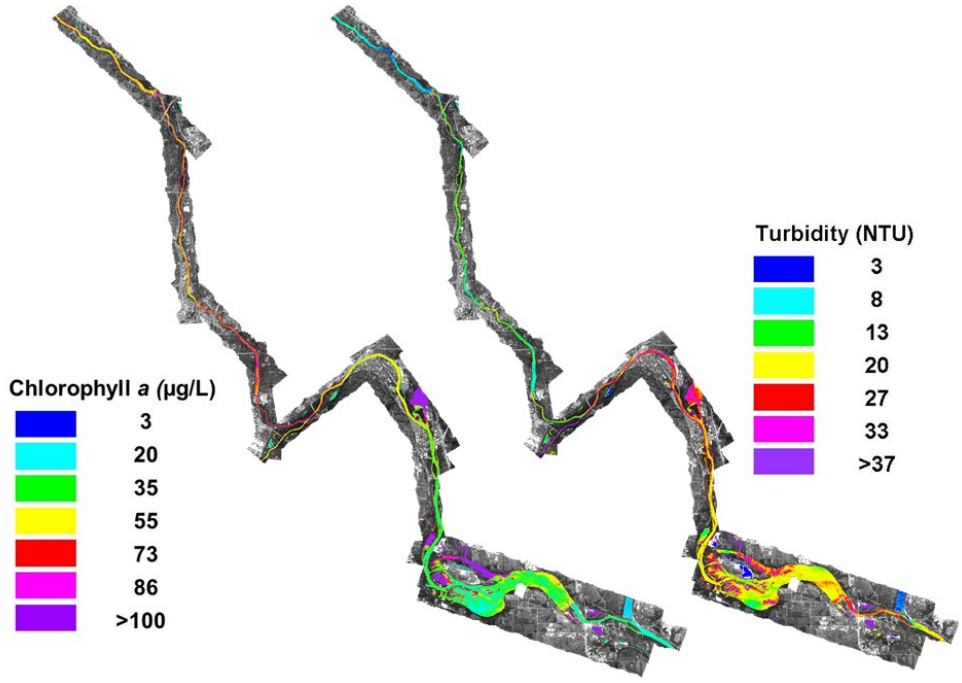

Figure 5.7 Mississippi River Water quality maps (turbidity and chl a) from Rum River to past the confluence with the St. Croix River, August 30, 2007.

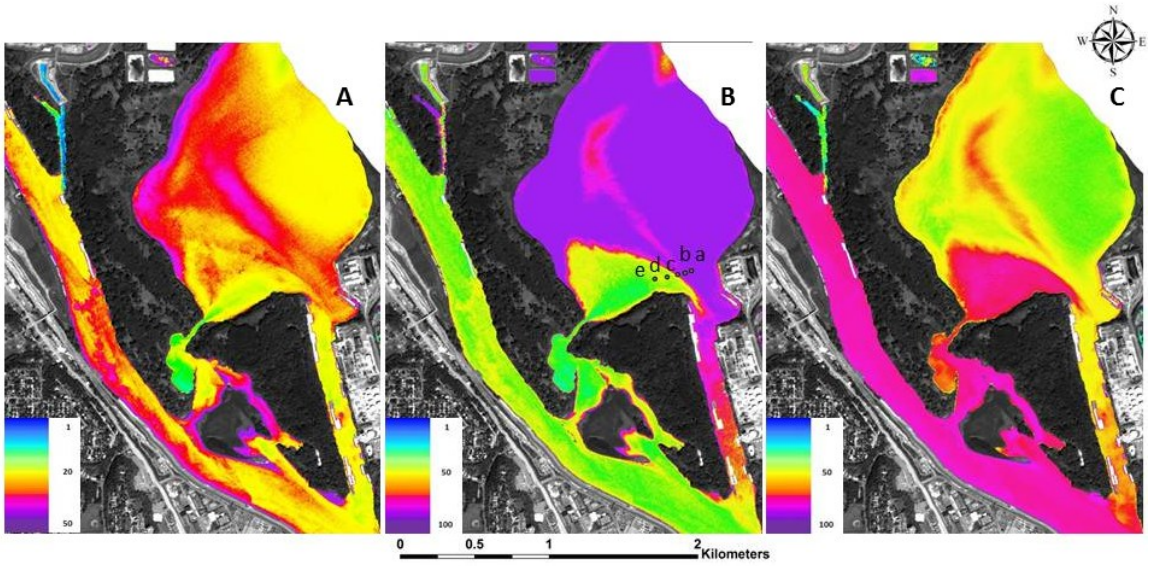

Figure 5.8 Maps of Pig's Eye Lake showing the transition from inorganic sediment dominated to phytoplankton dominated conditions ((A) turbidity, (B) chl *a*, and (C) NVSS/TSS); August 30, 2007.

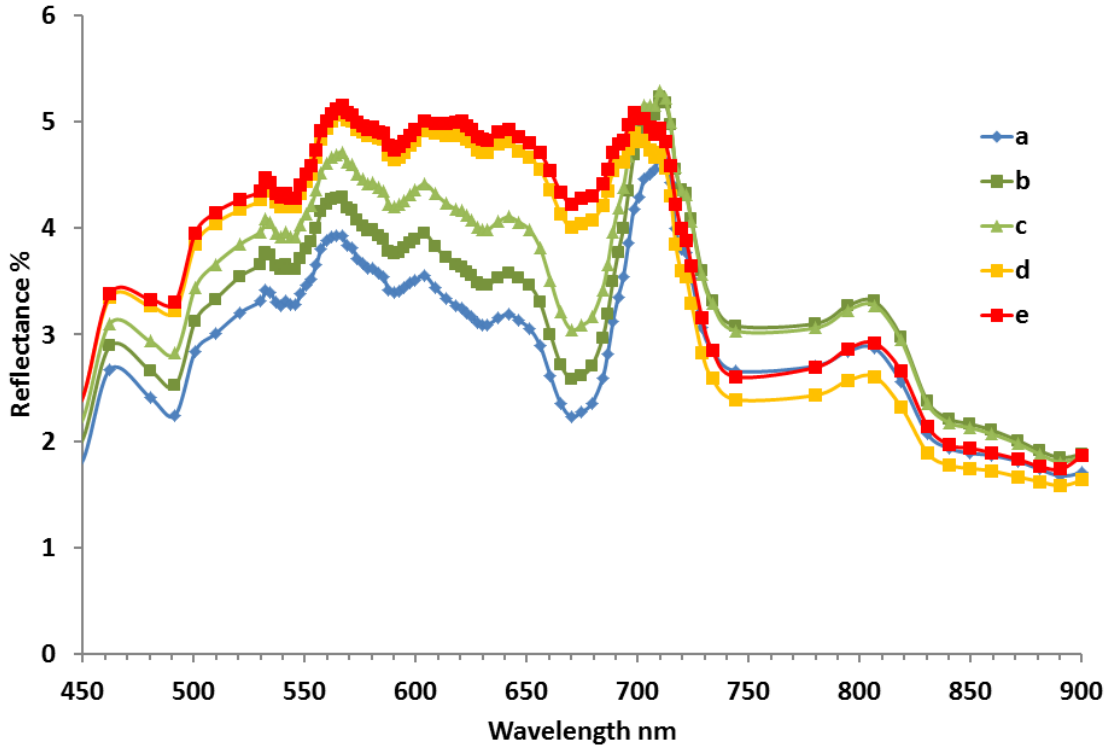

Figure 5.9 Reflectance spectra for the transition from inorganic sediment dominated to phytoplankton dominated conditions in Pig's Eye Lake, August 30, 2007.

The capability of airborne hyperspectral imagery for capturing fine-scale variations in water quality conditions is illustrated by the series of maps in Figure 5.8. Such variations typically are missed by conventional monitoring methods. The maps show the transition from sediment-dominated waters of the Mississippi River to phytoplankton-dominated water of Pig's Eye Lake. Although turbidity is similar in the river and Pig's Eye Lake (with some variations throughout both water bodies (Figure 5.8A), phytoplankton is dominant in most of the lake and much lower in the river (Figure 5.8B). An influx of water with a high load of inorganic sediment (i.e., high NVSS:TSS) from the river is evident in the southwestern portion of the lake (Figure 5.8C). The

transition from phytoplankton-dominated water at location “a” (Figure 5.8B) to inorganic sediment-dominated water at location “e” is captured in the reflectance spectra extracted from the imagery (Figure 5.9). Absorption characteristics of chlorophyll are clearly visible at location “a” but diminish towards location “e”. This example illustrates the vast amount of information available from a single image that would not be seen by conventional monitoring (which probably would involve one grab sample from entire area).

5.5 Discussion and Conclusions

Use of conventional monitoring methods would be prohibitively time consuming and expensive to capture the spatial heterogeneity of water quality exhibited by complex river systems like the Mississippi River and its backwater areas and tributaries in east-central Minnesota. Airborne hyperspectral remote sensing, as used in this study, was effective in capturing a much more comprehensive picture than obtained by typical ground-based sampling programs.

Our approach identified the spectral characteristics that distinguish waters dominated by different IOPs, and we used those characteristics to develop models to map different water quality characteristics in optically complex waters. For waters dominated by phytoplankton, solar radiation absorption by chlorophyll and phycocyanin (found in cyanobacteria) in the red (600-700 nm) wavelengths contrasted strongly with the lack of these absorption characteristics in inorganic sediment-dominated waters. The scattering peak at the red edge (~700 nm), which avoids the region where plant pigments absorb

light, was a strong predictor of variables related to water clarity (TSS, turbidity and T-tube). The ratios of the scattering peak at ~700 nm with the reflectance troughs caused by chlorophyll absorption at ~670 nm and other plant pigment absorption peaks at 592 and 620 nm all were strong predictors of chl *a* and VSS. The band and band combination models that worked for these complex waters have been found to work well by other researchers under varying water quality regimes (previously discussed) and thus appear to be generally robust predictors for chl *a* under a wide range of conditions. The results illustrated in Figures 5.8 and 5.9 for water quality conditions at the interface of Pig's Eye Lake and the Mississippi River also indicate that our predictive relationships can successfully distinguish and map key water quality variables under complex IOP conditions, i.e., separate and map inorganic suspended sediments independently of chlorophyll levels. For NVSS and the ratio NVSS:TSS, we found that a combination of the TSS and chl *a* relationships described above were the most robust because this model corrects for the scattering of phytoplankton at ~700 nm.

High spatial and spectral resolution imagery thus is well suited for regional river water quality assessments in spatially heterogeneous systems with complex IOP conditions. This complexity is not measured by conventional (ground-based) sampling methods that typically represent large areas with one sample. As illustrated in Figure 5.8, the location of a single sample may be representative of only a very small area, but high resolution hyperspectral imagery overcomes these limitations. This is important in waters with complex IOPs because it allows us to distinguish between phytoplankton and inorganic suspended sediments that contribute to the water clarity conditions. Aircraft-

mounted hyperspectral sensors are especially well-suited to capture water quality conditions in complicated systems like the Upper Mississippi River with extensive backwater areas that are difficult to reach by conventional sampling methods, and thus may allow analysis of the effects of contributing factors that could be missed by ground-based monitoring.

Although aircraft-mounted hyperspectral sensing has many advantages for river water quality assessments, it does have limitations. The expense of airborne hyperspectral imagery may be too high for local agencies that oversee natural resources with small budgets. Remote sensing methods also are limited to data collection when atmospheric conditions are clear, and conditions that can alter the spectral radiometric response, such as haze, cloud cover and cloud shadows, should be at a minimum. Imagery thus may not be available when needed. Although hyperspectral imagery is useful to develop water quality models, it is not needed for operational monitoring when only a few key bands are needed. A multispectral system that has well-positioned bands (e.g., those found useful in this study) to capture the key spectral characteristics to measure important water quality variables and also has high spatial resolution (~1-3 m) thus would be sufficient. Technical advancements, such as satellites with higher spectral and spatial resolution and unmanned drones, may reduce the costs of imagery collection and make remote sensing of river water quality a cost-effective and routinely used technique in coming years.

List of References

Abrams, M.J., Ashley, R., Rowan, L.C., Goetz, A.F.H. & Kahle, A.B. (1977). Mapping of hydrothermal alteration in the Cuprite mining district, Nevada, using aircraft scanner imagery for the 0.46–2.36 μm spectral region. *Geology*, 5, 713−718.

Alexander, R.B, Smith, R.A., Schwarz, G.E., Boyer, E.W., Nolan, J.V. & Brakebill, J.W. (2008). Differences in Phosphorus and Nitrogen Delivery to the Gulf of Mexico from the Mississippi River Basin. *Environ. Sci. Technol*., 2008, 42(3), 822–830, doi: 10.1021/es0716103.

Alikas, K and Reinart, A. (2008). Validation of the MERIS products on large European lakes: Peipsi, Vänern and Vättern. *Hydrobiologia*, 599, 161–168, doi:10.1007/s10750-007-9212-0.

Ammenberg, P., Flink, P., Lindell, T., Pierson, D. & Strombeck, N. (2002): Bio-optical modelling combined with remote sensing to assess water quality. *International Journal of Remote Sensing*, 23(8), 1621–1638, doi: 10.1080/01431160110071860.

Arbuckle, K.E. & Downing, J.A. (2001). The influence of watershed land use on lake N:P in a predominantly agricultural landscape. *Limnol. Oceanogr.,* 46, 970–975.

ASTM, (1994). ASTM Standards. Water and Environmental Technology (I). *American Society for Testing and Materials*, Vol 11.01.

Baker, R.J., Anderson, Y.C., Gelvin-Innvaer, L., Hamady, M., Haws, K. & Perry, P.S. (2004). Tenth Anniversary Report - Minnesota Loon Monitoring Program 1994 - 2003. Nongame Wildlife Program, Minnesota Department of Natural Resources Report. 12 pp.

Battin, T.J., Luyssaert, S., Kaplan, L.A., Aufdenkampe, A.K., Richter, A. and Tranvik. L.J. (2009). The boundless carbon cycle. *Nat. Geosci*., 2, 598–600, doi:10.1038/ngeo618.

BEAM. (2010). The Basic Toolbox for ENVISAT (A)ATSR and MERIS (BEAM) version 4.7. Online at: http://www.brockmann-consult.de/cms/web/beam/ downloaded Feb. 25, 2010.

Belmont, P., Gran, K.B., Schottler, S.P., Wilcock, P.R., Day, S.S., Jennings, C., Lauer, J.W., Viparelli, E., Willenbring, J.K., Engstrom, D.R. & Parker, G. (2011). Large shift in source of fine sediment in the Upper Mississippi River. *Environmental Science and Technology,* 45 (20), 8804–8810, doi: 10.1021/es2019109.

Berka, C., Schreier, H. & Hall, K. (2001). Linking water quality with agricultural intensification in a rural watershed. *Water, Air, Soil Pollut.,* 127, 389–401.

Brezonik, P.L. (1978). Effect of organic color and turbidity on Secchi disk transparency. *J. Fish. Res. Bd. Canada,* 35, 1410–1416.

Brezonik, P.L.& Stadelmann, T,H. (2002). Analysis and predictive models of stormwater runoff volumes, loads, and pollutant concentrations from watersheds in the Twin Cities metropolitan area, Minnesota, USA. *Water Research*, 36(7), 1743–57.

Brooks, D.J. (1975). Landsat measures of water clarity. *Photogrammetric Engineering and Remote Sensing,* 41(10), 1269–1271.

Brown, D.R., Warwick, R., & Skaggs, R. (1977). Reconnaissance analysis of lake condition in east central Minnesota. Minnesota Land Management Information System Report 5022. Center for Urban and Regional Affairs, University of Minnesota, Minneapolis, Minnesota. 19 pp.

Carlson, R. E. (1977). A trophic state index for lakes. *Limnology and. Oceanography, 22*, 361–369.

Carroll, M.W., Glaser, J.A., Hellmich, R.L., Hunt, T.E., Sappington, T.W., Calvin, D., Copenhaver, K. & Fridgen, J. (2008). Use of spectral vegetation indices derived from airborne hyperspectral imagery for detection of European corn borer infestation in Iowa corn plots. *Journal of Economic Entomology*, 101(5), 1614–1623, doi: 10.1603/0022-0493(2008)101[1614:UOSVID]2.0.CO;2.

Chen, Z.Q., Hu, C.M., and Muller-Karger, F. (2007). Monitoring turbidity in Tampa Bay using MODIS. *Remote Sensing of Environment*, 109(2), 207–220, doi:10.1016/j.rse.2006.12.019.

Chipman, J.W., Lillesand, T.M., Schmaltz, J.E., Leale, J.E., & Nordheim, M.J. (2004). Mapping lake water clarity with Landsat images in Wisconsin, USA. *Canada Journal of Remote Sensing,* 30, 1–7.

Chipman, J.W., Olmanson, L.G., & Gitelson, A.A. (2009). Remote Sensing Methods for Lake Management: A guide for resource managers and decision-makers. Developed by the North American Lake Management Society in collaboration with Dartmouth College, University of Minnesota, University of Nebraska and University of Wisconsin for the United States Environmental Protection Agency.

Choi, J., Engel, B., Muthukrishnan, S. & Harbor, J. (2003). GIS based long term hydrologic impact evaluation for watershed urbanization. *J. Am. Wat. Resour. Assoc*, 39(3), 623–635.

Clark, R.N., King, T.V.V., Klejwa, M., Swayze, G.A. & Verga, N. (1990). High spectral resolution reflectance spectroscopy of minerals. *Journal Geophysical Research-Solid Earth Planets*, 95, 12653−12680, doi: 10.1029/JB095iB08p12653.

Dall'Olmo G and Gitelson A.A. (2005). Effect of bio-optical parameter variability on the remote estimation of chlorophyll *a* concentration in turbid productive waters: experimental results. *Applied Optics,* 44, 412–422, doi:10.1364/AO.44.000412.

Dekker, A.G., & Peters, S.W.M. (1993). The use of the thematic mapper for the analysis of eutrophic lakes - a case-study in the Netherlands. *International Journal of Remote Sensing,* 14(5), 799–821.

Dekker, A.G., Vos, R.J. & Peters S.W.M. (2002). Analytical algorithms for lake water TSM estimation for retrospective analyses of TM and SPOT sensor data. *International Journal of Remote Sensing*, 23(1), 15–35.

Department of Natural Resources. (1968). An Inventory of Minnesota Lakes. Bulletin 25, Minnesota Department of Natural Resources, St. Paul, Minnesota.

Detenbeck, N.E., Johnston, C.A. & Niemi, G.J. (1993). Wetland effects on lake water quality in the Minneapolis/St. Paul metropolitan area. *Landscape Ecology*, 8, 39–61.

Doerffer, R. and Schiller, H. (2008a). MERIS lake water algorithm for BEAM ATBD, GKSS Research Center, Geesthacht, Germany. Version 1.0, 10 June 2008.

Doerffer, R. and Schiller, H. (2008b). MERIS regional, coastal and lake case 2 water project — atmospheric correction ATBD. GKSS Research Center, Geesthacht, Germany. Version 1.0, 18 May 2008.

Doxaran, D., Cherukuru, R. & Lavender, S. (2005). Use of reflectance band ratios to estimate suspended and dissolved matter concentrations in estuarine waters. *International Journal of Remote Sensing*, 26, 1763–1770, doi: 10.1080/01431160512331314092.

Duan, H.T., Zhang, Y.Z., Zhan, B., Song, K.S. & Wang, Z.M. (2007). Assessment of chlorophyll-a concentration and trophic state for Lake Chagan using Landsat TM and field spectral data. *Environmental Monitoring and Assessment*, 129, 295–308, doi: 10.1007/s10661-006-9362-y.

Engstrom, D.R., Almendinger, J.E. & Wolin , J.A. (2009). Historical changes in sediment and phosphorus loading to the Upper Mississippi River: mass-balance reconstructions from the sediments of Lake Pepin. *Journal of Paleolimnology,* 41, 563–588, doi: 10.1007/s10933-008-9292-5.

GEO, (2007). Inland and nearshore coastal water quality remote sensing, in: GEO group on earth observation, edited by: Bauer, M., Dekker, A., DiGiacomo, P., Greb, S., Gitelson, A., Herlevi, A., and Kutser, T.

Giardino, C., Candiani, G. and Zilioli, E. (2005). Detecting chlorophyll *a* in Lake Garda using TOA MERIS radiances. *Photogrammetric Engineering and Remote Sensing,* 71(9), 1045–1051.

Giardino, C., Bresciani, M., Bartoli, M., and Razinkovas, A. (2010). *In situ* measurements and satellite remote sensing of case 2 waters: first results from the Curonian Lagoon. *Oceanologia,* 52(2), 197–210.

Gitelson, A. (1992). The peak near 700 nm on reflectance spectra of algae and water: relationships of its magnitude and position with chlorophyll concentration. *Int. J. Remote Sensing,* 13(17), 3367–3373.

Gitelson, A.A., Dall'Olmo, G., Moses, W., Rundquist, D.C., Barrow, T., Fisher, T.R., Gurlin D., and Holz, J. (2008). A simple semi-analytical model for remote estimation of chlorophyll *a* in turbid waters: Validation, *Remote Sensing of Environment,* 112, 3582–3593, doi:10.1016/j.rse.2008.04.015.

Gitelson, A., Garbuzov, G., Szilagyi, F.,Mittenzwey, K., karnieli, A. & Kaiser, A. (1993). Quantitative remote sensing methods for real-time monitoring of inland waters quality. *Int. J. Remote Sensing*, 14, 1269–1295.

Gitelson, A.A., Gurlin D., Moses and W.J., Barrow T. (2009). A bio-optical algorithm for the remote estimation of the chlorophyll *a* concentration in case 2 waters. *Environmental Research Letters,* 4(4), doi:10.1088/1748-9326/4/4/045003.

Gitelson A.A. & Merzlyak M.N. (1996). Signature analysis of leaf reflectance spectra: algorithm development for remote sensing of chlorophyll. *J. Plant Physiol*., 148, 494–500.

Gitelson A.A., Zur Y., Chivkunova, O.B. & Merzlyak M.N. (2002). Assesing carotenoid content in plant leaves with reflectance spectroscopy. *Photochem. Photobiol*, 75, 272–281.

Goetz, A.F.H. & Srivastava, V. (1985). Mineralogical mapping in the Cuprite mining district, Nevada. Proceedings, Airborne Imaging Spectrometer Data Analysis Workshop. Pasadena, California. JPL Publication 85-41, Jet Propulsion Laboratory, pp. 22−31.

Gons, H.J., (1999). Optical teledetection of chlorophyll a in turbid inland waters. *Environmental Science and Technology,* 33, 1127–1132, doi: 10.1021/es9809657.

Goolsby, D.A., Battaglin, W.A., Aulenbach, B.T. & Hooper, R.P. (2001). Nitrogen input to the Gulf of Mexico. *J. Environ. Qual*., 30, 329–336.

Gordon, H., and Wang, M. (1994). Retrieval of water-leaving radiance and aerosol optical-thickness over the oceans with SeaWiFS-A preliminary algorithm. *Applied Optics*, 33(3), 443–452.

Gove, N.E., Edwards, R.T. & Conquest, L.L. (2001). Effects of scale on land use and water quality relationships. *J. Am. Wat. Resour. Assoc,* 37(6), 1721–1734.

Gran, K.B., Belmont, P., Day, S.S., Jennings, C., Johnson, A., Parker, G., Perg, L. & Wilcock, P.R. (2009). Geomorphic evolution of the Le Sueur River, Minnesota, and implications for current sediment loading. eds. In James, L.A., Rathburn, S.L. and Whittecar, G.R., eds., Management and Restoration of Fluvial Systems with Broad Historical Changes and Human Impacts: *Geological Society of American Special Paper,* 451, 119–130, doi: 10.1130/2008.2451(08).

Greenberg, A.E., Clesceri, L.S. & Eaton, A.D., (1992). Standard methods for the examination of water and wastewater. 18th Edition, American Public Health Association, Washington, D.C.

Guan, X., Li, J., and Booty, W. (2011). Monitoring Lake Simcoe water clarity using Landsat-5 TM images. *Water Resources Management,* 25(8), 2015–2033, doi:10.1007/s11269-011-9792-3.

Hakvoort, H., De Haan, J., Jordans, R., Vos, R., Peters, S. & Rijkeboer, M. (2002). Towards airborne remote sensing of water quality in The Netherlands – validation and error analysis. *ISPRS Journal of Photogrammetry and Remote Sensing*, 57, 171–183, doi: 10.1016/S0924-2716(02)00120-X.

Haboudane, D., Miller, J.R., Pattey, E., Zarco-Tejada, P.J. & Strachan, I.B. (2004). Hyperspectral vegetation indices and novel algorithms for predicting green LAI of crop canopies: modeling and validation in the context of precision agriculture. *Remote Sens. Environ*, 90(3), 337–352, doi:10.1016/j.rse.2003.12.013.

Haboudane, D., Miller, J.R., Tremblay, N., Zarco-Tejada, P.J. & Dextraze, L. (2002). Integrated narrow-band vegetation indices for prediction of crop chlorophyll content for application to precision agriculture. *Remote Sens. Environ,* 81(2–3), 416–426.

Härmä, P., Vepsalainen, J., Hannonen, T., Pyhalahti, T., Kamari, J., Kallio, K., Eloheimo, K. & Koponen, S. (2001). Detection of water quality using simulated satellite data and semi-empirical algorithms in Finland. *The Science of the Total Environment*, 268, 107–121.

Heiskary, S. & Lindon, M. (2005). Interrelationships among water quality, lake Morphometry, rooted Plants and related factors for selected shallow lakes of west-central Minnesota - Part of a series on Minnesota lake water quality assessment. Minnesota Pollution Control Agency Report. 133 pp.

Heiskary, S.A., & Walker Jr., W.W. (1988). Developing phosphorus criteria for Minnesota lakes. *Lake and Reservoir Management, 4*, 1–9.

Heiskary, S. & Wilson, B. (1988). Minnesota Lake Water Quality Assessment Report. MPCA. St. Paul MN, 95 pp.

Heiskary, S.A. & Wilson, C.B. (1989). The regional nature of lake water quality across Minnesota: An analysis for improving resource management. *J. Minn. Acad. of Sci*. 55, 71–77.

Heiskary, S.A. & Wilson, C.B. (2005). Minnesota lake water quality assessment report: Developing nutrient criteria. Minnesota Pollution Control Agency, St. Paul, Minnesota.

Horne, A.J. & C.R. Goldman. (1994). Limnology. 2nd edition. McGraw-Hill Co., New York, New York, USA.

Hoogenboom, H.J., Dekker, A.G. & De Haan, J.F. (1998). Retrieval of chlorophyll and suspended matter in inland waters from CASI data by matrix inversion. *Canadian Journal of Remote Sensing,* 24(2), 144–152.

Kallio, K., Kutser, T., Hannonen, T., Koponen, S., Pulliainen, J., Vepsalainen, J. & Pyhalahti, T. (2001). Retrieval of water quality from airborne imaging spectrometry of various lake types in different seasons. *The Science of the Total Environment*, 268, 59–77, doi:10.1016/S0048-9697(00)00685-9.

Keller P.A. (2001). Comparison of two inversion techniques of a semi-analytical model for the determination of lake water constituents using imaging spectrometry data, *Science of the Total Environment*, 268(1–3), 189–196.

Kloiber, S.M. (2006). Estimating nonpoint source pollution for the Twin Cities metropolitan area using landscape variables. *Water, Air and Soil Pollut.*, 172, 313–335.

Kloiber, S.M., Brezonik, P.L., Olmanson, L.G. & Bauer, M.E. (2002a). A procedure for regional lake water clarity assessment using Landsat multispectral data. *Remote Sensing of Environment,* 82(1), 38–47, doi: 10.1016/S0034-4257(02)00022-6.

Kloiber, S.M., Brezonik, P.L., & Bauer, M.E. (2002b). Application of Landsat imagery to regional-scale assessments of lake clarity. *Water Research,* 36*,* 4330–4340.

Koponen, S., Attila, J., Pulliainen, J.,Kallio,K., Pyhälahti, T., Lindfors,A., Rasmus, K. & Hallikainen, M. (2007). A case study of airborne and satellite remote sensing of a spring bloom event in the Gulf of Finland. *Continental Shelf Research*, 27, 228–244, doi: 10.1016/j.csr.2006.10.006.

Kutser, T., Arst, H., Miller, T., Kaarmann, L., and Milius, A. (1995). Telespectrometrical estimation of water transparency, chlorophyll-a and total phosphorus concentration of lake peipsi. *International Journal of Remote Sensing*, 16(16), 3069–3085.

Lathrop, R.G. (1992). Landsat Thematic Mapper monitoring of turbid inland water quality. *Photogrammetric Engineering and Remote Sensing,* 58, 465–470.

Lathrop, R.G., Lillesand, T. M., & Yandell, B.S. (1991). Testing the utility of simple multi-date Thematic Mapper calibration algorithms for monitoring turbid inland waters. *International Journal of Remote Sensing,* 12, 2045–2063.

Leone, A., Ripa, M.N., Boccia L. & Porto A.L. (2008). Phosphorus export from agricultural land: A simple approach. *Biosystems Eng*, 101, 270–280.

Lillesand, T.M., Chipman, J.W., Nagel, D.E., Reese, H.M., Bobo, M.R. & Goldmann, R.A. (1998). Upper Midwest Gap Analysis Program Image Processing Protocol. U.S. Geological Survey, Environmental Management Technical Center, Onalaska, Wisconsin. EMTC98-G001. 25 pp.+ appendices.

Lillesand, T. M., Johnson, W. L., Deuell, R. L., Lindstrom, O. M. & Meisner, D. E. (1983). Use of Landsat data to predict the trophic state of Minnesota lakes. *Photogrammetric Engineering and Remote Sensing, 49,* 219–229.

Lind, A.O. (1973). Application of ERTS-1 Imagery in the Vermont-New York Dispute Over Pollution of Lake Champlain. Burlington: Remote Sensing Laboratory, Vermont University. 5p.

Lindon, M., Heiskary, S., &Wiens, C. (2005). Status and Trend Monitoring of Select Lakes in Cass and Crow Wing Counties 2004. Lake Assessment Program, Minnesota Pollution Control Agency Report. 102 pp.

Matthews, M.W. (2011). A current review of empirical procedures of remote sensing in inland and near-coastal transitional waters. *International Journal of Remote Sensing*, 32(21), 6855–6899, doi: 10.1080/01431161.2010.512947.

Matthews, M.W., Bernard S., and Winter K. (2010). Remote sensing of cyanobacteria-dominant algal blooms and water quality parameters in Zeekoevlei, a small hypertrophic lake, using MERIS. *Remote Sensing of Environment,* 114, 2070–2087, doi:10.1016/j.rse.2010.04.013.

Mattikalli, N.M. & Richards, K.S. (1996). Estimation of surface water quality changes in response to land use change: application of the export coefficient model using remote sensing and geographic information system. *J. Environ. Manage*, 48, 263–282.

Martin, R.H., Boebel, E.O., Dunst, R.C., Williams, O.D., Olsen, M.V., Merideth, Jr.,R.W. & Scarpace, F.L. (1983). Wisconsin lakes – a trophic assessment using Landsat digital data. Wisconsin Lake Classification Survey Project. S00536601. 294 p.

McCauley, J.R. (1974). Skylab study of water quality. Lawrence: University of Kansas. 9 p.

Menken, K.D., Brezonik, P.L. & Bauer, M.E. (2006). Influence of chlorophyll and colored dissolved organic matter (CDOM) on lake reflectance spectra: implications for measuring lake properties by remote sensing. *Lake and Reservoir Management*, 22, 179−190.

Metropolitan Council, (2004). Regional Progress in Water Quality Analysis of Water Quality Data from 1976 to 2002 for the Major Rivers in the Twin Cities. *Metropolitan Council Environmental Services Regional Report.*

Minnesota Land Management Information Center (2006). Level III Ecoregions of the Conterminous United States (LMIC/MPCA Version of USEPA Omernik Map for Minnesota - 'ECOREG'). http://lucy.lmic.state.mn.us/metadata/ecoreg.html.

Mittenzwey, K., Gitelson, A., Ullrich, S. & Kondratiev, K. (1992). Determination of chlorophyll a of inland waters on the basis of spectral reflectance. *Limnology and Oceanography*, 37, 147–149.

Moore, G.F., Aiken, J. and Lavender, S.J. (1999). The atmospheric correction of water colour and the quantitative retrieval of suspended particulate matter in Case II waters: application to MERIS. *International Journal of Remote Sensing*, 20(9), 1713–1733.

Morel, A. & Prieur, L. (1977). Analysis of variations in ocean color. *Limnology and Oceanography,* 22, 709–722.

Moses, W.J., Gitelson, A.A., Berdnikov, S. & Povazhnyy V. (2009). Satellite estimation of chlorophyll *a* concentration using the red and NIR bands of MERIS—the Azov Sea case study. *IEEE Geoscience and Remote Sensing Letters*, 6(4), 845–849, doi: 10.1109/LGRS.2009.2026657.

Moses, W.J., Gitelson, A.A., Perk, R.L., Gurlin, D., Rundquist, D.C., Leavitt, B.C. Barrow, T.M. & Brakhage, P. (2011). Estimation of Chlorophyll-a Concentration in Turbid Productive Waters Using Airborne Hyperspectral Data. *Water Research,* 46(4), 993–1004, doi: 10.1016/j.watres.2011.11.068.

Mulla, D.J. & Sekely, A. (2009). Historical trends affecting accumulation of sediment and phosphorus in Lake Pepin. *J. Paleolimnology,* 41(4): 589–602, doi:10.1007/s10933-008-9293-4.

Myre, E. & Shaw, R. (2006). The Turbidity Tube: Simple and Accurate Measurement of Turbidity in the Field. Michigan Technology University, Houghton, Michigan.

Nelson, S.A.C., Soranno, P A., Cheruvelil, K.S., Batzli, S.A., & Skole, D.L. (2003). Regional assessment of lake water clarity using satellite remote sensing. *Journal of Limnology*, 62(s1), 27–32.

Odermatt, D., Heege, T., Nieke, J., Kneubuhler, M., and Itten, K. (2008). Water quality monitoring for Lake Constance with a physically based algorithm for MERIS data. *Sensors*, 8, 45824–599, doi:10.3390/s8084582.

Odermatt, D., Giardino, C., and Heege, T. (2010). Chlorophyll retrieval with MERIS Case-2-regional in perialpine lakes. *Remote Sensing of Environment,* 114(3), 607–617, doi:10.1016/j.rse.2009.10.016.

Olmanson, L.G., Bauer, M.E. & Brezonik, P.L. (2008). A 20-year Landsat water clarity census of Minnesota's 10,000 lakes. *Remote Sensing of Environment,* 112(11), 4086–4097, doi: 10.1016/j.rse.2007.12.013.

Olmanson, L.G., Brezonik, P.L. & Bauer, M.E. (2011). Evaluation of medium to low resolution satellite imagery for regional lake water quality assessments. *Water Resources Research,* 47, W09515, doi:10.1029/2011WR011005.

Olmanson, L.G., Brezonik, P.L., Kloiber, S.M., Bauer, M.E., & Day, E.E. (2002). Lake water clarity assessment of Minnesota's 10,000 lakes: A comprehensive view from space. *Proceedings, Virginia Water Research Symposium 2000*. In: Advances in Water Monitoring Research, T.Younos (Ed.), Water Resources Publications, LLC, Highland Ranch, Colorado. pp. 183–202.

Olmanson, L.G., Kloiber, S.M., Bauer, M.E. & Brezonik, P.L. (2001). Image processing protocol for regional assessments of lake water quality. Public Report Series #14. Water Resources Center and Remote Sensing Laboratory, University of Minnesota, St. Paul, MN, 55108, October 2001. 15 pp.

Omernik, J.M., (1987). Ecoregions of the Conterminous United States, Map. *Annals of the Association of American Geographers,* 77(1), 118–125.

Osgood, R.A., Brezonik, P.L. & Hatch L. (2002). Methods for classifying lakes based on measures of development. University of Minnesota Water Resources Center, Technical Report 143.

Peckham, S.D., and Lillesand, T.M. (2006). Detection of spatial and temporal trends in Wisconsin lake water clarity using Landsat-derived estimates of Secchi depth. *Lake and Reservoir Management*, 22(4), 331−341, doi:10.1080/07438140609354367.

Peterson SA, Urquhart NS, & Welch E.B. (1999). Sample representativeness: a must for reliable regional lake condition estimates. *Environmental Science and Technology,* 33(10), 1559–1565.

Pluhowski, E.J. (1973). Remote sensing of turbidity plumes in Lake Ontario. In NASA. Goddard Space Flight Center. Symposia on Significant Results obtained from the ERTS-1, Vol. 1 Sect. A and B, pp. 837–846.

Preisendorfer R.W. (1986). Secchi disk science: Visual optics of natural waters. *Limnol. Oceanogr.*, 3l(5), 909–926.

Rabalais, N.N., Turner, R.E. & Scavia, D. (2002a). Beyond science into policy: Gulf of Mexico hypoxia and the Mississippi River. *Bioscience,* 52, 129–142.

Rabalais, N.N., Turner, R.E. & Wiseman, W.J, Jr. (2002b). Gulf of Mexico hypoxia, A.K.A. the dead zone. *Annu Rev Ecol Syst,* 33, 235–263, doi: 10.1146/annurev.ecolsys.33.010802.150513.

Ramstack, J.M., Fritz S.C. & Engstrom, D.R. (2004). Twentieth century water quality trends in Minnesota lakes compared with presettlement variability. *Can J Fish Aquat Sci,* 61, 561–76.

Reinart, A., and Kutser, T. (2006). Comparison of different satellite sensors in detecting cyanobacterial bloom events in the Baltic Sea. *Remote Sensing of Environment*, 102, 74–85, doi:10.1016/j.rse.2006.02.013.

Ritchie, J. C., Cooper, C. M., & Schiebe, F. R. (1990). The relationship of MSS and TM digital data with suspended sediments, chlorophyll and temperature in Moon Lake, Mississippi. *Remote Sensing of Environment*, 33, 137–148.

Schalles, J.F., Gitelson, A.A., Yacobi, Y.Z. and Kroenke, A.E. (1998). Estimation of chlorophyll *a* from time series measurements of high spectral resolution reflectance in an eutrophic lake. *Journal of Phycology*, 34(2), 383–390.

Senay, G.B., Shafique, N.A., Autrey, B.C., Fulk, F. & Cormier, S.M. (2001). The selection of narrow wavebands for optimizing water quality monitoring on the Great Miami River, Ohio using hyperspectral remote sensor data. *J. Spatial Hydrol*. 1, 1–22.

Shafique, N.A., Autrey, B.C., Fulk, F.A. & Flotemersch, J.E. (2003). Hyperspectral remote sensing of water quality parameters for large rivers in the Ohio River Basin. First Interagency Conference on Research in the Watersheds. Benson, Arizona, October 27 - 30, 2003. USDA Agricultural Research Service, Washington, DC, 2003.

Shah, C.A., Arora, M.K., Robila, S.A. & Varshney, P.K. (2002). ICA mixture model based unsupervised classification of hyperspectral imagery. Proceedings of 31st International Workshop on Applied Imagery and Pattern Recognition. IEEE Computer Society, Washington DC, USA, 16–18 October 2002 (Los Alamitos, CA: IEEE Computer Society Press), pp. 29–35.

Shah, C.A., Manoj K. Arora & Pramod K. Varshney (2004). Unsupervised classification of hyperspectral data: an ICA mixture model based approach. *International Journal of Remote Sensing,* 25(2), 481–487, doi: 10.1080/01431160310001618040.

Shi, W., and Wang, M. (2009). An assessment of the black ocean pixel assumption for MODIS SWIR bands. *Remote Sensing of Environment,* 113, 1587–1597, doi:10.1016/j.rse.2009.03.011.

Song, C., Woodcock, C., Seto, K.C., Lenney, M.P., and Macomber, S.A. (2001). Classification and change detection using Landsat TM data–when and how to correct atmospheric effects? *Remote Sensing of Environment*, 75(2), 230–244.

Soranno, P.A., Wagner, T., Martin, S.L., McLean, C., Novitski, L.N., Provence, C.D. & Rober, A.R. (2011). Quantifying regional reference conditions for freshwater ecosystem management: A comparison of approaches and future research needs. *Lake Reserv Manage*, 27, 138–148.

Stadelmann, T.H., Brezonik, P.L. & Kloiber, S (2001). Seasonal Patterns of Chlorophyll a and Secchi Disk Transparency in Lakes of East-Central Minnesota: Implications for Design of Ground- and Satellite-Based Monitoring Programs. *Lake and Reservoir Management,* 17(4), 299–314.

Thorleifson, L.H. (1996). Review of Lake Agassiz history. *in* J.T. Teller, L.H. Thorleifson, G. Matile and W.C. Brisbin, eds. Sedimentology, Geomorphology and History of the Central Lake Agassiz Basin - Field Trip Guidebook B2; Geological Association of Canada/Mineralogical Association of Canada Annual Meeting, Winnipeg, Manitoba, May 27–29, 1996.

Tong, S. & Chen, W. (2002). Modeling the relationship between land use and surface water quality. *J. Environ. Manage,* 66(4), 377–393.

Tranvik, L.J., J. Downing, J. Cotner, S. Loiselle, R.G. Striegl, T.J. Ballatore, P. Dillon, K. Finlay, K. Fortino, L.B. Knoll, P. Kortelainen, T. Kutser, S. Larsen, I. Laurion, D.M. Leech, S.L. McCallister, D.M. McKnight, J.M. Melack, E. Overholt, J.A. Porter, Y. Prairie, W.H. Renwick, F. Roland, B.S. Sherman, D.W. Schindler, S. Sobek, A. Tremblay, M.J. Vanni, A.M. Verschoor, E. von Wachenfeldt, G.A. Weyhenmeyer, (2009). Lakes and impoundments as regulators of carbon cycling and climate. *Limnology and Oceanography*, 54, 2298–2314.

Turner R.E. & Rabalais N.N. (1994). Coastal eutrophication near the Mississippi River delta. *Nature* 368, 619–621, doi:10.1038/368619a0.

U.S. Environmental Protection Agency (1992). Methods for determination of chemical substances in marine and estuarine environmental samples. EPA/600/R-92/121, 95 pp.

U.S. FWS (1971). Wetlands of the United States. U.S. Fish and Wildlife, Circular 39.

Vollenweider R.A. (1968). Scientific fundamentals of the eutrophication of lakes and flowing waters, with particular reference to nitrogen and phosphorus as factors in eutrophication. Paris Organization for Economic Co-operation and Development, Tech. Rep. DAS/CSI/68.27, 250 p.

Vollenweider R.A. (1975). Input-output models with special reference to the phosphorus loading concept in Limnology. *Schweiz. Z. Hydrol*, 37, 53–84.

Wagner, T., Soranno, P.A., Cheruvelil, K.S., Renwick, W.H., Webster, K.E., Vaux, P. & Abbitt, R.J.F. (2008). Quantifying sample biases of inland lake sampling programs in relation to lake surface area and land use/cover. *Environ. Monit. Assess.,* 141, 131–147.

Werdell, P.J., Bailey, S.W., Franz, B.A., Harding Jr., L.W., Feldman, G.C., and McClain, C.R. (2009). Regional and seasonal variability of chlorophyll *a* in Chesapeake Bay as observed by SeaWiFS and MODIS-Aqua, *Remote Sensing of Environment*, 113(6), 1319–1330, doi:10.1016/j.rse.2009.02.012.

Wessman, C.A., Aber, J.D., Petersen, D.L. & Melillo, J.M. (1988). Remote-sensing of canopy chemistry and nitrogen cycling in temperate forest ecosystems. *Nature*, 335, 154−156, doi: 10.1038/335154a0.

Wilson, C.O. & Weng, Q. (2010). Assessing surface water quality and its relations with urban land cover changes in the Lake Calumet Area, Greater Chicago. *Environ Manage,* 45, 1096–111.

Wood, E. F., et al. (2011). Hyperresolution global land surface modeling: Meeting a grand challenge for monitoring Earth's terrestrial water. *Water Resour. Res.*, 47, W05301, doi:10.1029/2010WR010090.

Yarger, H.L., Mccauley, J.R., James, G.W., Magnuson, L.M. & Marzolf, G.R. (1973). Water turbidity detection using ERTS-1 imagery. In NASA. Goddard Space Flight Center. Symposia on Significant Results obtained from the ERTS-1, Vol. 1 Sect. A and B, pp. 651–658.